Eyes on the Sky: A Refracting Concentrator Approach to the SKA

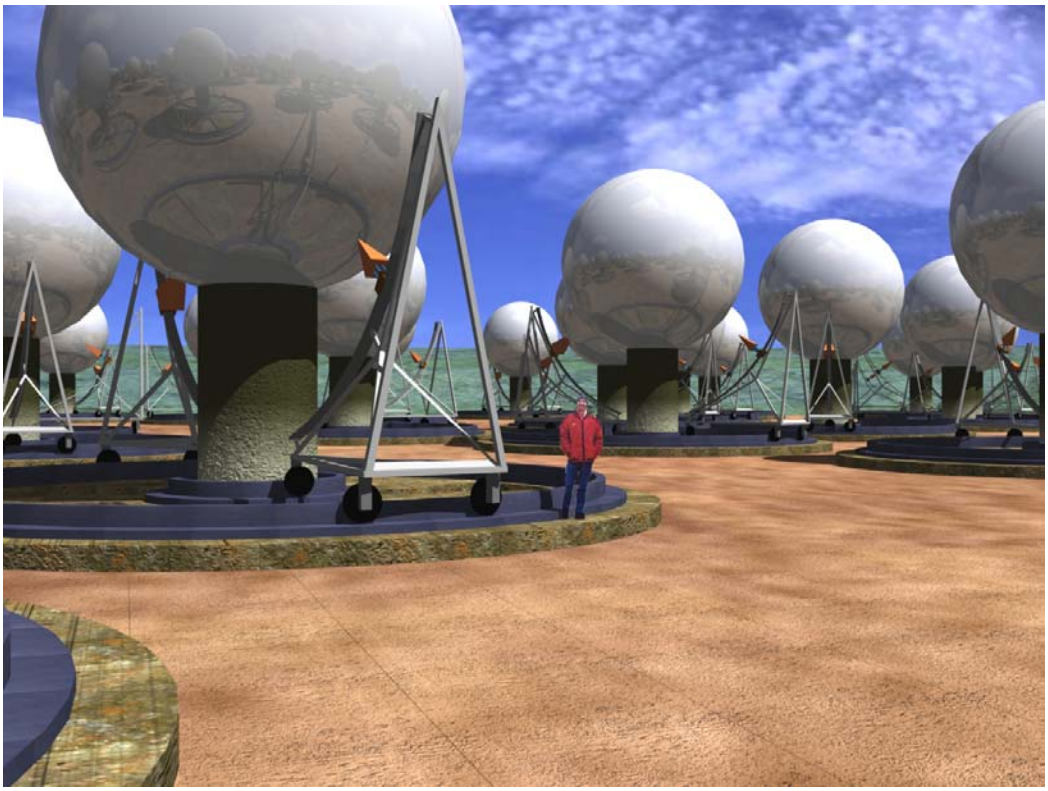

SKA
SQUARE KILOMETRE ARRAY

Eyes on the Sky: A Refracting Concentrator Approach to the SKA

By

Ron Beresford, Aaron Chippendale, Dick Ferris, Peter Hall, Carole Jackson, Graeme James and Mark Wieringa

Edited by

Peter Hall

Submitted to the SKA Engineering and Management Team by

The Executive Secretary
Australian SKA Consortium Committee
PO Box 76, Epping, NSW 1710, Australia.
June 2002

15 July 2002
(rev d)

TABLE OF CONTENTS

1. AUTHORS' PREFACE AND ACKNOWLEDGEMENTS

A concept description such as this one is guaranteed to leave writers with the feeling that it could all have been done so much better – if only the outcomes had been clear at the beginning! For us, the process has been simultaneously challenging, satisfying and sobering. We look forward to the discussions promoted by this first document.

We acknowledge with thanks the contributions of others, including Wim Brouw, John Bunton, Ron Ekers, Russell Gough, Colin Jacka, John Kot, David McConnell, Nasiha Nikolic, Andrew Parfitt, Elaine Sadler, Ravi Subrahmanyan, Paul Thompson, and Wei Wu. Special thanks to Chris Fluke from Swinburne University of Technology for visualizations of the Luneburg lens array stations.

2. EXECUTIVE SUMMARY

The Square Kilometre Array (SKA) is a proposed radio telescope which will be 100 times as sensitive as the best present-day centimetre-wave instruments, enabling it to unlock much of the early Universe and, via novel operational modes, to access an unprecedented volume of observing parameter space. This document describes a concept for the SKA based on Luneburg lens antennas: spherical refracting concentrators which, unlike conventional reflectors, allow simultaneous observation in widely differing directions.

The Luneburg lens concept, like all other ideas for the SKA, is a compromise based on a wide range of initial science goals set for the instrument. The thinking behind the proposal emphasizes an area re-use capability (multibeaming) for the billion-dollar SKA, the versatility of the instrument, and the ability to upgrade the telescope over perhaps a 30-40 year lifetime. The niche for the lens proposal is the frequency range 0.1 – 5 GHz, with the "soft" frequency limits set primarily by the seven-metre concentrator diameter and by its absorption of radio-frequency energy.

The lens concept gives astronomers access to the high-redshift Universe (including the epoch of re-ionization in the 100 – 150 MHz range), to full-sensitivity HI observations, and to the beginning of the thermal radiation spectrum. The multibeaming capability confers specific advantages in areas such as astrometry and pulsar astronomy and, while our cost analysis suggests that a two-beam SKA may be feasible initially, the ability to add beams progressively promises enormous further advantage in deeper studies of, for example, time-resolved or transient phenomena. This ability to add widely-separated beams, and to mix operational feeds and receivers, is unique to the lens concept. While some other proposals rely on split array modes to access different regions of the sky, the sensitivity loss per beam becomes prohibitive beyond a few sub-arrays.

Of course, the SKA will consist of much more than antennas. While not canvassing all aspects of the telescope design, this proposal includes practical suggestions in key areas such as receiver and data transport systems, array configuration and SKA siting. We have added most commentary in areas not widely addressed in SKA forums, simply to promote discussion within the SKA community. For example, an outline is given of a receiving system involving quantization at the antennas, station channelization and beamforming using digital signal processing, and data transport via fibre optic links, all modelled on advancing commercial technologies. At the same time, we have reserved detailed discussion of, for example, imaging correlators, noting extensive commentary elsewhere.

While construction and operating costs are important in designing the SKA, this first study deals mainly with major component costing. For a 300-station lens array with two independent beams, these costs total $US1.4 billion, dropping to $US1.1 billion for a single-beam instrument. A variational analysis is included to illustrate the sensitivity of SKA pricing to major system parameters and component costing assumptions. This analysis highlights a number of areas for attention in future studies; key areas include receiver noise performance, feed spillover, and the cost of artificial dielectric materials.

3. INTRODUCTION

Large radio telescopes of the future will be driven to aperture re-use through multibeaming for both scientific and economic reasons. While phased array technology has much to contribute in this evolution, it is unlikely that, for an SKA built by 2020, elemental receptors and purely electronic processing will provide the bandwidth and sensitivity demanded by the science community. Furthermore, no SKA model – phased array or other – can provide simultaneous all-sky coverage above 2 GHz, simply as a result of receptor and receiver costs alone.

We propose an SKA solution which invokes a spherical radio lens as the first stage beamformer. This "Luneburg lens" approach, with its wideband optical beamforming and intrinsic capability for placing multiple beams across the sky, is an intermediate one offering some of the signal processing flexibility associated with phased arrays, as well as most of the performance and versatility of reflecting concentrators. A particular advantage is that the lens approach allows progressive upgrades, not only to the primary receiving electronics but also in terms of number of widely-separable SKA beams.

Initial analysis of SKA imaging requirements leads us to favour a large number of antennas and about N = 300 stations ("medium-N"), similar in principle to an SKA designed around small or medium-diameter paraboloidal reflectors. Like other SKA solutions, especially those involving large or medium-N realizations, our design causes us to confront issues such as the cost of mass producing tens of thousands of antennas and associated receivers, the path to new data encoding and transport technologies, and the flexibility and financial costs of various signal aggregration schemes. In addition, the refracting concentrator approach raises challenges in fundamental and applied material science, particularly in the area of artificial dielectrics. Despite being first described in the 1940s [3-1], Luneburg lenses have had hitherto limited application, due mainly to the loss, density and cost of suitable dielectrics. Our proposal rests, in part, on favourable initial results from projects investigating the manufacture and forming of low-loss, lightweight, and cheap materials.

In compiling this summary we have not sought to canvass all possibilities for all parts of the sample SKA design. Most obviously, the proposal omits discussion of rather imaginative possibilities for robotic placement of Luneburg lens feeds, or for the population of the lens focal surface with phased arrays. Bearing in mind the ~10-year design timescale, the study presents a reference SKA based on more conventional feed translation systems. Overall, we have sought to outline a representative SKA based on what appear to us to be sensible, if ambitious, technology choices. As experimental work and commercial technology progresses, it will be important to re-visit critical design decisions. For completeness, details of a representative Australian SKA site are included; this exemplar site is for discussion purposes only and no endorsement by any technical or policy body is implied.

4. OVERVIEW

Our proposal is summarized in Table 4-1, while Fig. 4-1 illustrates the concept.

Table 4-1. Summary of SKA Proposal

Antenna type	Luneburg Lens
Antenna diameter	7.0 m
Frequency coverage (GHz)	0.1 – 5.0 GHz
Antenna beamwidth; field-of-view 0.1 GHz 0.3 GHz 1.4 GHz 5.0 GHz	 30.0° ; 705 deg^2 10.0° ; 78 deg^2 2.1° ; 3.6 deg^2 0.6° ; 0.3 deg^2
Equivalent number of stations	N = 300 (153 outside 4 km diameter central array)
Number of antennas per station	176
Station diameter	250 m
Total number of antennas	52 800
Longest baseline	3 000 km
Effective area	1.29 km^2
Sensitivity (A_{eff}/T_{sys}) 0.1 GHz 0.3 GHz 1.4 GHz 5.0 GHz	 7 x 10^2 m^2K^{-1} 6 x 10^3 m^2K^{-1} 2 x 10^4 m^2K^{-1} 1.3 x 10^4 m^2K^{-1}
Best array angular resolution 0.1 GHz 0.3 GHz 1.4 GHz 5.0 GHz	 0.25 arcsec 0.083 arcsec 0.018 arcsec 0.005 arcsec
Brightness sensitivity at 1.4 GHz (8 hrs integration, 800 MHz BW) Central array (13 arcsec res) 300 km array (0.1 arcsec res)	 0.3 mK 0.7 K
Number of independent feeds per antenna	2 (initially)
Number of polarizations per feed	2 linear
Number of spectral channels	8192
Number of simultaneous frequency bands	Flexible within station data transport limits (Section 9.4)

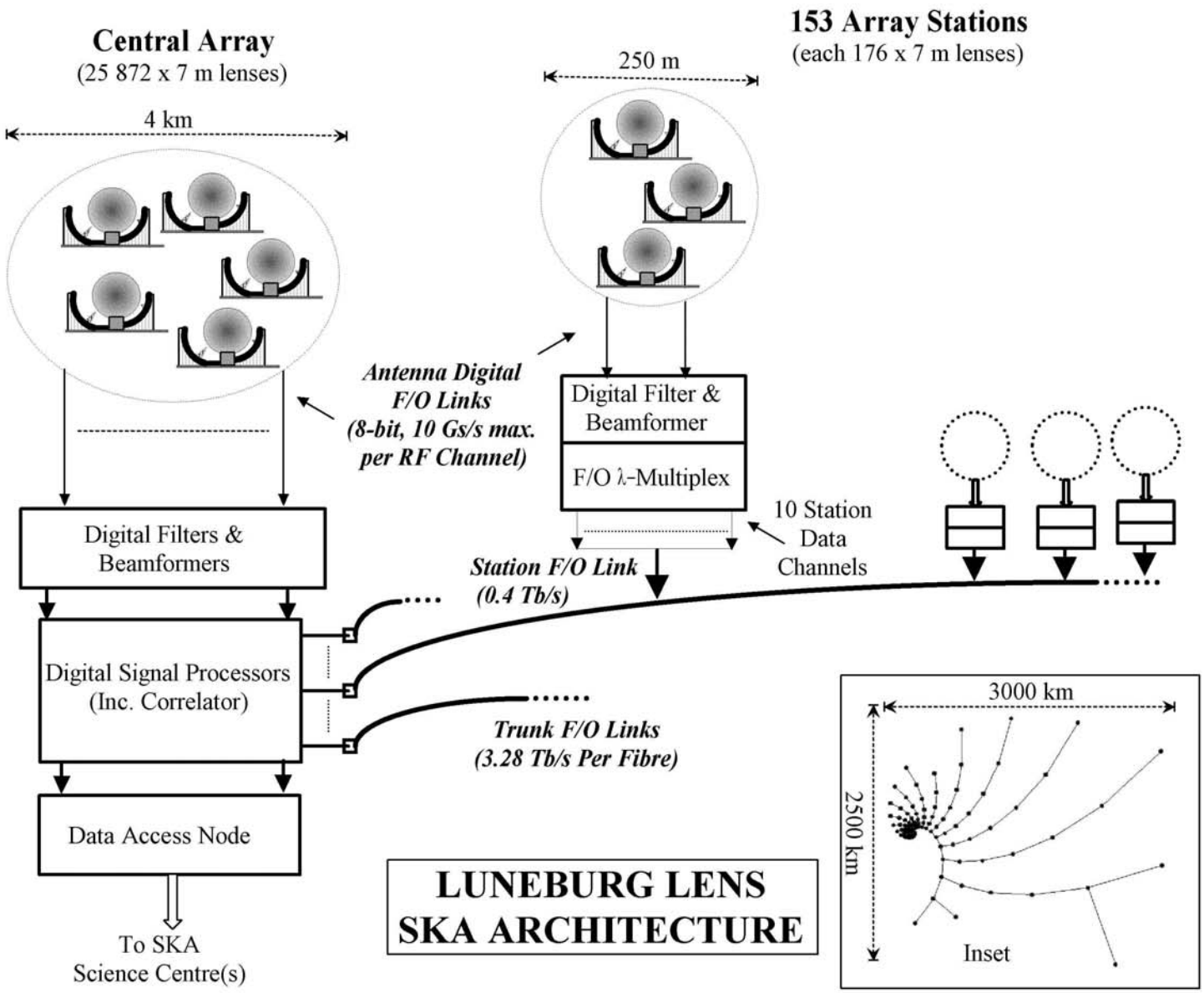

Fig. 4-1. Overview of an SKA based on Luneburg lens concentrators.

5. SCIENCE CONSIDERATIONS

5.1 Addressing the SKA Science Priorities

Radio astronomy is a unique window to the Universe: at centimetre wavelengths radio waves are largely unattenuated by intervening cosmic media, and the window gives an unobscured view of thermal and non-thermal processes at all cosmic epochs. Radio observations, and future results from other wavebands (mm, sub-mm, FIR), will combine to produce important insight into the evolution of primordial structure.

Radio astronomy has a rich history of outstanding astronomical discoveries including quasars, the cosmic microwave background and pulsars. The future of the science at centimetre wavelengths now rests with the development of the SKA: a highly-sensitive instrument with novel capabilities. SKA will complement other next-generation telescopes coming on-line over the next decade or so; these include NGST, ALMA, and very large (> 30 m) optical telescopes (including OWL & CELT).

The SKA science drivers as identified by the International Science Advisory Group fall into four categories, given as:

- probing the dark age - the detection of, and measurement of structures at, the re-ionization epoch, and of the objects responsible for this re-ionization;
- development of large scale structure of the universe, including the formation and clustering of galaxies and active galaxies;
- star life and death - Galactic and extra-Galactic studies of complete stellar populations (includes supernovae and pulsar studies to map galactic structure and dynamics); and
- cosmology and general relativity – including gamma-ray bursters as cosmological probes and pulsars as cosmic clocks.

As at 2002, there are outline specifications for each of the SKA science drivers. There is considerable overlap between some of these - unsurprising given the development of the SKA science case from the original “straw-man” SKA specification [5-1]. We now discuss briefly the capabilities and limitations of the Luneburg lens SKA concept with particular reference to the science driver specifications outlined in a series of memos from various Science Working Groups (SWGs) [5-2].

5.2 Proposed Features and Applicability to SKA Science

The Luneberg lens concept for the SKA is a solution capable of operating over a wide range of operating frequencies (<200 MHz to 5 GHz) with true wide-angle multibeaming capability. The large number of individual receptors and stations allows a highly-tailored solution of the array configuration (Section 6). We assume here the use of a scaled (or zoom) array, yielding an SKA with a large field of view and high sensitivity across a wide range of angular scales.

Early Universe science is an important driver for the SKA and recent results [5-3] make it clear that the epoch of re-ionization occurred at redshifts of six or more. The required frequency range for Early Universe science (SWG3 - The Early Universe and Large Scale Structure) is now between 100 and 220 MHz: a lower band than originally envisaged for the SKA. While this band is within the operating range of LOFAR, LOFAR sensitivity is 100 times worse than SKA at these frequencies and so will have limited capability to pursue this demanding science. The SKA, with its much higher effective collecting area, should therefore be the telescope to undertake most of these studies. Fortunately, the Luneburg lens concept can be extended to operate well at 100 MHz.

Our proposal is well-matched to the HI survey science drivers, both for very deep surveys in redshift space and the shallow, wide-angle, surveys outlined by SWG4 (Galaxy Formation). The resolution and sensitivity requirements for the HI and continuum surveys are both well accommodated (Table 4-1), with wide fields-of-view allowing each concentrator beam access to large areas of sky. The SKA will be able to detect galaxies to high redshifts, free of the effects of obscuration. The SKA science goals in this theme effectively extend the current redshift surveys (2dFGRS, SLOAN) by large factors, which are unmatchable by optical telescopes. Given a combination of (i) a wide-angle, shallow, HI survey to determine directly the evolution of large-scale structure from z~1.3 to the present and (ii) a deep pencil beam HI survey detecting galaxies and HI concentrations to $z > 4$, the HI mass function across a wide range of gas masses and cosmic epochs can be determined. Furthermore, because the HI mass function is an unbiased estimator of galaxy and proto-galaxy mass (unlike IR or optical luminosity), it can be used to constrain both star formation history and interaction/merger rates in galaxies throughout cosmic time. Both of these key surveys require high sensitivities, with ~50 mas angular resolution, over a wide frequency range (preferably extending down to 100 MHz).

The Luneburg lens concept cannot match the specification from the HI working group to observe CO at high frequencies, ideally beyond 20 GHz. We note though that the measurement of star-formation rates in ultraluminous IR galaxies at high redshift is expected to be addressed by the upgraded VLA (eVLA) and ultimately by ALMA.

The specifications from SWG5 (Active Galactic Nuclei and Supermassive Black Holes) are covered by our concept, at least to 5 GHz. A primary requirement is for a sensitive instrument with > 1000 km baselines and a self-similar (zoom) configuration. However, some aspects of AGN science require much higher observing frequencies (> 30 GHz); these applications include the investigation of the origin (base) of radio jets. Again though, the high-frequency, VLBI-like, requirements for these particular science goals will be realized by other telescopes, including the eVLA. The compact centre of the Luneburg array matches well the science specification for probing the non-thermal intergalactic medium (SWG8, The Intergalactic Medium). These objects include halo and relic sources which can be extremely diffuse and which exhibit structure on a wide range of angular scales, from milli-arcseconds to tens of arcminutes.

The multibeaming capabilities of our concept are particularly suited to the requirements for transient source science (SWG2, Transient Phenomena) where dedicated beams are suggested for particular experiments. However the Luneburg lens upper frequency limit of 5 GHz does not meet the required upper frequency (15 GHz)

necessary to avoid interstellar scattering of pulsar signals close to the galactic center and, with a 3000 km transcontinental baseline, yields only 5 mas (rather than the desired 1 mas) astrometric resolution. Importantly though, the ability to observe targets and calibrators simultaneously is a powerful one in astrometry and needs to be weighed against the reduced raw resolution. Still, the 5 GHz limit suggests to us that the eVLA and VLBI will remain more suitable for particular aspects of transient science. The Luneburg lens concept does offer large-area monitoring and surveying of the sky using a dedicated (or near-dedicated) beam, as well as near-instantaneous follow-up of transients if another beam can be allocated (Section 12.2). The high sensitivity of the central array will undoubtedly provide a high efficiency survey-like mode, vital for the discovery of many more pulsars.

The specifications from SWG6 (the Lifecycle of Stars) discuss very high-frequency observations, with 22 GHz capability being important. It is not obvious what, if any, aspects of this science the Luneburg lens concept would be able to address, given its projected high-frequency limit of 5 GHz. However, the science goals outlined by SWG1 (Milky Way and Local Neighbourhood Galaxies) are attainable with the proposed telescope, with the exception of those requiring observations up to 10 GHz. However, a large proportion of this science is centred on local HI (1.4 GHz) and OH (1.6 GHz) observations. We note though that H_2O maser observations at 22 GHz are excluded in our concept.

There are no recent SWG specifications for SETI or solar system science; we note here that the multibeaming concept is particularly compatible with targeted SETI applications. We also note that the frequency coverage of our concept does not include the bands required by the Deep Space Network for spacecraft tracking (SWG9); this is unfortunate since multiple beams could provide simultaneous support for missions requiring multiple probe tracking (e.g. Mars orbiters or L2 satellite clusters).

The Luneburg lens concept provides for independent beams, allowing significant sensitivity and speed advantages [5-5]. In concluding this Section we list briefly (below), from a science perspective, three major benefits of multibeaming.

- Response. A number of independent beams allows immediate response to many time-critical events (e.g., GRBs and new transient sources). This response can take place with other time-critical activities (e.g., pulsar timing) continuing uninterrupted.

- Scheduling. A number of science priority areas require multiple targets to be observed simultaneously (contrasting with the simultaneous multiple programs described above). This science includes, for example, monitoring a pair of pulsars, timed not against terrestrial clocks but against each other; quasar intra-day variables; and quasar lensing variability.

- Efficiency/efficacy. Having a number of independent beams re-uses the collecting area – each of n beams is worth $\sqrt{n}$ in collecting area. This capability makes the SKA a true community facility, akin to CERN, with many simultaneous users and separate science projects. In this respect the SKA will be unique amongst telescopes, perhaps expending large amounts of time on individual projects whilst dedicating other beams to shorter, targeted,

observations. Multibeaming also affords excellent calibration potential, perhaps with targets and calibrators observed simultaneously – an invaluable capability given the > 10^6 imaging dynamic range requirement of the SKA. Many of the advantages of multibeaming are realized only if widely-spaced, as opposed to cluster, beams are available.

6. ARRAY CONFIGURATION AND STATION LAYOUT

6.1 Configuration

Array configuration is basic to the SKA design with the designer needing to specify the number of stations, the layout at various scales, and the geographic and cost constraints. All SKA proposals to date have one thing in common: the antenna stations are fixed. This is contrary to the design of the existing large radio arrays with good frequency and resolution coverage. This means that, to be competitive in terms of instantaneous and half-day uv coverage, the SKA will need many more stations than current telescopes. For example, it will certainly need to cover at least the VLA A, B, C and D configurations with better uv coverage, implying at least 100 stations in the baseline range 300 m to 30 km.

To this basic requirement of covering the range of resolutions in common use now, we add both the user requirements for high brightness sensitivity on arcmin scales and high angular resolution (0.1 arcsec at 1.4 GHz). This means we need antenna and/or station separations which provide baselines which are both shorter and longer than the range mentioned: the revised spread is then from <100 m to 300 km. Finally, adding the requirement for VLBI capability extends the maximum baseline to beyond 1000 km. These requirements, taken together, indicate to us that at least N = 200 stations will be needed. From an economic and infrastructure perspective, there is value in keeping N as small as possible, consistent with acceptable imaging performance. Based on initial simulations, we have adopted N = 300 as a compromise but we note that SKA simulation tools are sorely needed to advance this important area of array design.

Some criteria on which to judge configurations are:

- good match to user requirements for sensitivity and resolution at various scales;
- good instantaneous uv coverage on baselines out to at least 300 km;
- good uv coverage with some time integration on VLBI scales; and
- synthesized beam pattern with low sidelobe levels.

A survey [6-1] of science preferences for array characteristics gave the following results:

- 40 % of the baselines in as compact a form as possible;
- 40 % of the baselines in configurations out to 300 km (0.1 arcsec at 1.4 GHz); and
- 20 % of the baselines in a VLBI array.

While there is no single optimum solution, and while the differences between sensible layouts decrease for large N, a series of simulations [6-2] does illustrate the limitations and strengths of various approaches. For example, uniform or Gaussian random arrays can produce good uv coverage on a 300 km scale, but not on other scales. In particular, they are unable to satisfy the short baseline requirements. We note the usefulness of the logarithmic spiral but identify the need to add a central close-packed array, boosting the baseline fraction to more than 40 % within 10 km radius.

Centrally condensed configurations, like the logarithmic spiral (and the VLA), have the disadvantage that the naturally-weighted synthesized beam has broad shoulders and a half-power beamwidth several times greater than that from a uniformly-weighted array. To obtain the required resolution of 0.1 arcsec at 1.4 GHz, the weights given to short spacing data need to be substantially reduced, resulting in a typical sensitivity degradation factors of 1.5 - 2. There is no way around this loss: an array designed with a large range of baselines and including a central core (for high brightness sensitivity) will be only about 50% efficient for an experiment at one particular scale.

The sensitivity loss may be alleviated by using robust weighting schemes and/or more sophisticated deconvolution algorithms. For example, the use of super-resolution should be possible since the naturally weighted beam already has a narrow central spike; a Gaussian fit to the beam above 85% power will yield close to the resolution obtained with uniform weighting. Having good uv coverage gives much greater flexibility in creating a low sidelobe point spread function by appropriate weighting schemes. Most logarithmic spirals will give good uv coverage with sufficient time integration, so the challenge is to design spirals with good snapshot coverage. Spirals that cover the plane uniformly with roughly equilateral triangles are best in this regard.

While site details and communications infrastructure are discussed more in Section 14, the spiral layout is known to provide economical connectivity, at least for an SKA built around a new communications network. We also note that, due to the strong central concentration of the SKA, asymmetric arrays perform as well as symmetric arrays, but use only about half the number of antennas [6-3]. They also allow for longer baselines (e.g., across a continent) if most of the array area is placed near a seaboard rather than centrally. With these points in mind, and noting that the requirement to place the central 40% of the array area as densely as possible forces a departure from a strict spiral form on the most compact scale, we offer the configuration shown in Fig. 6-1 as a representative one for the SKA.

This configuration, based on a seven-arm spiral, is arranged such that artifacts are minimized and good instantaneous imaging is achieved on baselines extending to 1000 km. Figure 6-2 shows the area and baseline distribution, and the resulting uv coverage. While we emphasize the representative nature of the suggested configuration, we note the following additional advantages:

- logarithmic (scale-free) uv coverage on baselines > 3 km, allowing imaging at different frequencies with very similar uv coverage and resolution, and not imposing instrumental constraints on the size of astronomical objects that can be imaged well;

- good snapshot coverage;
- non-identical spiral arms, i.e. the uv coverage fills in for longer integrations;
- dense uv coverage in about 2 hours;
- compact core for high brightness sensitivity;
- robust against failure of up to 10% of antennas; and
- freedom in positioning of stations (10% of radial distance).

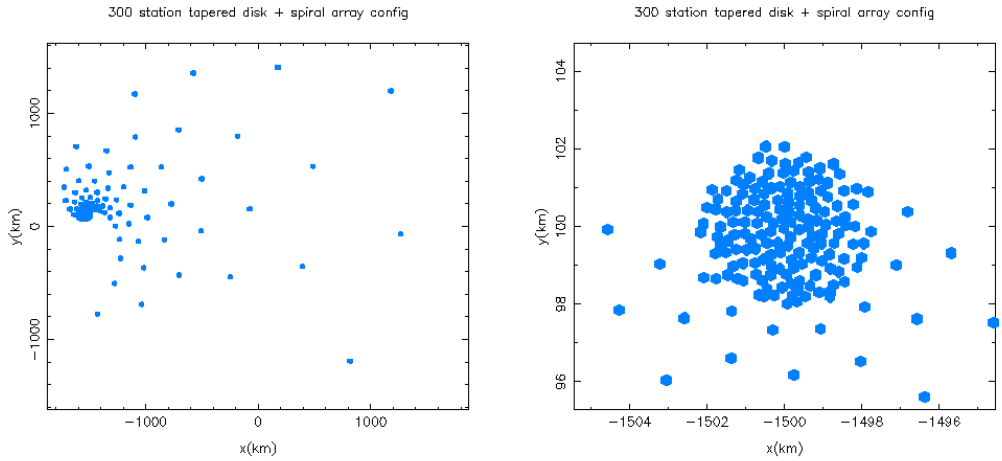

(a) (b)

Fig. 6-1. Seven-armed, 300-station, spiral configuration for the SKA. In (a) the whole array is shown out to VLBI scales. A zoomed view of the central 10 km section is shown in (b); the spiral pattern makes more than a complete turn on intermediate scales. In this and Fig. 6-2 the central array packing is for a 30° elevation limit (Section 6.2).

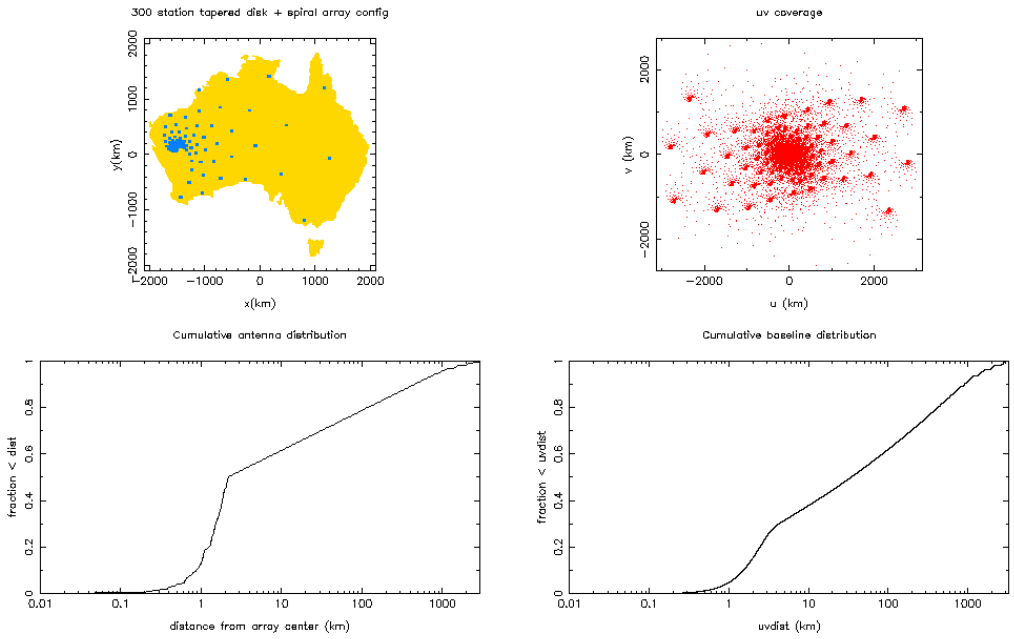

Fig. 6-2. Characteristics of a seven-armed, 300-station, spiral with dis-similar arms. The central array is shown located at the Mileura site (Section 14).

6.2 Station Layout

The layout of SKA stations composed of smaller elements has not been studied in detail so far. Two basic design parameters are the:

- layout form - close packed grid (rectangular or hexagonal) versus randomized arrangements; and
- minimum elevation coverage for no shadowing of antennas.

Compact stations are favoured because they have lower beamforming and connection costs. Regular station layouts produce station beams with very large secondary responses (up to 99% of the central peak) which may introduce spurious signals in station-to-station correlations; these artifacts could be hard to remove without imaging the entire field-of view of a single element. We therefore favour randomized layouts which, although slightly less compact, can produce well-shaped station beams with low (1-2%) sidelobes. Making the layout truly random, as opposed to "dithering" a regular configuration, is preferred, since dithered responses still tend to show rather large sidelobes. Our currently preferred station is a random, close-packed, arrangement with a minimum spacing constraint that avoids excessive shadowing. Making the minimum spacing constraint slightly "fuzzy" avoids ringing in the beam pattern (due to a sharp inner cutoff). We note that with area filling factors ~0.1, mosaicing observations are likely to be a staple SKA mode, if only to recover missing spacing information.

In a station composed of 176 elements of 7 m diameter, the corresponding station diameters are 500 m and 250 m for elevation limits of 15° and 30°, respectively. With this composition, each station is equivalent in collecting area to a 93 m diameter dish.

Fig. 6-3 is a visualization of an array station giving slightly better than 30° unshadowed elevation coverage.

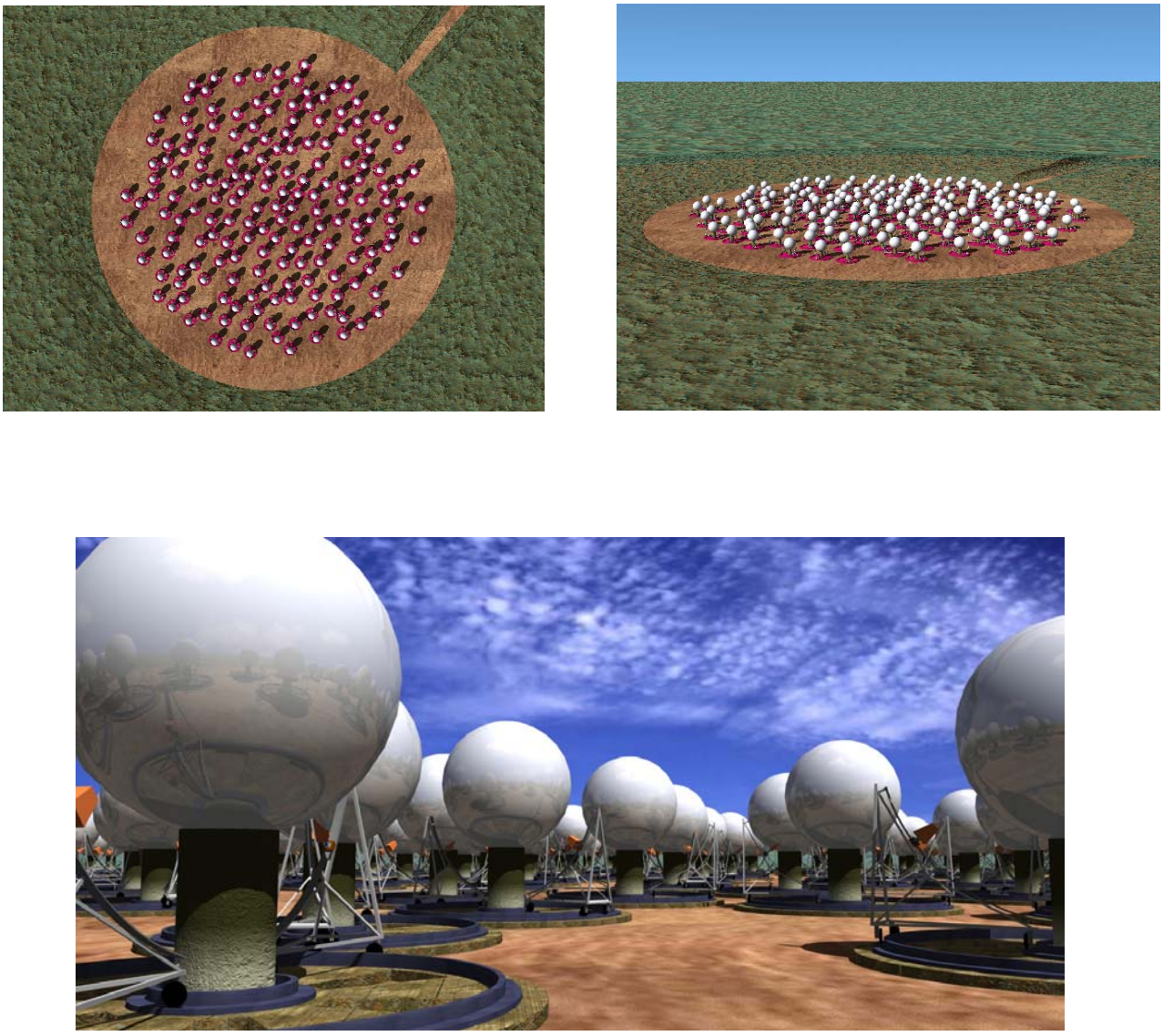

Fig. 6-3. Views of an array station (about 250 m across) composed of 176 seven-metre diameter Luneburg lens antennas.

7. THE LUNEBURG LENS CONCENTRATOR

7.1 Introduction

From the outset there has been a desire for the SKA to provide distinctive capabilities (aside from increased sensitivity) not available with other radio telescopes. One of the more exciting possibilities is that of having a multibeam instrument with independent beams placeable anywhere on the sky. Multibeaming capability was, in fact, a major consideration in the early NFRA proposal for a phased array SKA antenna element [7-1]. While there have been several subsequent suggestions for the antenna element, the only other option to-date which provides independent, widely-separated, multiple beam, capability is the Luneburg lens (Fig. 7-1). Other proposals have, in principle, more limited multibeaming capability, ranging from the cylindrical reflector proposals [7-2, 7-3] where multibeaming is possible within a fan beam, down to cluster-beaming within the main beam of a conventional reflector antenna [7-4 to 7-6].

Two major considerations driving all SKA antenna design have been economics and extendability. Like other designs of interest, the Luneburg lens has the potential to be manufactured cheaply. In addition, its "one feed per beam" characteristic gives it a distinct advantage over other proposals in that it is possible to add, incrementally, widely-separated beams. Beams can be generated using different feed types (e.g. general-purpose, cluster, high efficiency), all available on the telescope simultaneously. Although mechanical movement is necessary in the concept presented here, the movement is confined to skeleton feed carriers and light-weight feeds; this gives great economy relative to the cost of pointing accurately large concentrators.

Attributes of the Luneburg lens in the SKA application have been described previously by Russian and Australian (CSIRO) authors [7-7, 7-8]. The CSIRO proposal has, from the outset, rested on the successful development of artificial dielectrics where weight, loss and cost are reduced significantly relative to presently-available materials. In this Section we give a summary of our current thinking (more details are provided in Appendix B) in four practical areas of Luneburg lens design and we describe an exemplar SKA element.

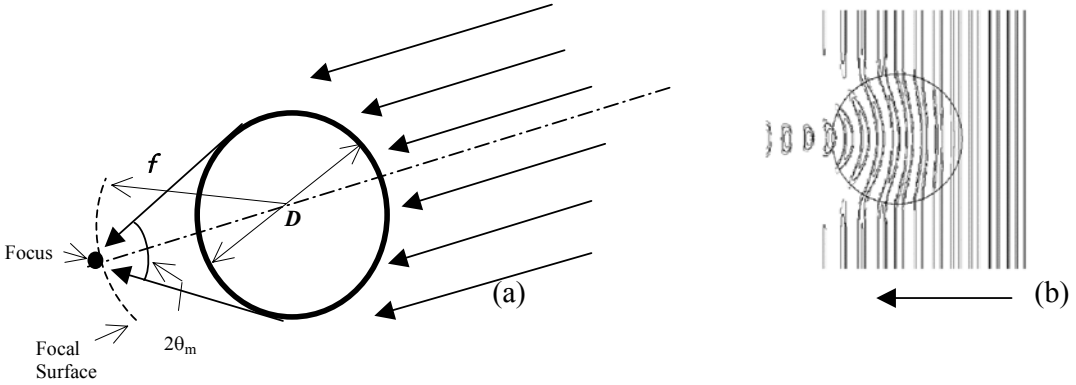

Fig. 7-1. In (a) the geometry of the Luneburg lens is shown, while (b) is a superposition of electric field snapshots showing the focussing action on a wavefront travelling from right to left.

7.2 Lens Material

A Luneburg lens requires dielectric material ranging in relative permittivity from a maximum in the centre, the value depending on the value of *f/D* as shown in Fig. 7-2, to unity on the outer surface. Since the lens is volumetric in nature, a low-loss material is required to minimize the receiver noise loading.

To construct the SKA lenses out of conventional dielectric materials is not a viable proposition given weight, loss and cost considerations. CSIRO is attempting to develop suitable artificial dielectric materials for constructing lenses and, despite patents pending on some of the processes involved, a brief overview of the work can be given. In outline, low-density (20 kg m^{-3}) foam (loss tangent < 10^{-4}) is being doped with small amounts of high dielectric index ceramic such as rutile (TiO_2), to produce artificial, low-loss (loss tangent ~ 10^{-4}), dielectrics. Initial results have confirmed that simple static mixing formulas are applicable at the microwave frequencies of interest to the SKA and we expect to translate readily laboratory fabrication methods to a manufacturing environment.

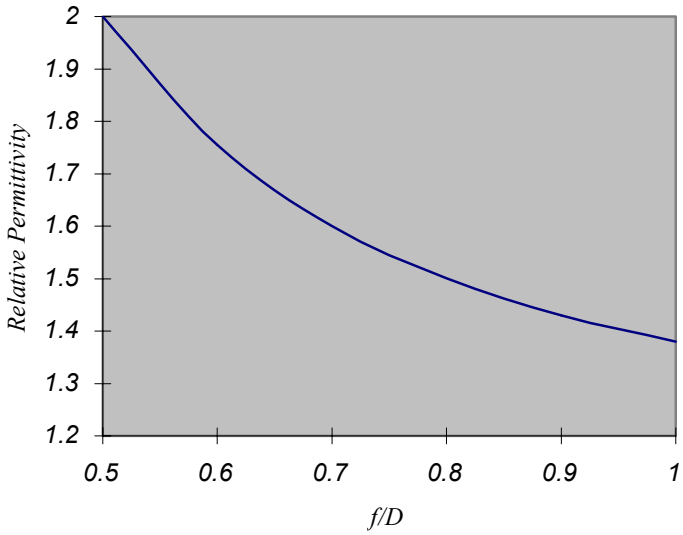

Fig. 7-2. Maximum permittivity as a function of f/D.

7.3 Lens Construction and Architecture

Assuming that a practical artificial dielectric will be manufactured, we can make some estimate as to the loss, weight and the cost of constructing the lenses. The choice of parameters for the lens is basically very simple: *f/D* and *D*. It became clear from an earlier parametric study (Appendix B) that the limits on lens diameter, *D*, were such that for $D < 5$ m the number of lenses required by the SKA, and hence the cost of signal channels, became excessive. Furthermore, operation at low frequencies is not effective when the lenses become much smaller than a few wavelengths in diameter; a 7 m lens is certainly suitable above 200 MHz (being more than 5λ in diameter) and our investigations show reasonable beamshapes as low as 100 MHz, even with simple dipole feeds (Appendix E). For larger lenses, where $D > 7$ m, the quantity and weight of the materials required to construct the lenses start to become a problem. Also, the

larger lenses limit the upper frequency of operation given the non-negligible absorbtion in the lens. Weight and cost were also shown to be related to the *f/D* ratio, in that small values of *f/D* require a larger range of permittivity (Fig. 7-2), leading to greater cost and weight. In addition, the choice of *f/D* is a crucial parameter in the feed design (discussed below). We find that $f/D \sim 0.7$- 0.8 (where the maximum permittivity in the centre of the lens is 1.5 to 1.6), and $D \sim 5$ - 7 m, are sensible design starting points.

An alternative to the full spherical Luneburg lens is the hemispherical 'virtual source' Luneburg lens [7-8]. Here the half lens is placed on a perfectly conducting ground plane and the resultant mirror image provides a complete lens for operation in the upper half-space. The main advantages of this arrangement are that only half the material is required and that the lens is fully supported by the ground plane. However, the disadvantages are that an adequately large, accurate, ground plane must be provided - not a trivial or cheap task - and the feeds will, in many observations, block the signal path. These disadvantages lead us to favour the full spherical Luneburg lens over the 'virtual source' configuration, although a more detailed design study should be undertaken before large-scale use is made of the Luneburg antenna.

Another practical advantage of the full Luneburg lens solution is that, with a little thought, it can involve minimal earth works, particularly important if the antennas are located in remote sites. As the lenses are static they need only be placed high enough above the ground to allow for feed movement (Appendix B).

7.4 Feed Systems

A variety of feed types can be used to simultaneously illuminate a Luneburg lens, and we first consider the variation of maximum feed illumination half-angle, θ_m, with *f/D* (Fig. 7-3). With our preferred values of *f/D*, we find $\theta_m \sim 42^\circ$. To a first approximation, if we set the half power beamwidth (HPBW) equal to θ_m, the feed radiation pattern level at θ_m will be about 12-15 dB below the on-axis value, giving a good compromise between antenna efficiency and sidelobe levels.

Given the two engineering drivers of low cost and wide bandwidth, frequency-independent antennas are an obvious place to start in the feed design. From a survey of possible suitable feed designs, and having in mind the need for HPBW ~ 42º, the pyramidal zigzag antenna described in [7-9] seems to be a good initial choice. It provides dual linear polarization, is very simple in construction, is compact in size for its beamwidth and is essentially self-scaling in frequency, with a main beam which is highly symmetrical. This type of feed is currently favoured in the design of the Allen Telescope Array [7-5]. The main disadvantage, which applies to all end-fire antenna types, is that the phase centre moves along the antenna with frequency. Thus, radial movement of the feed is necessary to retain optimum performance.

While the zig-zag feed is attractive, it becomes bulky at frequencies below 300 MHz (Appendix B). Much simpler feeds, such as a single or crossed dipoles placed $\lambda/4$ above a ground plane, can be used if science imperatives demand low-frequency coverage. The physical distance between the antenna and plane could be reduced substantially by mounting the dipoles on a sheet of artificial magneto-dielectric material. Depending on the bandwidth required, the dipoles can be physically short and tuned accordingly. Such simple feeds have a broad beamwidth and need to be

placed closer to the lens surface but, at these wavelengths, de-focussing is not an issue.

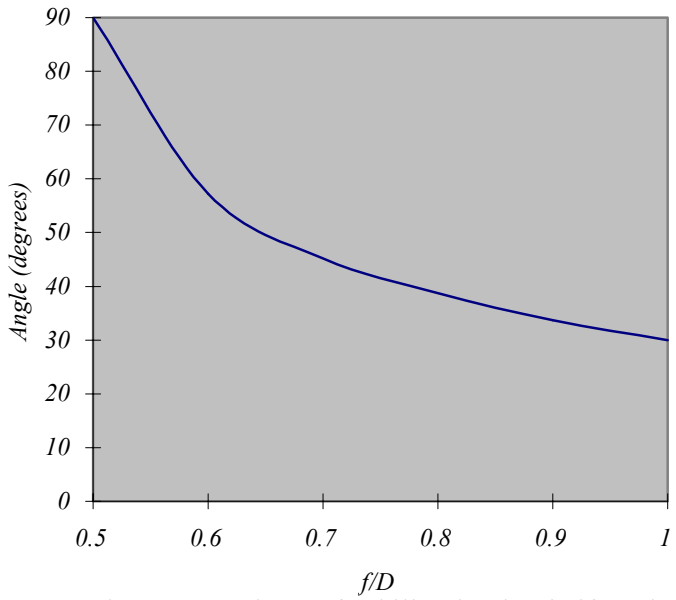

Fig. 7-3. Maximum feed illumination half-angle.

7.5 A Possible Antenna Design

Fig. 7-4 is a general view of a basic alt-az SKA antenna design. The Luneburg lens is supported atop a pillar, the pillar being surrounded by an azimuth slewing assembly. Frame structures (feed arms) both support and translate arcs, which themselves guide feed movement in altitude. A given antenna can have a number of feed arms and each feed arc can support multiple feeds; there is no requirement for feeds to be of the same type. Table 7-1 summarizes some of the more important design projections for the antenna. Finite element modelling of the lens has been undertaken (Appendix C) to ensure that required deformation and deflection limits for the concentrator itself are not exceeded.

Advanced foam structures are a possibility for some of the external antenna components, but more conventional materials and fabrication techniques are also envisaged in the antenna construction. In particular, finite element analysis and costings of the feed support and translation arrangements have assumed steel members and pre-fabricated assemblies, all manufactured using production line welding techniques. However, foam support techniques for the lens and azimuth track (Appendix B) have also been adopted in initial cost models. A preliminary mechanical and structural design study by consulting engineers is expected by July 2002; this will provide more details of sub-assemblies not shown in Fig. 7-4.

Reliability is paramount and we anticipate that the variant of a simple wheel-on-track design will give repeatable performance in harsh conditions. Both the azimuth and elevation loads are low and, with modest positioning accuracy requirements, economical and robust motors and controllers can be used. We envisage an antenna-based computer providing servo, general control and monitoring functions (including the obvious anti-collision system for the various moving parts). A very limited set of

hardware safety features would be provided although, with tens of thousands of antennas, the cost and reliability implications of using such devices needs to be considered carefully. One encoder option being investigated involves bar-code scanning of printed surfaces, giving absolute positions.

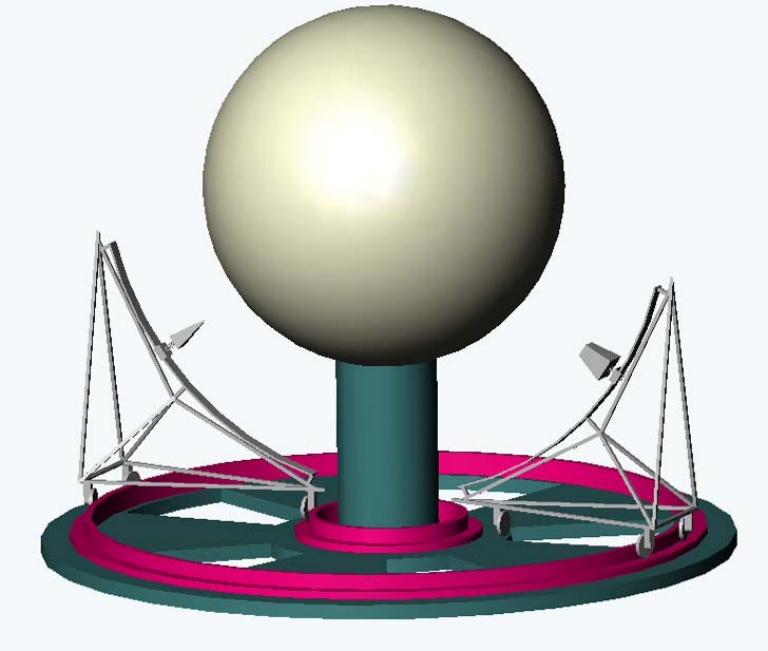

Fig. 7-4. General arrangement of a Luneburg lens antenna using two zig-zag (pyramidal) feeds, each mounted on a separate feed arm. The high-frequency feed is shown on the left. It is possible to add more feed arms, and/or more feeds – either single beam or cluster types.

Table 7-1. Typical Parameters of Luneburg Lens Antenna

Luneburg lens diameter	7 m
Lens mass	7000 kg
Feed mass	< 5 kg each
Mass of feed arm assembly	~ 400 kg each
Elevation coverage	15° to 80° (typical)
Maximum drive speed	40° per minute (both axes)
Pointing error	< 1.8 arcmin (beamwidth/20 at 5 GHz)
Maximum operating wind speed	35 km hr^{-1} (10 ms^{-1})
Survival wind speed	180 km hr^{-1} (50 ms^{-1})

8. RECEIVERS AND RF SYSTEMS

With hundreds of thousands of RF channels implicit in a phased array or small concentrator approach to the SKA, the cost and physical complexity of traditional radio astronomy receivers exclude them from consideration. It is certain, for example, that the SKA will require highly-integrated receiving systems based around MMICs. We show in this Section that it is feasible to construct the telescope using uncooled receivers, reducing initial costs and greatly simplifying maintenance. Should low-cost, high-reliability, cryocoolers become available, the Luneburg lens concept (with its flexibility in feed and RF options) is well-placed to use them, either to reduce the built area of the SKA or to provide a high-sensitivity upgrade path.

With the concentrator and feed selected (Section 7), consider the noise contributions prior to the receiver. Fig. 8-1 plots a representative noise budget for a 7 m Luneburg lens antenna. The Galactic contribution and lens dielectric loss dominate at low and high frequencies, respectively, and the system performs best near 1 GHz. In compiling this summary the Galactic foreground was taken as 30 K at 400 MHz and scaled with a spectral index of –2.9 to be representative of about 70% of the sky. The atmosphere contribution was calculated with Miriad's OPPLT task (assuming sea level location, 20% relative humidity, 1013 hPa pressure, and zenith observation). The lens loss was derived from Appendix B (equation B2), assuming $f/D = 0.7$ and loss tangent = 10^{-4}. Spillover was taken as 8% of total response, with equal contributions from the sky and ground. Feed loss was taken as 0.1 dB at f = 1.4 GHz and scaled as √f. An allowance for a switchable noise calibration signal of 2 K has been made.

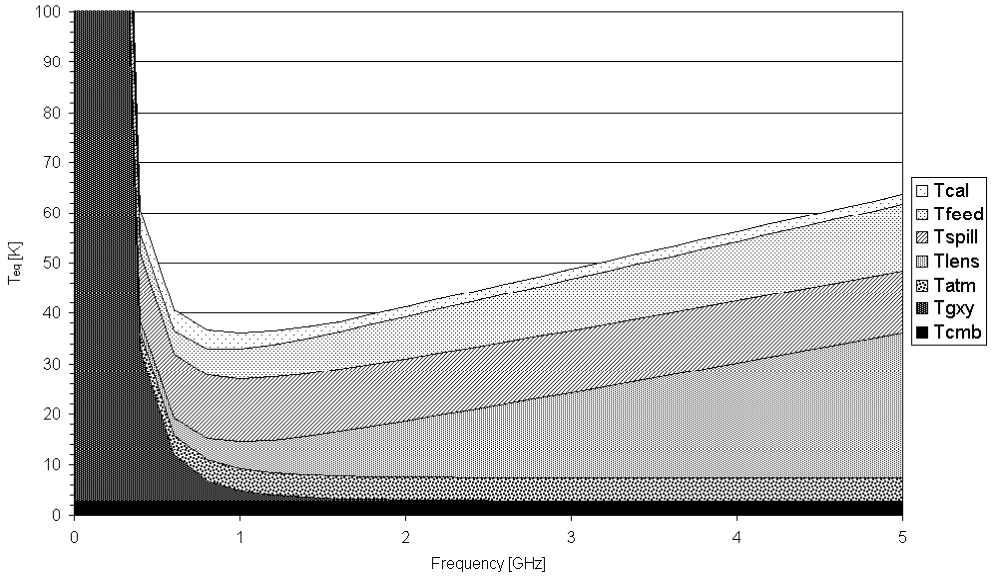

Fig. 8-1. Contributions to system temperature for a 7 m diameter Luneburg lens antenna, excluding the receiver. With the small lens losses involved, the noise components can be added directly with little error.

Cuts through this model at 1.4 GHz and 5 GHz are given in Table 8-1.

Table 8-1. External System Temperature Contributions

Noise Contributor	Value (K)		Comment
	1.4 GHz	5 GHz	
Cosmic microwave background	2.7	2.7	
Galactic foreground	0.8	0.0	True for ~70% of sky
Atmosphere	4.4	4.7	At zenith
Luneburg lens dielectric loss	7.8	28.7	Artificial, low-loss dielectric
Feed spillover	12.3	12.3	Half sky, half ground
Feed loss	7.0	13.2	0.1 dB at 1.4 GHz; √f scaling
Injected calibration signal	2.0	2.0	
TOTAL (T_{PRE-RX})	37.0	63.6	

Given this model, a specification for A_e/T_{sys}, and an assumed effective collecting area, the required receiver performance can be specified. Fig. 8-2 summarizes in graphical form the allowable receiver noise contribution for various values of array A_e/T_{sys}, assuming A_e is 1 x 10^6 m^2. Also shown are noise temperatures for a range of present and future receivers; for a given technology to exceed a chosen A_e/T_{sys} specification, its plot must fall below the appropriate contour line.

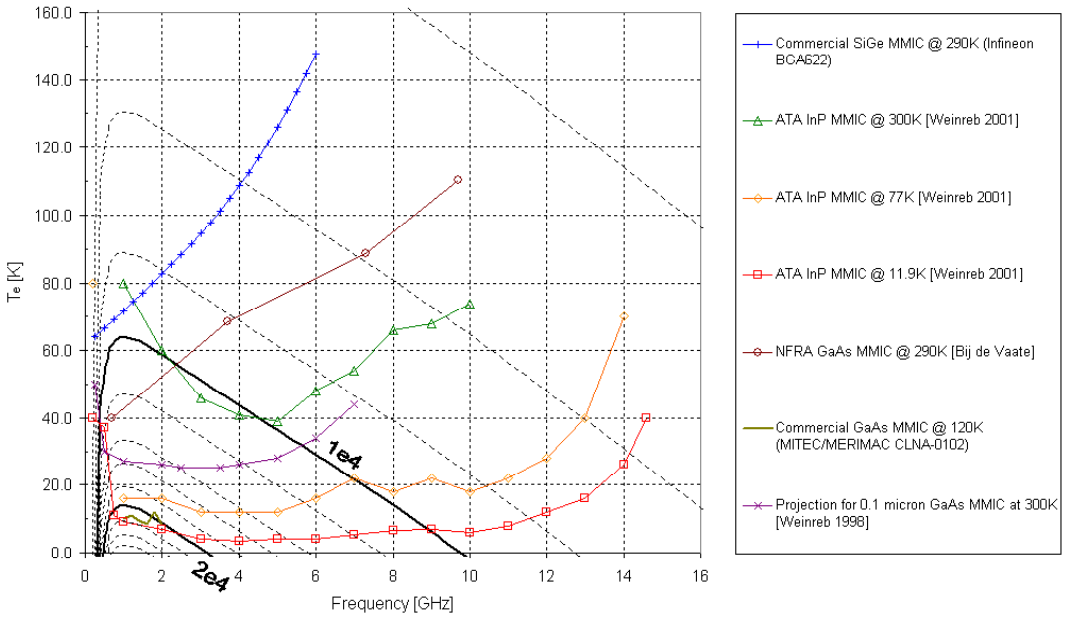

Fig. 8-2. Allowable receiver noise contributions (T_e) versus frequency for various values of SKA A_e/T_{sys} (assuming A_e = 1 x 10^6 m^2 and external noise contributions as shown in Fig. 8-1).

Bearing in mind the goal of uncooled receivers, we see that the projection for a 0.1μm gate length GaAs MMIC [8-1] yields an A_e/T_{sys} of order 1.6 x 10^4 m^2K^{-1} at 1.4 GHz. Thus, to meet the SKA goal of A_e/T_{sys} = 2.0 x 10^4 m^2K^{-1}, we need to build an effective collecting area of 2.0/1.6 times the reference, or 1.3 x 10^6 m^2.

Assuming this collecting area, we can now plot the array performance with frequency, as well as examine the sensitivity with other receiver options. Figure 8-3 shows the performance of this putative array equipped with a variety of receivers. The uncooled 0.1 μm gate length GaAs MMIC is our reference and, interestingly, we see that adding a second feed and computing the √2 area re-use (or speed) advantage yields a sensitivity very similar to that obtainable with an ATA-style cryogenic receiver [8-2]. Plotting the approximateVLA sensitivity (A_e/T_{sys} ~ 280) on the same scale underlines the two-orders-of-magnitude SKA advantage.

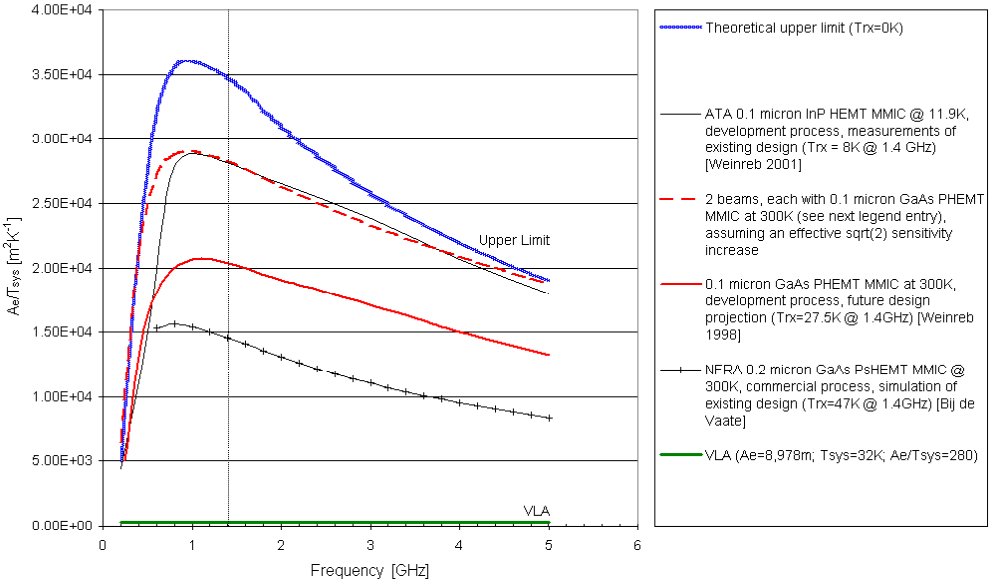

Figure 8-3. A_e/T_{sys} plots for a 7 m diameter Luneburg Lens SKA with an effective collecting area of 1.3×10^6 m^2 and illustrative receiver technologies.

9. SIGNAL ENCODING, BEAMFORMING AND TRANSPORT

9.1 Overview

In this Section we describe an all-digital SKA data encoding and transport solution – receiver outputs are quantized at the antenna and sent as binary data on high-speed optical fibre links. We believe that the signal path linearity requirements for the SKA make alternative analog transmission strategies difficult. Until the advent of coherent optical communications, optical links will continue to use envelope modulation and demodulation, limiting the dynamic range of low-cost components to < 30 dB. Furthermore, we are unconvinced that wideband analog transmission is an industry priority. By contrast, high-speed analog-digital conversion and highly-integrated digital fibre links are mainstream developments for consumer and telco applications.

Fig. 9-1 is an overview of the arrangement proposed for the Luneburg lens SKA. Separate RF bands in the range 0 – 2.5 GHz (low-band) and 0 – 5 GHz (high-band) are provided, principally to achieve optimum RF performance from different receiver technologies. Fig. 9-2 shows the data transmission scheme in more detail. The central array and intra-station transmission is done with short-haul digital links. For more distant stations, signal aggregation is done using station-level digital beamformers; the resultant smaller data bandwidth is then transmitted via a trunk, or long-haul, arrangement compatible with industry-standard arrangements. As well as being suitable for custom SKA installations, the long-haul proposal is well-placed to take advantage of access to small numbers of "dark fibres", possibly accessible via arrangements with telcos.

The main advantages of the all-digital system are the high dynamic range signal path, robustness to fibre and electro-optic component variations, and ease of diagnostics. The principal disadvantage is the need to carefully engineer the high-speed circuitry at the antenna in order to minimize self-generated RFI. However, in the receiver architecture outlined below, any residual RFI has minimal impact on system performance.

9.2 The Signal Path

The receivers used in our concept are "baseband" or "video" types in which the signal is amplified, band-limited, digitized, then transported on fibre to beamforming machinery. The absence of local oscillators, mixers, analog filters and LO distribution schemes represents a saving in cost, complexity and maintenance. This architecture also removes the sources of many systematic spurious responses, including mixer images. Parasitic spurii from causes such as the imperfect linearity of analog circuits, and subtleties such as in-channel noise from out-of-band interferers interacting with LO noise, are also avoided. High resolution (8-bit) quantizing and accurate digital signal processing stages provide a near-ideal, high dynamic range, signal path. A more detailed overview, including aspects of data framing etc., will be given in [9-1].

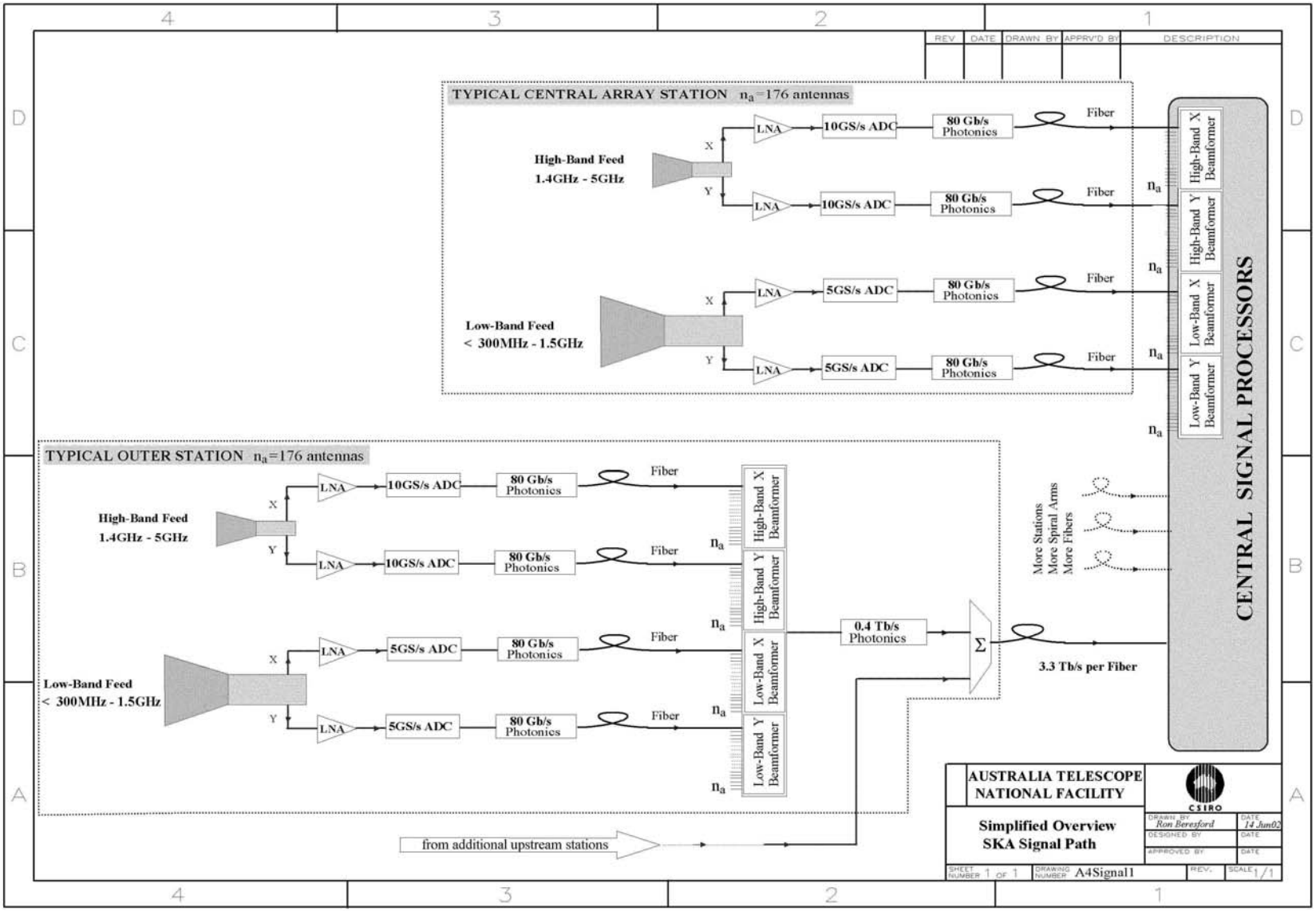

Fig. 9-1. Simplified SKA Signal Path.

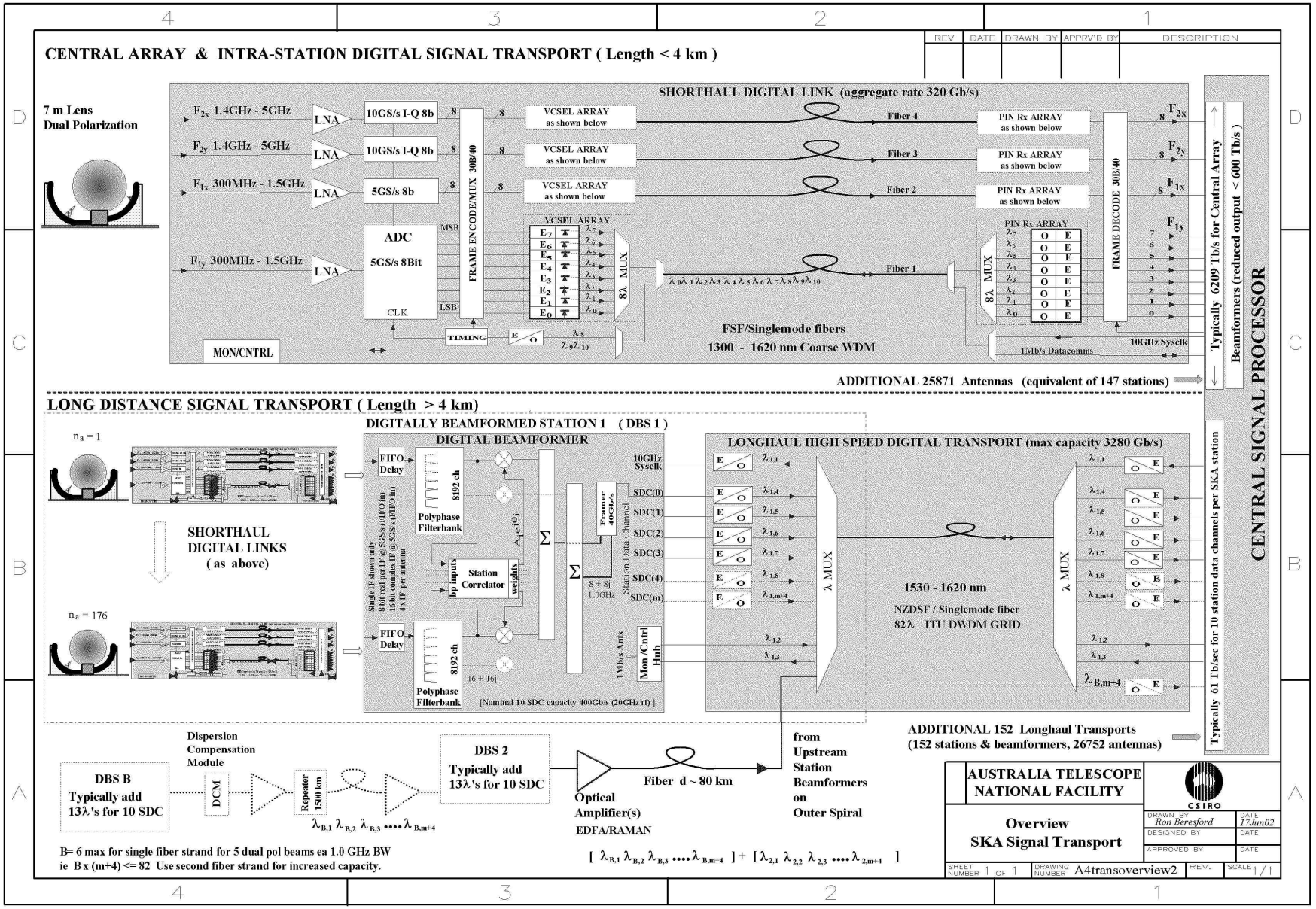

Fig. 9-2. SKA data transport scheme shown in more detail.

An important part of our thinking involves the use of digital filterbanks at stations physically separating, in effect, the frequency splitting and correlation functions inherent in an F/X correlation scheme. The channelization confers many advantages including:

- the ability to localize RFI sources in frequency and to reject channels with intractable interference;
- the ability to pre-select the bandwidth to be processed by the beamformer and transmitted by the digital fibre optic links; and
- flexibility in allocating station beamforming resources across (possibly) non-contiguous channels and multiple receivers, giving the option of a large number of simultaneous frequency bands.

We envisage perhaps 8192 and 4096 channels for high and low-band, respectively, giving $\Delta f = 0.61$ MHz channels in both cases. There is spectrum overlap between the receivers, with the common high-band and low-band channels having identical shapes and centre frequencies; this gives seamless continuity across the available RF spectrum.

Station beamforming is done in the interesting regime in which d_s/c (the light travel time across the station) ~ $1/\Delta f$, where the station diameter, d_s, is about 250 m. Thus, delay, phase and coherence effects are all important. A suitable beamforming scheme involves sample (or multiple sample) delay tracking prior to the filterbank, and phase rotation of the channelized outputs. The channel phasors may incorporate phase and amplitude twiddles for spatial nulling, as well as the usual fine delay compensation. Since the station beams are constrained by the concentrator field-of-view, multiple beams may be formed by applying different sets of phasors to the same filterbank outputs, avoiding the need for one filterbank per station beam and allowing a significant cost saving.

While the filterbank processes the entire 5 GHz feed bandwidth, the beamformers need only supply the ~ 1.5 GHz maximum bandwidth required by the SKA specification for a telescope with a 5 GHz upper frequency limit (Appendix A). The chosen architecture supports a linear increase in beamforming and signal transmission capabilities as time drives down the costs of the relevant technologies.

It is worth noting that the all-digital approach relies on at least two key technology developments being realized by 2010-2015 (see also Section 13). First, it is assumed that high resolution (8-bit) A/D converters sampling at 10 Gs s^{-1} will be available. (Though even 6-bit devices yield better dynamic range than analog fibre links). A second key component is the multi-wavelength VCSEL (integrated-circuit laser) array with integrated wavelength division multiplexing. There is intense commercial pressure for these devices but an alternative might involve 40 Gs s^{-1} serial links; these systems are also being pushed strongly by the telecommunications industry.

9.3 Station Calibration

Accurate beamforming to provide stable station beams, possibly with interference nulling, probably requires cross-correlation of all antennas within a station. However, a full correlator may not be required; it is already common practice in geodetic VLBI experiments to model entire signal bands using a small number of channels placed

across the observed spectrum. A set of interference-free filterbank channels may be all that is required in the SKA application. Of course, extra channels containing candidates for interference nulling could also be correlated. While the process of (adaptive) beamforming is likely to operate on the entire station and to be invoked at the station, the small total calibration bandwidth suggests that spectral samples from all antennas could be transmitted to a central signal processor (e.g. correlator) at little expense; this would allow an array-wide calibration strategy, such as that proposed for LOFAR [9-2]. As a first estimate, we assume a station correlator with 32 calibration channels plus an additional eight channels devoted to RFI processing.

9.4 Comments on Beamforming

With our proposal implementing configurable, digital, beamforming at the station level, the number of expensive trunk signal channels is reduced. However, all beamforming forces the SKA user(s) to select which parts of the wide concentrator field(s)-of-view are accessed. Digital beamforming from configurable sub-arrays gives the signal processing flexibility to support arbitrary (including random) antenna placement. This, together with the inherent accuracy and stability of the digital processing, leads to cleaner and more easily calibrated station beams.

In the imaging context our proposal, like all pre-correlation signal aggregation schemes, is inferior to the theoretical ideal of correlating tens-of-thousands of antennas in a (very) large-N array. To match the full correlation result, where information over the entire concentrator field-of-view is available, a beamforming approach would need to form and transmit every possible station beam, giving no saving in information transmission or processing costs. In practical beamforming models, sub-arrays are used to reduce the information from the station by more than an order of magnitude, saving on long-haul transmission and central signal processor cost.

In practice, sub-arrays will be of order of the station diameter in size, leading to 1.4 GHz station beams of order 0.06° in extent for a 250 m station. An individual station beam therefore images much less than 1 square degree. It is important though to relate the SKA goal of 1 square degree imaging field at 1.4 GHz to the HI science driver. When this is done, the design guide is actually to produce a large field-of-view instrument on central array scales. In our approach, the individual connections to antennas in the central array, together with a flexible central beamforming and correlation system, mean that the wide-field imaging can be achieved (Appendix F). Significantly though, flexibility limits at larger array scales are imposed by the station-level beamforming and finite bandwidth data links. However, the ability to re-allocate beamforming and transmission resources allows credible sky coverage; Table 9-1 is a summary of a few operational modes and illustrates some resource allocation possibilities with the links specified in Fig. 9-2. Of course, increased data bandwidth from stations would allow still more coverage and Appendix G describes some options. Note that the proposed correlator bandwidth of 3 GHz (full Stokes) is the relevant limit in some observing modes. Finally, from a construction perspective, it makes sense to install extra optical fibres during initial trenching, even if they remain unterminated until required.

Table 9-1. Examples of Station Data Channel Resource Allocation

Instantaneous Bandwidth (MHz)	**Number of Station Beams (Dual Polarization)**	**Total Sky Coverage at 1.4 GHz (Deg^2)**	**Comments**
5000	2	0.006	BW > specified maximum for 5 GHz SKA
1500	6	0.02	BW = specified maximum for 5 GHz SKA
500	20	0.06	BW = specified minimum for 5 GHz SKA
50	200	0.6	
5	2000	6	Sky coverage > lens beam area of 3.6 deg^2

10. SIGNAL PROCESSING

10.1 Introduction

SKA signal processing studies have tended to focus on correlator requirements and there are now a number of reviews outlining possible approaches in this area [10-1, 10-2]. The general conclusion is that F/X architecture leads to lower cost and better scaleability. With 2010 components, a 3 GHz (full Stokes) correlator with 2500 inputs (antennas, sub-arrays, or stations), 8192 channels and "lossless" (8-bit accuracy DSP) is certainly feasible, at least for capital costs of order $US50 million (Section 15). The refracting concentrator proposal is similar to other large or medium-N concepts in its signal processing demands and a number of alternative approaches could obviously be substituted. However, there are important issues yet to be incorporated into SKA discussions. These include:

- non-imaging back-ends (including tied-array and pulsar processors);
- baseband buffer arrangements (for capturing transient events); and
- interference mitigation (IM) requirements.

Australian experiments in the last area have led to the development of post-correlation IM [10-3] which, while not a panacea for the SKA interference problem, will be important in system design. We discuss below some factors relevant to IM in the SKA context.

10.2 The SKA Interference Environment

Perhaps the most significant lesson already learned from IM experiments is that no one strategy is likely to be effective against all interferers. Designers can strive to reduce the probability of "loss of service" (LOS) to an acceptably low level but must recognize that the cost and complexity of making the probability approach zero rises exponentially with performance. Robust IM involves a hierarchy of solutions, beginning with the need to locate the SKA in a radio-quiet area, minimizing the impact of strong terrestrial transmitters. The LOS concept underlines the need to include temporal statistics in RFI survey data so that the type and level of engineering investment in IM matches the LOS risks involved.

With a benign terrestrial RF environment and well-implemented strategies to minimize self-generated interference, the most pressing problem for the SKA will be RFI from satellites. Low-earth-orbiting (LEO) satellites will produce interference via the main SKA beam(s) or near sidelobes, but a more persistent challenge will come from signals in low-level sidelobes – including those from geostationary satellites or constellations. Natural interferometer filtering will provide a large measure of protection for the SKA, provided a linear signal path of sufficient dynamic range exists – hence the choice of linear architectures described in Section 9.2. Linearity also ensures that techniques such as post-correlation IM and spectral excision can function to their full potential.

10.3 Practical Interference Mitigation

Choice of a linear, channelized, signal path (such as that described in Section 9.2) constitutes avoidance of the RFI problem in that the baseband receiver avoids the systematic and parasitic problems of mixers while the filterbank localizes interference in frequency, allowing rejection of affected channels if the problem cannot be dealt with by downstream signal processors. The degree to which uncontaminated spectrum between interferers can be used depends on the channel bandwidth relative to the interference spectral separation; the importance of determining this design parameter from site survey information has been demonstrated by LOFAR investigators.

While post-correlation algorithms of the type described in [10-3] hold great promise in terms of retaining astronomy information in affected channels, strong or recalcitrant interferers may need to be dealt with via spatial nulling in the beamformers. This will be most effective for interference entering via far sidelobes, as relatively small perturbations of the combining function can steer the nulls with minimal distortion of the main beam. Nulling of close-in sources will require a more sophisticated calibration process which accounts for a (probably) time-variable main beam. In all cases it will be desirable to cross-correlate signals from all station antennas in order to drive the beamformer, at least at the frequency of the interference. As mentioned in Section 9.3, such an architecture is inevitable to optimize normal beamforming. However, high performance beam nulling is likely to impose higher response speed requirements on the signal processing, and greater complexity in the beamformer, than would otherwise be required.

While the architecture described in this proposal is inherently resistant to LOS through interference, it is compatible with existing IM techniques and allows for their progressive implementation during development of the SKA - or subsequently, should a worsening RFI environment so dictate.

11. SOME SKA DATA MANAGEMENT ISSUES

SKA data management arrangements will depend on a number of factors, including:

- the type of (hardware) data processors available (for example, imaging correlator(s), pulsar timers, etc.);
- the hierarchal structure of the element connections, and the possibility of progressive extension of (for example) the correlator to process data from smaller sub-arrays (and more baselines);
- the possibility of switching from hardware to software processing in any part of the data stream;
- the operational modes of the telescope (is completely automatic hands-off operation in all modes a realistic or desirable goal?); and
- the most common mode of operation (for example, summary observations of selected fields, large surveys in any mode, or measurement of the electric field to be interpreted with high precision at a later stage).

Regardless of the form of the SKA, the limitations of the correlator impose the need to include non-imaging modes if the telescope is to be used efficiently. Even with these scientifically desirable modes and their associated backends, it will be necessary to manage carefully integration times across a variety of (possibly simultaneous) imaging observations, simply in order to control data volume – the biggest single determinant of the scale of operations such as archiving.

Considering the extraction of science from the instrument, we envisage that the processing of SKA data for end users may be done in a number of modes, including:

- standard processing (used in making, for example, continuum images of a given field) handled by the SKA data processing center using an automatic pipeline mode and, most likely, grid computing;
- remote and quasi-interactive programming of the pipeline by specialists for users interested in obtaining the highest possible sensitivity, dynamic range, or other performance parameters;
- virtual pipeline processing, where the pipeline is a grid computer which is data driven and, most likely, has its centre nearer the astronomer than the SKA;
- pipeline processing from an archive which is part of a Virtual Observatory [11-1]; and
- hands-on system tests and calibrations by specialists.

12. SKA OPERATIONS

12.1 Introduction

Although the SKA will not be fully functional for at least 15 years, even superficial thought makes it clear that the design and operations are linked closely. For example, operational activities include:

- collection of astronomical data;
- calibration;
- array diagnosis and repair; and
- facility upgrades.

The processes involved in each of these activities depends strongly on the form of the instrument and its systems. At this early stage in the SKA design the most illuminating approach may be to consider what is feasible operationally, then assess the design implications. Such an analysis is beyond the scope of this report but we note below a few specific points requiring consideration. In general terms, we expect the annual operating costs of the SKA to be ~5% of the construction costs, or about $US 75 million.

12.2 Operational Issues

12.2.1 Multibeaming

SKA beams may be widely spaced or clustered in one region of the sky. In either case, a number of different experiments may collect data simultaneously via different beams. It is also conceivable that independent experiments may share data from a given beam. (An example is the case where spectral line, pulsar and SETI observations are all proceeding in parallel). SKA designers therefore need to decide early which modes are supported and to design appropriate signal path branching and backend availability.

12.2.2 Sub-arraying and Configurations

It is likely that, for many experiments, an effective area less than that of the full SKA will suffice. The sub-arrays themselves could form multiple beams, making the number of simultaneous experiments potentially very large. Some experiments may require repeated observations with identical configurations (sub-array, hour angle, etc) whilst for others configuration is unimportant. Again, designers need to establish which modes will be possible; this will require close liaison with the science community to prioritize requirements such as those flowing from configuration issues.

12.2.3 Scheduling and Target-of-Opportunity Observations

While optimized, automated, scheduling has eluded the radio astronomy community to date, the sheer complexity of the SKA observing domain reinforces the view that automatic queue scheduling must be used, at least for the great majority of observations. With the SKA science requirement to study non-stationary phenomena in many forms, it is especially important that the instrument scheduling be able to respond effectively to target-of-opportunity (ToO) requests. In a telescope capable of

widely spaced multibeaming, a simple mode might be to dedicate at least one beam and associated backends to such requests, making maximum sensitivity available for ToO observers.

12.2.4 Calibration

Calibration will be central to the SKA, and effective instrumental and observational methods will need to operate in parallel if the instrument is to meet its science goals, especially the goal of imaging with a dynamic range of better than 60 dB. In a multibeam instrument it is likely that continuous, or near-continuous, availability of a calibration beam placed near the target field could yield substantial dividends. Whatever strategies are adopted, continuous calibration will be central to SKA operations.

12.2.5 Maintenance

The scale of the SKA makes it certain that, at any given time, parts of the system will be malfunctioning and will require diagnosis and repair. Depending on the location of the fault, astronomy operations will be affected to a greater or lesser extent. Most likely, faults will be associated with individual antennas which, in a well-designed large or medium-N array, should have minimal impact on overall operation. Station-level or central signal processor faults will be progressively more serious. Signal routing and prioritized scheduling arrangements must be designed to give high priority science programs access to functional hardware. At the same time, the diagnosis and repair process will require simultaneous access to other parts of the instrument, in some cases extending to the need for a sub-array or beam for test observations. Despite the advantages of a large or medium-N solution in facilitating maintenance, we note the probable higher absolute failure numbers flowing from this design philosophy and we stress the need for at least representative reliability analyses for various topologies – preferably early in the design process. In the absence of detailed analysis, we note that if each of ~53 000 antennas in the Luneburg lens SKA requires one hour of attention per year by a two-person team, the labour cost for the field crew amounts to about $US2 million per annum.

12.2.6 Facility Upgrades

Different realizations of the SKA have different optimum upgrade strategies but, just as the large-N approach minimizes the operational impact of many failures, it also makes a continuous (or at least frequent) upgrade process less disruptive. In the Luneburg lens approach, installation of the best available initial infrastructure (concentrators, intra-station and trunk fibres, etc) makes a variety of upgrades feasible. Examples include additional feeds, receivers (perhaps giving a mix of cooled and un-cooled types), A/D converters, beamformers, and expanded long-haul fibre capacity. At the central signal processor end, the designer should factor in the continuous improvement in computing capacity. One could, for example, imagine the provision of at least two entirely separate platforms (with associated signal distribution) commutated as new hardware and software becomes available.

13. PIVOTAL TECHNOLOGIES

As with other SKA solutions, the feasibility of the Luneburg lens concept depends heavily on the availability of efficient, low-cost, collecting elements as well as economical signal encoding and transport solutions. While realization of a practical refracting concentrator is a major challenge, initial experimental results do indicate that new composite materials can yield good electrical performance at costs compatible with SKA antenna budgets. Advice from specialist manufacturing engineers also leads to optimism about mass production possibilities for the lenses themselves (Appendix B). However, cost analyses (Section 15) show that the cost of material as basic as the rutile dopant for the dielectric has a substantial impact on the SKA budget. It is essential therefore to show the feasibility of lens production and to establish links with expert commercial players in the materials field. We also note that the associated antenna mechanical components are, as yet, untested. The aim though is to test thoroughly all aspects of the antenna design in the demonstrator described in Section 16.

While some of the antenna uncertainty flows from basic physics, we are also concerned at the need to pick winners in the commercial development of signal encoding and transport technologies. The central importance of fast A/D conversion and fibre optic signal transport to any SKA design makes it important that the SKA community takes market advice in these areas (Section 17). Two examples are illustrative here. Section 9.2 identified key components in the signal path shown in Fig. 9-2. We assume the availability, by 2010 – 2015, of 8-bit A/D converters sampling at 10 Gs s^{-1}; the unit cost of these devices (in quantity) is taken as around $US1000. While A/D converters certainly do not follow Moore's law, a couple of examples are useful. Rockwell is now advertising a 6-bit, 3.2 Gs s^{-1}, device as available in autumn 2002 for a price of $US300; a 5-bit, 6 Gs s^{-1}, is currently under development. The estimate for the 8-bit device, 10-15 years hence, does not seem implausible, but it is important that SKA designers have an early grasp of trends.

The key optical component in the signal path is the VCSEL laser chip with integrated DWDM. With prices for individual 850 nm devices now at < $US10, and intense industry pressure, there is clearly a path forward to our assumed package costing $US400, despite known difficulties in translating the semiconductor processes to the 1550 nm band.

14. A REPRESENTATIVE SKA SITE

14.1 Introduction

Australia is an island continent about the size of the conterminous USA. Despite the mythology of the Outback, the population is highly urbanized, with over 80% of the population living in cities. The vast, often flat, inland of the continent is sparsely inhabited but, despite the low population density, activities such as agriculture and mining make it possible to find remote – and radio quiet – locations which offer reasonable infrastructure.

Australia has a stable political environment, with the eight states and territories having federated in 1901 to form a Commonwealth governed by a Westminster-style parliamentary democracy. Perhaps to combat the "tyranny of distance" so feared by European settlers, the uptake rate of technology is especially high. For example, a 2002 survey combining 23 indices ranked Australia third (behind the US and Sweden) of 14 developed countries in a measure of progress in the information economy [14-1].

In recent years there have been attempts at returning the title of some land to the Aborigines, the indigenous occupants of the continent; social justice considerations will ensure that this trend continues. Early reaction of Aboriginal interest groups to the SKA project has been favourable, partially because the impact is minimal compared with agriculture or mining. In general, country communities in Australia are keen to see new activities established and many rural development bodies exist to attract initiatives to regional areas.

14.2 The Mileura Site

It is certain that Australia offers a large number of potentially suitable SKA sites. Our work to date has been concerned with choosing and characterizing representative candidate sites and, in this Section, we describe the best known of these: Mileura Station, in the mid-West region of Western Australia. While Mileura is the most thoroughly studied potential site, we stress that it is presented for illustrative purposes only; no national determination or ranking of candidate Australian sites has yet been made by any technical or policy body.

Mileura (117°31'E, 26°38'S, elevation 440 m) is a typical cattle station of the mid-West region. It is 70 x 40 km in extent and is on marginal agricultural land. The station is surrounded by similar holdings, the population of each being typically four, rising to 15 in the mustering and shearing season. The nearest town is Meekatharra (population 2000) located about 100 km to the east. Mileura is 600 km north-east of Perth (population > 1 million), the WA state capital and an international air and sea port. The site is less than 100 km from an existing high-bandwidth optical fibre network and is about 200 km from a major natural gas pipeline; a tentative plan for a pipeline extension would bring gas to within 100 km (significant for the SKA as there is no large-scale electric power distribution in the area). There is ample space available for development of on-site airstrips and related facilities. Road access is via all-weather gravel roads, with provisional plans in place to improve regional access via sealed roads.

In world terms, the site is meteorologically benign, with the Meekatharra Airport weather data (Table 14-1) being representative of the region.

Table 14-1. Climate Summary for Meekatharra Airport (50-Year Data)

Mean daily maximum temperature in hottest month (January)	38.2 °C
Mean daily minimum temperature in coldest month (July)	7.4 °C
Mean annual rainfall	228 mm
Mean monthly maximum rainfall in wettest month (June)	35.2 mm
Percentage of time wind exceeds 30 km hr^{-1} (8.3 ms^{-1}) in worst case (January)	13
Maximum recorded wind gust	148 km hr^{-1}

Snow is never recorded; occasional frosts are recorded in June, July and August (giving a figure of 1.3 for the annual mean number of days with frost); and occasional hail has been recorded in April, September and November (0.4 days mean annual).

14.3 First RF Environment Measurements

Being one country, Australia is unique among the continents in having a single licensing authority (the Australian Communications Authority – ACA) for radio communication services. The ACA spectrum management database is in the public domain and is available in electronic form (excluding military and associated communications). The ATNF has used the database as a tool for planning and conducting radio astronomy observations, and some of the capabilities developed are available via the Web [14-2]. Combining the ACA database and relatively simple propagation models allows prediction of the RF environment at a given location. However, uncertainties relating to the transmitting antenna orientation and channel usage statistics makes the prediction a guide only. Still, the presence of a single, vigilant, licensing authority and the ready availability of a comprehensive database does simplify the task of a radio astronomy planner.

Of course, real measurements are the only effective way of characterizing a site and a preliminary round of RFI testing has been carried out at Mileura. The tests covered the frequency range 30 – 1800 MHz and lasted four weeks. Detailed outcomes are summarized in [14-3] but, in general terms, the site proved extremely radio-quiet, with large numbers of test bands showing less than a few percent occupancy in frequency. For example, a 700 MHz band above 1060 MHz had a band vacancy better than 99%. Terrestrial broadcast signals were also weak by global standards, with peak levels near –90 dBm m^{-2} being common. Indications are that the ACA database is indeed useful as a prediction tool and a communications industry contractor is currently working on refining a software package which should allow a more comprehensive comparison with measured data.

While the initial tests do illustrate an extremely radio-quiet site, the minimum signal identification levels for RFI measurements taken with any conventional scanning spectrum analyzer are typically around -130 dBm m^{-2} – too high to establish compliance with existing ITU radio astronomy recommendations or likely future SKA guidelines. Recognizing this, the ATNF is completing an autocorrelator-based spectrum analyzer, allowing more realistic measurements to be made at sensitivities closer to those needed for radio astronomy. This new instrument, together with more sophisticated data acquisition and visualization software, will be used first at Mileura in 2003.

14.4 A Radio-Quiet Reserve

In parallel with studies of representative sites the ATNF, on behalf of the Australian SKA Consortium, has been pursuing the creation of a radio-quiet reserve (typically 50 x 50 km). The reserve is ostensibly to accommodate the central portion of the SKA (where baselines are shorter and natural interferometer filtering of RFI is weakest), but it also has application in other areas of science and engineering. The proposal has been received with interest by Commonwealth and state authorities. A meeting of government representatives was held in June 2002 to discuss national co-ordination of the SKA site project and, in particular, administrative aspects of setting up the radio-quiet reserve. Representatives resolved that, regardless of individual regional interests, establishing the best candidate Australian SKA sites was the paramount concern. It was further agreed that the Australian SKA Consortium should be the body responsible for overseeing the characterization of candidate sites, as well as the advancement of the radio-quiet reserve.

15. COST SUMMARIES

15.1 Reference Array Cost

We have estimated the cost of a "reference" SKA built using 7 m diameter Luneburg lenses and achieving A_e/T_{sys} of 2×10^4 m^2 K^{-1} at 1.4 GHz. Figure 15-1 gives a summary of this estimation and Appendix D contains the details behind it. Note that all costs in this section are expressed in 2002 US dollars (but performances of key components are taken as those available in 2010). In compiling the estimates in this and Section 15.2, the "nominal" values of parameters listed in Table 15-3 were used. Costs for beamforming and station correlators are generally small and occasionally round to zero in high-level summaries.

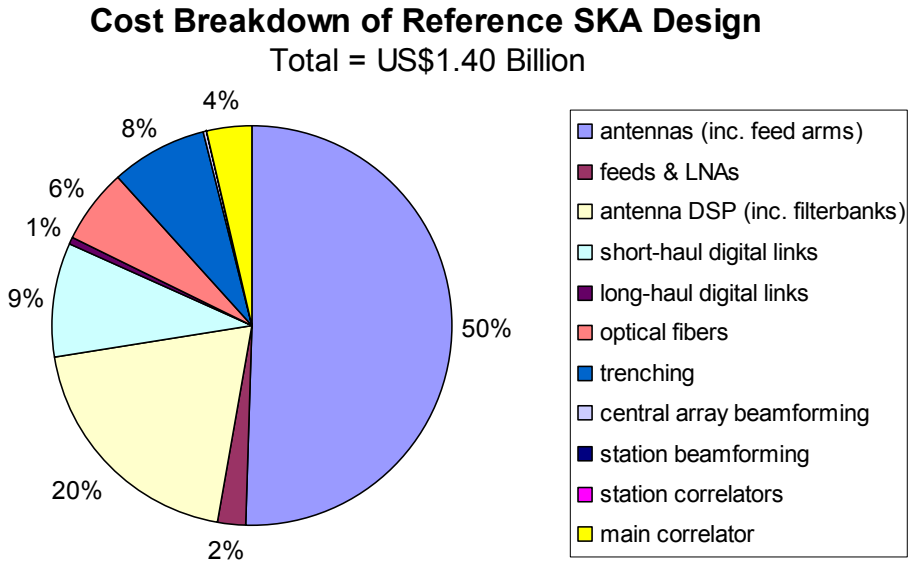

Fig. 15-1**.** Cost breakdown of a 7 m Luneburg lens SKA. This array has two widely placeable feeds per antenna (Section 9.1) and operates using uncooled LNAs. Refer to Fig. 9-2 for more details of sub-systems. The main correlator has a 3 GHz (maximum) bandwidth, full Stokes processing, 8192 channels, 8-bit DSP and 2500 inputs. (Note that beamforming and station correlator costs are small).

15.2 Cost Variation with Feed Numbers and LNA Physical Temperatures

Table 15-1 shows the variation of cost with number of widely placeable feeds for the reference array. This array has 52 800 elements, 1.29 km^2 effective collecting area, and a system temperature at 1.4 GHz of 64 K. The receiver RF stages are based on GaAs MMICs operating at ambient temperature and each front-end costs $US340. For illustration, it is assumed that the feeds do not share feed arms, and that the additional receivers are low-band types (Section 9.1).

Table 15-1. Costs for Reference Array (Uncooled Receivers)

	Number of Moveable Feeds		
	(1 High)	**(1 High, 1 Low)**	**(1 High, 2 Low)**
Cost Component	*Million USD*	*Million USD*	*Million USD*
Antennas (inc. feed arms)	617	709	800
Feeds & LNAs	16	33	49
Antenna DSP (inc. filterbanks)	184	276	368
Short-haul digital links	69	127	185
Long-haul digital links	9	9	9
Optical fibres	72	84	102
Trenching	113	113	113
Central array beamforming	1	1	1
Station beamforming	1	1	1
Station correlators	0	0	0
Main correlator	51	51	51
TOTAL	**1,133**	**1,403**	**1,678**
Relative cost increment over one high-band beam		**24%**	**48%**

Table 15-2 shows cost variations with number of moveable feeds for an SKA using 7 m lenses, this time with receivers cooled to a physical temperature of 60 K. Such an array will have 34 237 elements, 0.835 km^2 effective collecting area and a system temperature of 42 K. The receiver and feed package is based on ATA-style components and costs $US 6310.

Table 15-2. Costs for Array (Cooled Receivers)

	Number of Moveable Feeds		
	(1 High)	**(1 High, 1 Low)**	**(1 High, 2 Low)**
Cost Component	*Million USD*	*Million USD*	*Million USD*
Antennas (inc. feed arms)	400	460	519
Feeds & LNAs	216	432	648
Antenna DSP (inc. filterbanks)	119	179	239
Short-haul digital links	45	82	120
Long-haul digital links	9	9	9
Optical fibres	62	74	79
Trenching	113	113	113
Central array beamforming	0	0	0
Station beamforming	0	0	0
Station correlators	0	0	0
Main correlator	51	51	51
TOTAL	**1,016**	**1,400**	**1,779**
Relative cost increment over one high-band beam		**38%**	**75%**

15.3 Further Variational Analysis

15.3.1 SKA Cost Variation with Key Parameters

Table 15-3 lists the results of a sensitivity analysis on the reference SKA budget. Minimum and maximum values of a number of parameters were estimated, and the impact of each on the total cost of the reference system was calculated.

Table 15-3. Effect of Various Parameter Variations on Cost

Parameter	Description	Nominal Value	Likely Variation		Resulting Total Cost Variation	
			max	min	for max value	for min value
α	Percentage rutile inclusions in foam, by volume, in order to achieve an artificial ε_r of 2	1.5%	2%	1%	+6.5%	-6.5%
η_a	Aperture efficiency of Luneburg lens	65%	70%	60%	-5.9%	+7.3%
f/D	Focal ratio of Luneburg lens	0.7	1	0.5	-4.5%	+8.6%
δ	Loss tangent of foam	0.0001	0.00015	0.00005	+7.4%	-6.8%
T_{lna}	Equivalent noise temperature of the first LNA stage	25 K	30 K	20 K	+7.8%	-7.4%
T_{spill}	Spillover noise contribution	12 K	12 K	7 K	+0.0%	-7.0%
c_{adc10}'	Cost of 8 b 10 Gs/s ADC in 2010	1000 USD	1500 USD	500 USD	+5.6%	-5.6%
MF_{dig}	Factor for reduction in digital electronics costs from 2002 to 2010	32	40	16	-1.9%	+9.3%
c_{rutile}	Cost of rutile	1.5 USD.kg^{-1}	2.0 USD.kg^{-1}	1.0 USD.kg^{-1}	+6.5%	-6.5%
c_{foam}	Cost of foam	1.0 USD.kg^{-1}	1.5 USD.kg^{-1}	0.5 USD.kg^{-1}	+7.7%	-7.7%
k	Fraction of long-haul fibre supplied at "no cost" (telcos etc.)	30%	50%	0%	-2.3%	+3.4%

15.3.2 Cost Variation With Diameter

An interesting special case of SKA cost variation is that which occurs as the diameter of the concentrator is varied. In the case of the Luneburg lens array, the behaviour is plotted in Fig. 15-2 over the range of interest. An obvious strategy is to build for minimum cost but an alternative might be to build the smallest diameter lens affordable, giving maximum upgrade potential as data transmission and signal processing costs fall with time.

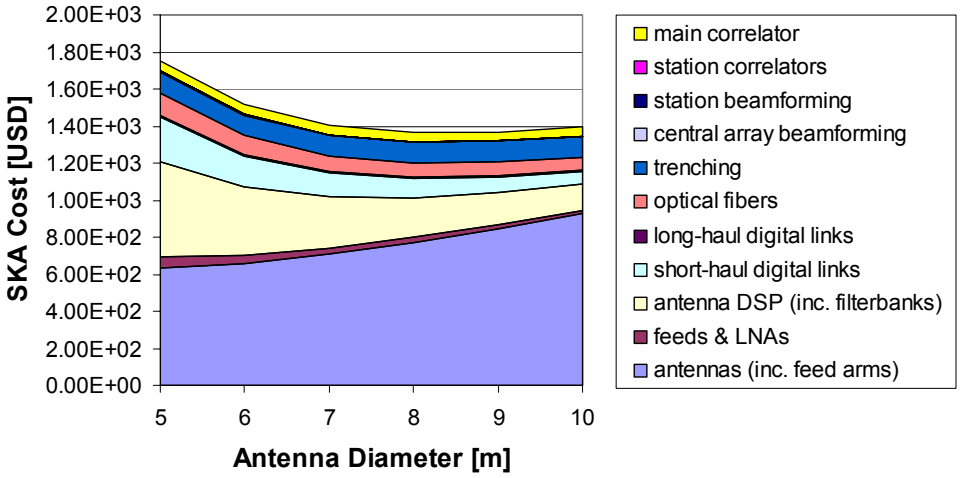

Fig. 15-2. Variation of array cost with lens diameter. Note that beamforming and station correlator costs are very small.

16. THE NEW TECHNOLOGY DEMONSTRATOR (NTD)

A previous contribution [16-1] has summarized thoughts on what an SKA demonstrator should actually demonstrate. While there is a place for laboratory and early prototyping, it is clear that satisfactory treatment of issues such as stability and calibration require a functional astronomical capability. With limited funding available ($US 6 million), we have specified the integration of new trial SKA systems with an existing synthesis array – the Australia Telescope Compact Array (ATCA).

The demonstrator concept is shown in Fig. 16-1. Approximately half the funds will be spent developing a highly scaleable SKA-style FX correlator; the remainder will be used to construct either one or two mini SKA stations based on Luneburg lens technology. The intention is to investigate the feasibility of the lens concept, the digital receiver implementation, and the elements of the high bandwidth signal transport described in this document. At the same time, the project will provide, at a minimum, an astronomically useful ATCA upgrade in the form of the wideband correlator. Table 16-1 outlines some NTD characteristics as they are currently envisaged. Economics of the prototyping are still being assessed and the outcome will determine whether one or two mini-stations will be built. In either case, the intention is to have the demonstrator available for international evaluation by the end of 2005.

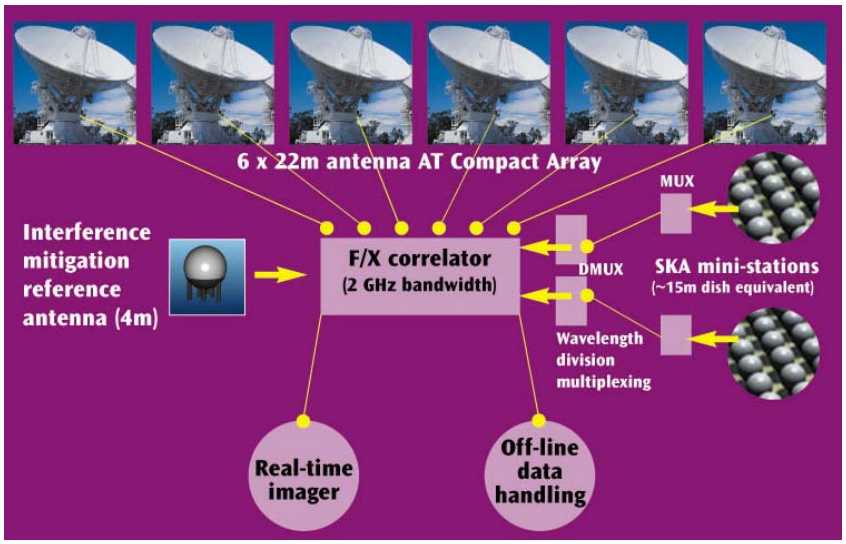

Fig. 16-1. NTD concept. Either one or two mini SKA stations will be integrated with the six-antenna ATCA. An F/X correlator (minimum 2 GHz bandwidth) build around scaleable technology replaces the existing ATCA signal processor. The interference mitigation reference antenna is in fact a first-prototype Luneburg lens and allows early incorporation of post-correlation interference mitigation into the upgraded array.

Table 16-1. NTD Characteristics

Number of stations	1 (or 2)
Antenna type	Luneburg lens
Antenna diameter	5 m
Number of antennas per station	8
Station diameter	38 m
Operating frequency range	1-5 GHz
Antenna field-of-view (1.4 GHz)	2.9°
Station beam width (1.4 GHz)	23 arcmin.
Station equiv. geometrical aperture	~ 15 m
Number of RF beams	2
Receiver type	Uncooled LNA
Number of dual-polarization receivers	16 (or 32)
Signal encoding	4 or 8-bit digital at antenna
Signal transport	Wavelength division optical
Longest data link	< 10 km

Practical large or medium-N SKA realizations will require station beamforming but the NTD, in the interests of test-bed flexibility, will convey all antenna signals to the central site, an arrangement similar to that proposed for the SKA central array. Beamforming can, of course, still be demonstrated prior to correlation of the station beam with the remainder of the ATCA. Alternatively, a versatile signal routing scheme will allow many, if not all, NTD antennas to be correlated with their peers, or with some ATCA dishes.

17. SYNERGIES AND LINKS WITH OTHER SKA CONCEPTS

All SKA concepts have considerable infrastructure and technical common ground. The biggest commonality lies within the medium-to-large-N (phased arrays, Luneburg lens, small dish) and small-N (large dishes, cylindrical reflectors) groupings but, even so, technical questions relevant to the whole SKA community certainly exist. For example, the provision of many long-haul, wideband, optical fibre data links is a major cost and technical challenge in any SKA model.

In specific terms, the Luneburg lens concept is allied most closely with the small dish proposal for SKA realization; simply interchanging the two types of concentrator in the two concepts is a worthwhile thought experiment. Apart from system level similarities, we suspect that these two SKA models are also comparable in terms of practical considerations such as feeds, antenna mechanics and mass production challenges. It is quite likely therefore that individual contacts, being built now, in areas such as materials, structural and manufacturing engineering may prove invaluable in the wider SKA project.

While our favoured approach has Luneburg lens antennas equipped with ambient-temperature receivers – as in a phased array SKA – cryogenically cooled systems such as variants of those currently proposed for the Allen Telescope Array are a possibility. We also note the wide applicability of phased array technology across a range of SKA concepts. Whether the array is used as a primary receptor, or as a focal plane or focal surface array in a concentrator, it is clear that development of dense, active, wideband, arrays is central to the SKA effort. Interestingly, although the small or medium diameter concentrators benefit from the availability of arrays providing cluster beam options, it is the extreme technologies which provide the real imperatives. The phased array primary receptor is an obvious driver, but large concentrators also need arrays (two-dimensional or line) to meet field of-view or multibeaming requirements.

Noting the fractional cost of signal encoding and transport (Section 15), we stress the importance of SKA concept groups establishing common metrics and costings in this area. Given the need to estimate trends in volatile commercial environments (including the telco and consumer markets), it is likely that the whole SKA community would benefit from a jointly-funded global market and technology forecast, perhaps along the lines of those provided by, for example, ElectroniCast Corporation [17-1].

Signal processing is the easiest area in which to establish functional international working groups and there have already been profitable exchanges resulting in new insights in areas such as correlator design. It is important that all SKA system design incorporate interference mitigation concepts from the outset. With demonstrators such as the ATA and NTD emphasizing interference mitigation, it will be valuable for international project groups to have access to these test beds.

While not part of any one SKA concept, we note the importance of urgent international collaboration in the technical aspects of site testing. Only by establishing common metrics, and preferably standardizing techniques and equipment, can meaningful comparisons of candidate SKA sites be made.

18. REFERENCES

[3-1] R. K. Luneburg, in *Mathematical Theory of Optics*, Brown University Course Notes, 1944.
[5-1] "SKA Preliminary Specifications", see http://www.atnf.csiro.au/projects/ska/archive/prelim.html
[5-2] "SKA Memoranda", see http://www.ras.ucalgary.ca/SKA/ska_memos.shtml
[5-3] X. Fan et al., "Evolution of the Ionizing Background and the Epoch of Reionization from the Spectra of z~6 Quasars", *Astron. J.*, in press, 2002.
[5-4] K. v.d. Schaaf, "LOFAR System Definition", ASTRON-LOFAR-00134, see http://www.lofar.org/archive/engineering/SystemDefinition_1.4.pdf
[5-5] J. Bell and R. Ekers, "Multiple Widely Spaced Beams for the SKA?", see http://www.jb.man.ac.uk/ska/workshop/Bell1.pdf
[6-1] R. D. Ekers, survey at Amsterdam SKA Workshop, April 1999.
[6-2] M. H. Wieringa, "SKA Configuration Simulations", see http://www.narrabri.atnf.csiro.au/~mwiering/skasim/
[6-3] J. D. Bunton, "Array Configurations that Tile the Plane", *Experimental Astrophys*, vol. 11, no. 3, pp. 193-206, 2001.
[7-1] G. A. Hampson, R. De Wild and A. B. Smolders, " Efficient Multi-Beaming for the Next Generation of Radio Telescopes", in *Perspectives on Radio Astronomy: Technologies for Large Antenna Arrays*, A. B. Smolders and M. P. van Haarlem Eds. ASTRON, pp. 265-276, 1999.
[7-2] G. L. James and A. J. Parfitt, "A Proposal for the 1kT Antenna", URSI General Assembly, Toronto, Canada, pp. 549, August 1999.
[7-3] J. D. Bunton et al., "Cylindrical Reflector SKA", submitted to EMT, June 2002.
[7-4] P. Dewdney, "The Large Adaptive Reflector for the SKA", URSI Large Telescope Working Group Meeting and 1kT International Technical Workshop, Sydney, Australia, Section C2, December 1997.
[7-5] J. W. Dreher, "The One Hectare Telescope (1HT) project", in *Perspectives on Radio Astronomy: Technologies for Large Antenna Arrays*, A.B. Smolders and M.P. van Haarlem Eds. ASTRON, pp. 33-36, 1999.
[7-6] B. Peng et al., "The Technical Scheme for FAST", ibid., pp. 43-48.
[7-7] N. Kardashev, "Luneburg Lens", SKA Workshop, Greenbank, West Virginia, October 1998.
[7-8] A. Parfitt et al., " A Case for the Luneburg Lens as the Antenna Element for the Square Kilometre Array Radio Telescope", *Radio Science Bulletin*, no. 293, pp. 32-37, June 2000.
[7-9] P. E. Mayes, "Frequency-Independent Antennas", in *Antenna Handbook* ,Y. T. Lo and S. W. Lee Eds. Van Nostrand Reinhold, 1993.
[8-1] S. Weinreb, "Noise Temperature Estimates for a Next Generation Very Large Microwave Array," *IEEE MTT-S International Microwave Symposium Digest*, vol. 2, pp. 673-676, 1998.
[8-2] S. Weinreb & D. Bargri, "Progress at JPL Concerning Antenna and Wideband Receiver Design", Presented at SKA: Defining the Future, Berkeley, 2001.
[9-1] R. H. Ferris, "A Baseband Receiver Architecture for a Medium-N SKA", in preparation.
[9-2] J. E. Nordam, "LOFAR Calibration and Calibratability", ASTRON-LOFAR-00227, see http://www.lofar.org/archive/engineering/noordam-calib_1.0.pdf

[10-1] C. J. Lonsdale and R. J. Capello, "Concepts for a Large-N SKA", in *Perspectives on Radio Astronomy: Technologies for Large Antenna Arrays*, A.B. Smolders and M.P. van Haarlem Eds. ASTRON, pp. 243-250, 1999.
[10-2] J. D. Bunton, "Cost of an Imaging Correlator for the SKA", see http://www.atnf.csiro.au/projects/ska/techdocs/Correlator_cost_for_the_SKA.pdf
[10-3] M. J. Kesteven and R. J. Sault, "Post-Correlation Ineterference Mitigation", *Proc. IUCAF Workshop*, Bonn, March 2001 (in press).
[11-1] "Australian Virtual Observatory – Background Information", see http://www.atnf.csiro.au/projects/avo/background.html
[14-1] Allen Consulting Group, "Australia's Information Economy", see http://www.noie.gov.au/index.htm
[14-2] ATNF, "RFI Characterization Page", see http://www.parkes.atnf.csiro.au/people/jsarkiss/rfi
[14-3] B. M. Thomas, "Radio Quietness Measurements at Mileura Station – 27 March to 17 April 2001", Report No. 4, CSIRO ATNF, 2002.
[16-1] P. J. Hall et al., "New Roles for Today's Telescopes", see http://www.skatelescope.org/skaberkeley/html/posters/html.htm
[17-1] ElectroniCast Corporation, see http://www.electronicast.com/

APPENDIX A: SKA DESIGN GOALS

Parameter	Design Goal
A_{eff}/T_{sys}	2×10^4 m^2K^{-1}
Total Frequency Range	f = 0.15 - 20 GHz
Imaging Field of View	1 square degree at 1.4 GHz
Number of Instantaneous Pencil Beams	100
Maximum Primary Beam Separation low frequency high frequency	 100 degrees 1 degree at 1.4 GHz
Angular Resolution	0.1 arcsec at 1.4 GHz
Surface Brightness Sensitivity	1 K at 0.1 arcsec (continuum)
Instantaneous Bandwidth	0.5 + f/5 GHz
Number of Spectral Channels	10^4
Number of Simultaneous Frequency Bands	2
Imaging Dynamic Range	10^6 at 1.4 GHz
Polarization Purity	-40 dB

APPENDIX B:

DESIGN OF A LUNEBURG LENS ANTENNA ELEMENT FOR THE SKA

GRAEME JAMES
CSIRO TELECOMMUNICATIONS AND INDUSTRIAL PHYSICS
PO BOX 76, EPPING, NSW 1710, AUSTRALIA
graeme.james@csiro.au

B1 INTRODUCTION

In this appendix we provide details from an earlier study, augmenting the overview of the Luneburg lens as the SKA antenna element. Being an earlier study, there are a number of minor differences relative to the main text but the essence of the case remains the same.

The SKA radio telescope [B1] is planned for construction around 2012-2015. From the outset there has always been the desire for the SKA to provide a distinctive capability (aside from increased sensitivity) not currently available on any other radio telescopes. To this end, one possibility is that of having a multi-beam instrument with several independent beams anywhere on the sky at any one time has scientific applications as well as opening-up new ways of how one observes the radio sky. This multi-beaming capability was the major consideration behind the NFRA proposal for a phased array as the SKA antenna element [B2]. While there have been several alternative schemes subsequently put forward for the antenna element, the only other option to date providing truly independent widely-separated multiple beam capability is the Luneburg lens proposal outlined in [B3]. All the other proposals have, in principle, limited multi-beaming capability, ranging from cylindrical reflectors [B4], [B5] where multi-beaming is possible within a fan beam, down to multi-beaming within the main beam of a conventional reflector antenna [B6]-[B8].

Some of the main features of the SKA, such as a large collecting area, a wide frequency range and the desire for multi-beaming, have meant from the outset that cost has been a major parameter driving the design. To build the SKA at an affordable price within the next 10-15 years, heavy reliance is being placed on Moore's law, the economies of scale and some clever engineering. To these main parameters we would add another: upgradeability. In building such an expensive multi-national telescope, the ability to readily upgrade and extend the instrument's capability over its lifetime is an obvious attractive feature in any design. In this regard, the Luneburg lens approach has a distinct advantage over all other proposals.

B2 THE SKA SPECIFICATIONS

While the final and detailed specifications for the SKA remain under discussion and development, the main features are clear. In this section, only those features that impact on the design of the antenna element will be considered.

The lowest frequency of operation desirable is to ensure the SKA overlaps with LOFAR [B9] where operation up to about 0.3 GHz is envisaged. The highest frequency of operation for the SKA is more problematical with 1.42 GHz being an

absolute minimum to enable all of red-shifted hydrogen to be observed. However, if the upper frequency range could be extended to around 5 GHz much more science of interest would be covered [B10]. At higher frequencies still there is interest around 12 GHz, 22 GHz and even in the 40-100 GHz range. However, it has been argued that at these higher frequencies different specifications are required (for example the provision of multi-beaming may be unnecessary; see [B11]). Furthermore, as discussed below, the size of Luneburg lens required to operate as low as 0.3 GHz will manifest increasingly unacceptable losses at frequencies 12 GHz and above. Therefore, it is assumed here that 0.3 – 1.5 GHz is the prime frequency range of interest with extension to 5 GHz highly desirable.* For higher frequencies, other telescopes will become available (such as the EVLA and, for frequencies above 30 GHz, ALMA) albeit without the sensitivity of the mid-range SKA.

A key specification for the SKA is the sensitivity, A_{eff} / T_{sys} , where A_{eff} is the effective collecting area and T_{sys} the system temperature. Proceeding from the SKA specification of $A_{eff} / T_{sys} = 2 \times 10^4$ m^2K^{-1} at 1.4 GHz, for an antenna radiating from a physical aperture of area A_{ant}, the specification can be expressed as

$$A_{ant} = 2 \times T_{sys}\,(K) \,/\, \eta\,(\%);\ km^2 \qquad (B1)$$

where η is the antenna efficiency (typical values lie in the range 60-70%). Given the limited control over this parameter, the crucial role of T_{sys} in minimising the collecting area of the array is evident from the above relationship. While, initially, it may be thought that cooled LNAs be essential to minimise the size (and therefore cost) of the array, cryogenics are expensive. However, with room-temperature devices in the low gigahertz region already having noise figures as low as 0.2 dB [B12], the need for cryogenically-cooled LNAs for the SKA at these frequencies is expected to reduce over the next 10-15 years. Given these technological advances, it is possible that T_{sys} could be as low as 35K in the 0.3 – 5 GHz frequency range using room-temperature LNAs. With this value of T_{sys} together with the range of antenna efficiencies quoted above, the required antenna collecting area from equation (B1) comes to around one square kilometre.

The SKA imaging specification is for an instantaneous one square degree field-of-view (FOV) at 1.4 GHz. Based on the half-power beamwidth of the equivalent circular aperture antenna with 60-70% antenna efficiency, the diameter of the element antenna cannot be greater than 17 metres. This implies a minimum of 4,400 antenna elements to form the complete array. Within the FOV a number of instantaneous pencil beams is desired. Currently this number is set at 100 but this may be unreasonably high [B13]. How these beams are formed is not particular to the Luneburg lens design and there are several options applicable to all proposals such as a focal plane array and/or beam forming at the station level. As the number of beams necessary is a somewhat 'rubbery' figure and that the case for the Luneburg lens is not contingent on it, we need not consider it further here. Of more relevance is the capability for independent instantaneous multi-beaming by the Luneburg lens. Provided the basic infrastructure of the SKA is constructed with sufficient foresight (especially with regard to laying enough optical fibre capacity between stations to

* It is worth noting that while operation to 5 GHz is possibly achievable using Luneburg lenses, it becomes a more formidable task for one alternative to the Luneburg lens: the phased array. Achieving the basic 0.3 – 1.5 GHz frequency range with a multi-beaming array the size of the SKA would be technically challenging and expensive, even taking into account Moore's law.

allow for possible future extensions), the Luneburg lens solution allows, at relatively low cost, additional beams to be added as resources permit thus providing a straightforward ongoing upgrading path for the SKA not possible with other designs. It is worth noting that widely spaced beams are desired in nearly 40% of the science driver proposals [B10]. Furthermore, the provision of multiple beams will provide an instrument with great versatility and likely change in a profound way as to how the radio sky is observed**.**

When adding additional beams to the SKA it is most likely, at least in the first instance, they will be simplified depending on the resources available and the intended scientific objectives. Reduced capability could include their confinement to the inner part of the array, not providing instantaneous pencil beams or imaging capabilities, or in other cases, having limited frequency coverage. As the provision of additional beams is clearly an obvious path for continual upgrading of the SKA, it is worth considering providing this capability from the outset, albeit in limited way, to demonstrate the possibilities of multi-beaming. To this end we propose an additional non-imaging single beam be provided on the innermost part of the array.

Other features of the SKA that affect the antenna design include dual polarisation (either linear or circular with a preference here for linear polarisation) and, as appears to be coming increasing in favour, a large-N (where N, the number of array stations, is > 200) solution to beam forming. A large-N SKA places considerable demands on the correlator but the advantages as outlined in [B14] seem to be formidable.

From the above discussion, the specifications of immediate concern for the design of the Luneburg lens antenna element are summarised in Table B1.

TABLE B1: SPECIFICATIONS FOR THE DESIGN OF THE LUNEBURG LENS

Parameter	Specification
Antenna efficiency, η	60-70%
System temperature, T_{sys}	~ 35K (optimistic)
Antenna area, A_{ant}	1 km^2
Imaging Field of View	1 square degree @ 1.4 GHz
Antenna diameter, $\mathcal{D}$	≤ 17 metres
No. of antenna elements, n	≥ 4,400
Frequency Range	0.3 – 5 GHz
Polarisation	Dual linear
No. of independent beams	≥ 2 (initially limited second beam)
Sky coverage	Maximum possible

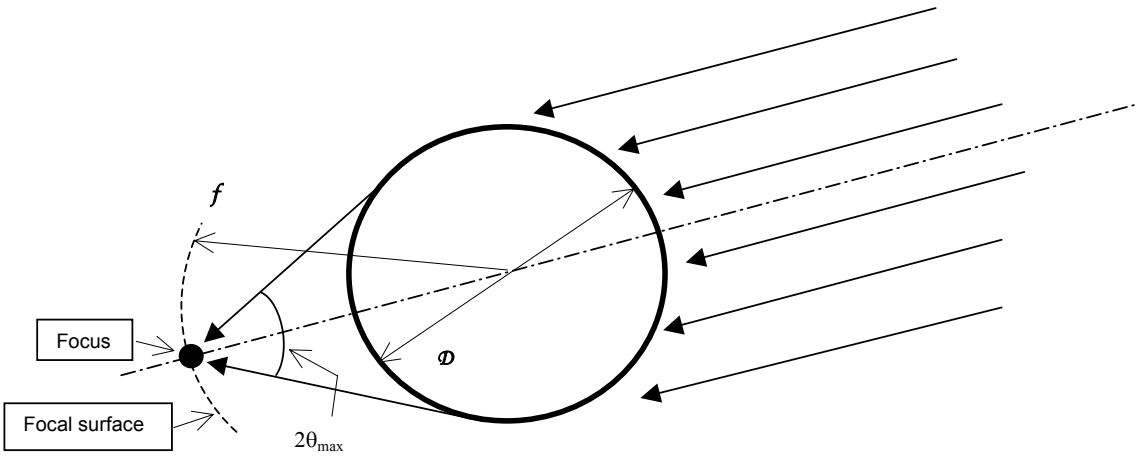

Figure B1: Luneburg lens focussing an incoming plane wave

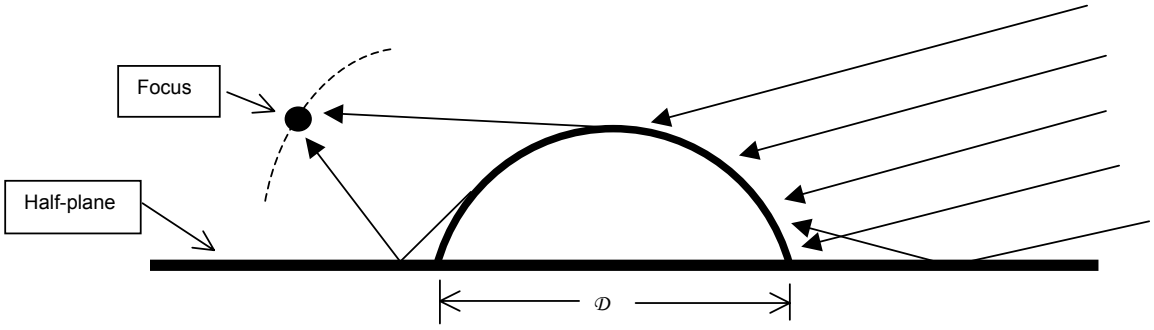

Figure B2: 'Virtual-source' Luneburg lens

B3 THE LUNEBURG LENS

B3.1 GENERAL CONSIDERATIONS

The Luneburg lens is a spherical lens characterised by an inhomogeneous but spherically symmetric refractive index profile. The basic action of the lens is illustrated in Figure B1. Energy from a plane wave incident on the lens is focussed to a feed point, *f*, on the opposite side of the sphere. Given the spherical symmetry of the lens, perfect focussing is obtained from all directions to feed positions on the focal surface of radius *f*. Multiple independent beams may be produced by increasing the number of feeds on the focal surface and each beam can track a source by simply moving the feed over this surface.

An alternative to the full spherical Luneburg lens for astronomy applications is the hemispherical 'virtual source' Luneburg lens shown in Figure B2. Here the half lens is placed on a perfectly conducting ground plane and the resultant mirror image provides a complete lens for operation in the upper half-space. The advantages of this arrangement are that only half the material is required and that it is fully supported by the ground plane. Furthermore, there are mechanical advantages in providing feed movement with this configuration. The disadvantages are that a large, accurate, ground plane must be provided (not a trivial task and found to cost considerably more than the savings in the cost of material to make the lens) and the feeds will, in many instances, block the signal path. It is for these reasons that the full spherical Luneburg lens is preferred where possible to the 'virtual source' configuration.

The Luneburg lens was first proposed by Luneburg in 1944 [15]. Since that time a number have been built ranging in size from a diameter of 26 metres (configured as a 'virtual source' lens) down to a few centimetres; the lenses have been used successfully as scanning and multi-beam antennas. Some researchers have investigated variants of the lens in the form of discrete shell structures. An example of one of the earlier successes of this approach is reported in [16] and the results of a more recent investigation can be found in [17]. While a number of lenses are currently commercially available, utilisation of the Luneburg lens to-date has been somewhat limited. The problem relates to one of low-volume manufacture and the availability of suitable dielectric materials in terms of cost, weight and loss. For example, the commercially available KONKUR lens [18] has a diameter of 0.9 m and weighs 90 kg. Despite innovation construction techniques, the transmission loss (~ 1 dB) is unacceptably high for radio astronomy applications. However, with the SKA and the need for a large number of antenna elements, the economies of scale exist to develop and improve the Luneburg lens in ways which make it viable, both for the SKA and communications applications.

B3.2 ADVANTAGES AND LIMITATIONS

The Luneburg lens combines the advantages of optical beam forming over a complete field of view with inherently very wide bandwidth capability. Its main attraction for the SKA is the ease in which multi-beaming and source tracking can be achieved.

For multi-beaming the Luneburg lens offers the following unique set of features:

1) a single feed per beam;

2) by symmetry, the beam shapes are invariant with scan angle, and, by implication, no gain loss on scan;
3) because of the continuous aperture, frequency dependent scan blindness (a phenomenon common in phased arrays) does not occur;
4) the optical beam forming is inherently wide band, giving true time-delay beam forming throughout;
5) each beam can access any part of the sky.

The primary disadvantages of the Luneburg lens are:

1) the inevitable loss through the lens (this will always be a limiting factor on the maximum size of lens and upper frequency of operation that can be used);
2) the weight of the lens and the need to support it in a way which minimises the distortion of the dielectric material under gravity;
3) the unknown longevity of the dielectric, given its potential susceptibility to UV radiation and moisture ingress;
4) the cost, especially for larger diameters, as the volume increases by D^3;
5) possible difficulties in manufacturing the lens.

These issues will be addressed in the appropriate sections below.

B3.3 DESIGN CONSIDERATIONS

B3.3.1 GENERAL

We consider the general design parameters for the Luneburg lens. In Fig. B1, the maximum illumination half angle, θ_{max}, by the feed on the lens is a function of f/D and this dependency is shown in Fig. B3. For the focus close to the lens surface a wide beamwidth feed is required but the feed beamwidth required reduces significantly as f/D increases from 0.5 to around 0.7. The refractive index profile is also dependent on the f/D ratio of the lens. For a range of f/D ratios of practical interest, the relative permittivity of the dielectric material within the lens is plotted in Fig. B4 as a function of the normalised lens radius. It is seen that the maximum value of permittivity, ε_{max}, occurs in the centre of the lens and that this maximum value reduces in inverse proportion to f/D. This is demonstrated further in Fig. B5 where ε_{max} is plotted as a function of f/D. As we will discuss below, a low a value of ε_{max} (consistent with other requirements) is desirable to minimise the weight and loss of the lens and the ability to manufacture. From Fig. B5 we note that increasing f/D above 0.5 to around 0.7 to 0.8 makes an initial substantial reduction in ε_{max}. To utilise this desirable reduction in the maximum value of refractive index we note from Fig. B3 that a relatively narrow-beam feed is required with $\theta_{max} < 45°$.

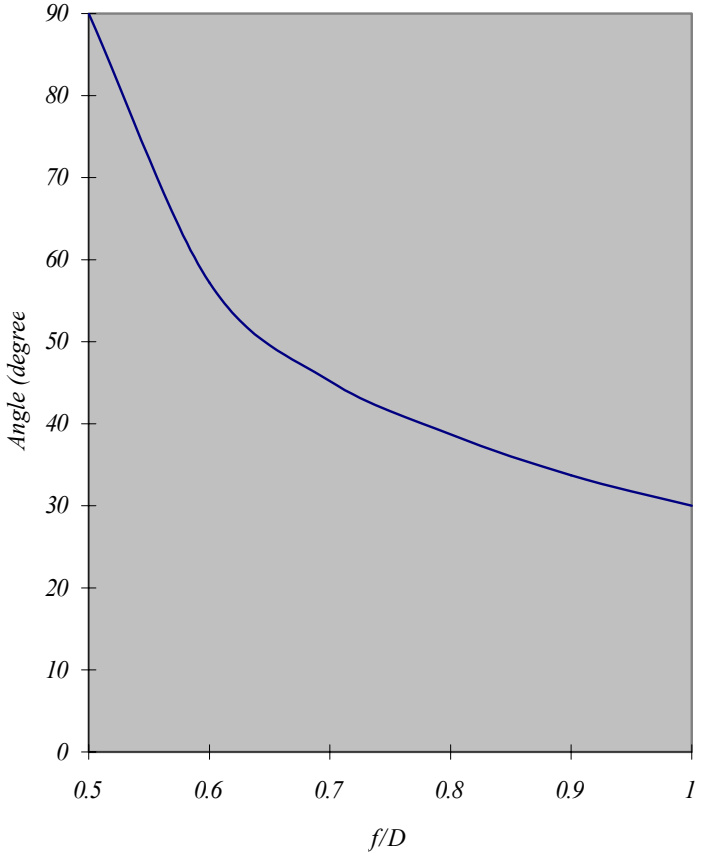

Figure B3: Maximum Feed Illumination Half-Angle

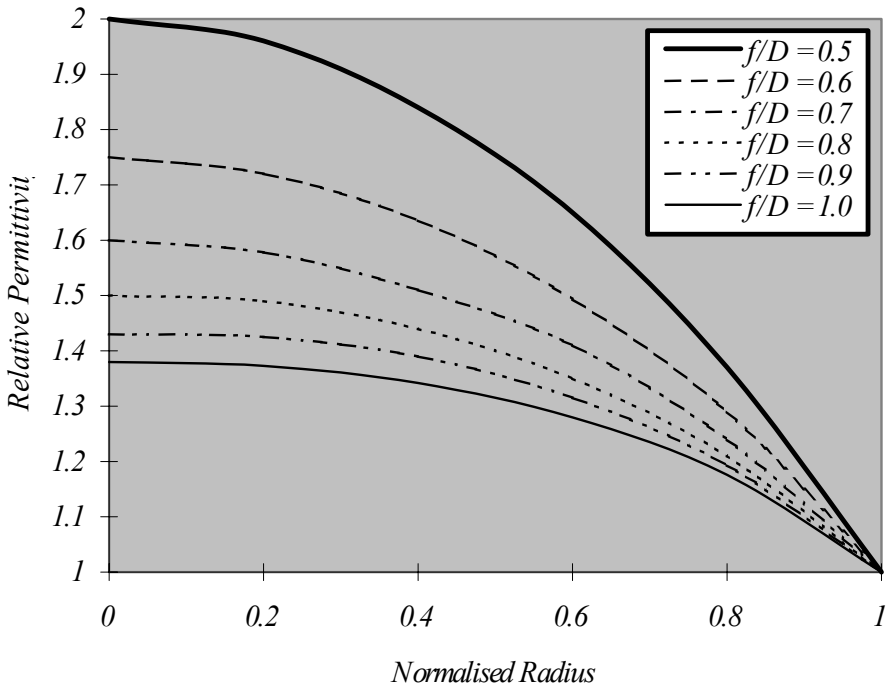

Figure B4: Permittivity Profiles for Luneburg Lens

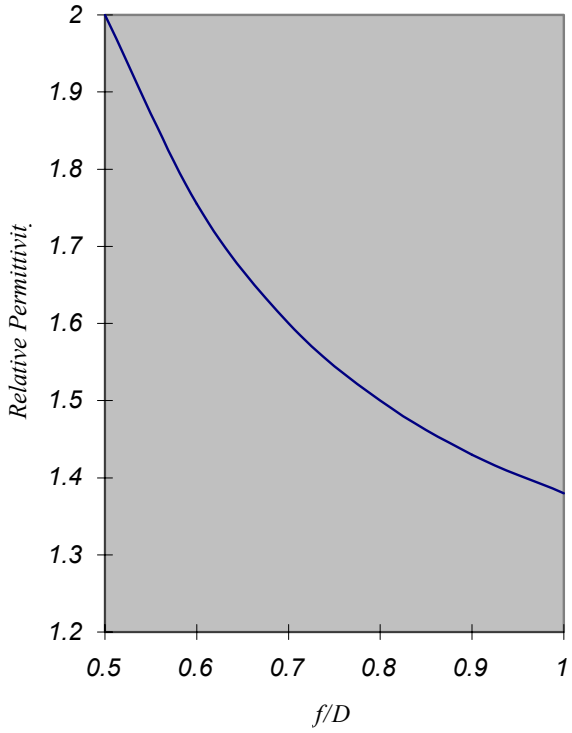

Figure B5: Maximum Permittivity as a function of f/D

B3.3.2 SKY COVERAGE

Given suitable mechanical arrangements, a stand-alone Luneburg lens with an appropriate feed can place a beam anywhere on the sky. Furthermore, this beam is free from blockage. In practice structure supporting the lens will modify this ability to some extent. Furthermore, when extra feeds are added some additional blockage is possible under some circumstances. For example, for an $f/D = 0.5$ where the lens surface is also the focal surface, feeds on opposite sides of the lens will be in the signal path of each other for beams less than 45° in elevation. Unless there are a large number of multiple feeds this will not be of great concern. (Such blockage is common in many reflector antenna installations.) Nevertheless, the region of totally unblocked aperture is a measure of the 'quality' of the antenna element. For the Luneburg lens the elevation angle at which blockage can occur is a function of f/D and this is plotted in Fig. B6. It is seen that the minimum blockage angle decreases rapidly initially with increasing f/D to a value around 0.65 after which the decrease is much less pronounced.

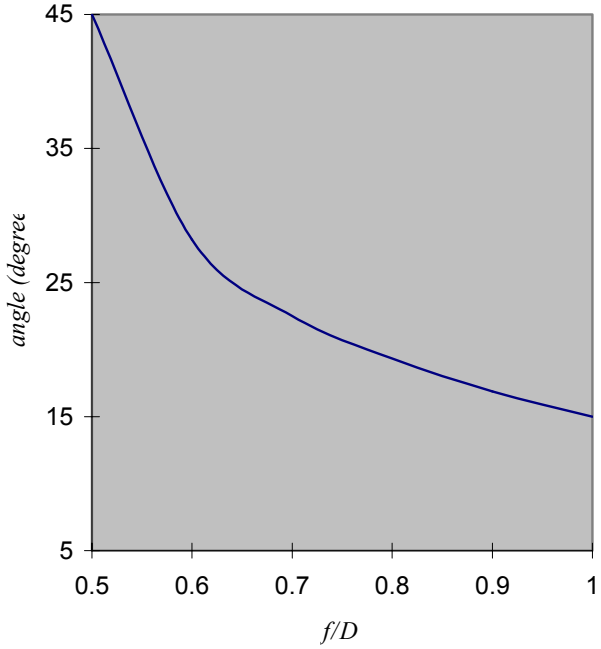

Figure B6: Minimum elevation angle for no blockage effects in the beam from a Luneburg lens

When elements are placed in an array station blockage will occur between adjacent elements and, depending on the configuration and spacing between the elements, the blockage elevation angle will vary with azimuthal direction. In some directions, for example, coverage to the horizon may be desired and to accomplish this the station elements will need to be configured to avoid inter-element blockage.[*]

[*] This problem of inter-element blockage is also common to other designs such as a steerable reflector antenna where the effect is the same as a full spherical lens. For the cylindrical reflector 'doublet' design [4], where the antenna is fixed in elevation, the spacing is reduced slightly and the problem is avoided altogether in a design such as the phased array tile [2].

B3.3.3 DIELECTRIC MATERIALS

To construct the lenses for the SKA out of conventional dielectric materials is not a viable proposition given weight, loss and cost considerations. From the outset, the CSIRO SKA proposal utilising the Luneburg lens has been contingent on the successful development of artificial dielectrics where weight, loss and cost are reduced to a significant degree compared to presently available materials. A joint project between four CSIRO divisions* is underway to develop suitable artificial dielectric materials for constructing the Luneburg lens. While details cannot be given here as there are patents pending on some of the processes involved, in outline, low density (20 kg/m^3) low loss (loss tangent < 0.0001) foam is being doped with graded small amounts of high dielectric low loss ceramics such as rutile (4,250 kg/m^3; $\varepsilon_r \approx$ 100; loss tangent < 0.001) to produce artificial low loss (loss tangent ~ 0.0001) low permittivity ($\varepsilon_r < 2$) dielectrics.

Assuming an artificial dielectric can be constructed from the materials above, we can make some estimate as to the loss, weight and the cost of the lenses.

B3.3.4 LOSS

With regard to loss through the lens, our calculations show that it can be given to a good approximation by the simple formula

$$\text{Loss (dB)} \approx \sqrt{\underline{\varepsilon}_r} \times \delta \text{ (loss tangent)} \times \mathcal{D}\,\text{(m)} \times \text{Frequency(GHz)} \times 100 \qquad \text{(B2)}$$

where $\underline{\varepsilon}_r$ is the mean value of permittivity through the lens as shown in Fig. B7.

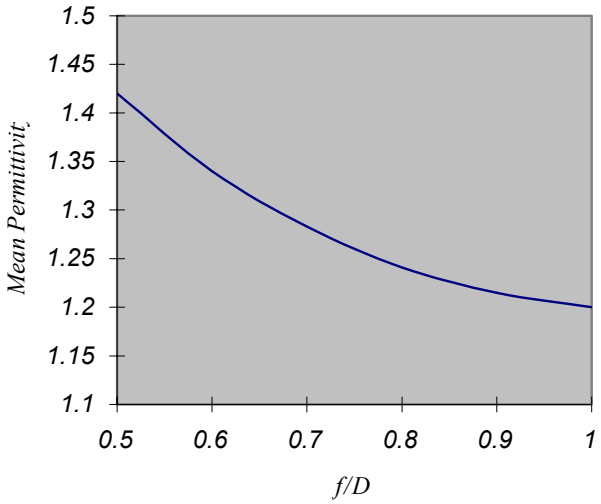

Figure B7: Mean permittivity as a function of f/D

Assuming a loss tangent of 0.0001, Fig. B8 plots the loss through a 10m-diameter lens at a frequency of 1 GHz. The loss is only weakly dependent on $f/\mathcal{D}$ with small gains made when $f/\mathcal{D} \geq 0.7$. At 1 GHz it is seen that the loss introduced by the lens is relatively modest at ~ 0.1 dB. For other diameters and frequencies a simple multiplication is required. For example, at 5 GHz (the highest operating frequency

* CTIP (CSIRO Telecommunications and Industrial Physics) and ATNF (Australia Telescope National Facility) based at Marsfield, Sydney, and CMS (CSIRO Molecular Science) and CMST (CSIRO Manufacturing Science and Technology) based in Clayton, Melbourne.

anticipated for the Luneburg lens) the loss is 0.5-0.6 dB and at 12 GHz the loss increases to ~ 1.3 dB. The latter figure may be unacceptable in some instances and, even at 5 GHz, the loss may be higher than desirable. Thus, if we wish the lens to operate up to 5 GHz a somewhat smaller diameter may be preferable. Therefore, we assume for our purposes here that a 10m-diameter represents an upper limit for the size of the lens.

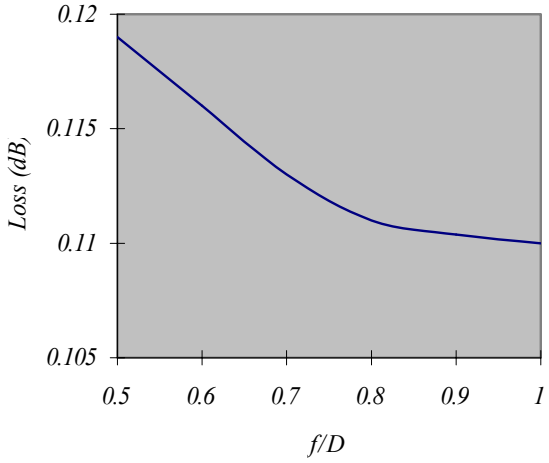

Figure B8: Loss for a 10 m diameter lens at 1 GHz (loss tangent of dielectric = 0.0001)

B3.3.5 WEIGHT AND SUPPORTING STRUCTURE

The weight for a 10 m-diameter lens (the maximum diameter we are likely to use) as a function of f/D is plotted in Fig. B9 assuming it is constructed from the materials discussed in section 3.3.3. (The weight for smaller lenses is of course given by multiplying these results by the factor $0.001 \times D^3$(m)). The parameter α refers to the amount of doping of rutile assumed (where α is the percentage of doping required to achieve a maximum permittivity of 2). The special case $\alpha = 0\%$ is for an un-doped foam sphere. With $\alpha = 1\%$ representing our most optimistic estimate of how much doping is required, the inclusion of rutile increases the weight considerably, especially for low f/D where higher values of permittivity are required. We anticipate at this stage that the doping required will be between 1-2%, so in Fig. 9 we have given the case for 2% doping (an expected upper limit) to show the degree of increase in weight.

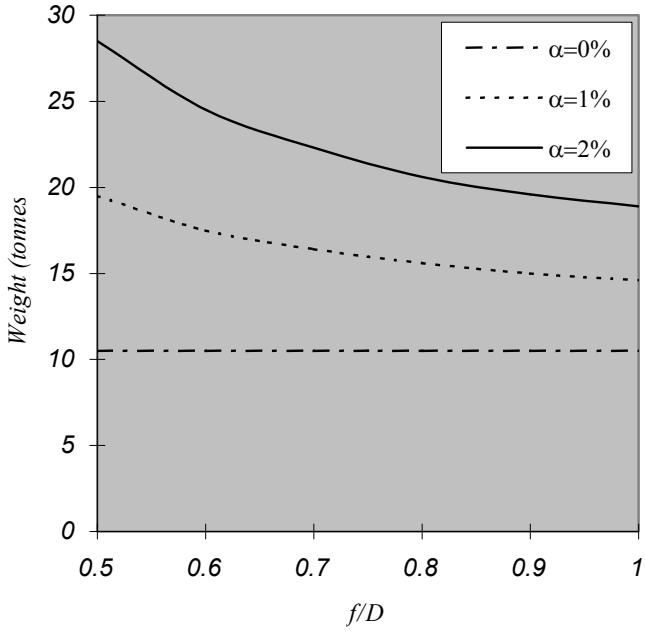

Figure B9: Estimated Weight for a 10m-Diameter Lens Constructed from Artificial Dielectrics

To support the lens above the ground and to allow for maximum feed movement, a simple circular post of diameter d as shown in Fig. B10 will suffice where, for small θ (< 60°), $d/D \approx 0.5 \times \theta$. Depending on the d/D ratio and the characteristics of the material, the sphere will deflect by an amount δ due to gravity. As a first approximation for low-density foam (20 kg/m^3), we get*

$$\delta/D \approx 5\tau \times D \text{ (metres)} \times \ln [4/\theta \text{ (radians)}] \times 10^{-5}\,;\ 0^\circ << \theta < 60^\circ \qquad \text{(B3)}$$

where τ is the ratio of the weight of doped to an un-doped lens deduced from Fig. B9; note τ is function of both f/D and doping factor α. For values of diameter of interest here, where D ≤ 10m, the maximum value for the ratio δ/D is < 0.003 assuming acceptable values of d/D (and hence θ). Detailed calculations on the effect of this lens distortion for specific examples using an accurate finite element approach are given in Appendix C, where the results confirm that the values of deflection are small enough to have only a minor impact on the performance of the lens. Two other points to note here: 1) it is possible in the manufacture of the lens to pre-distort its shape if necessary so that, with gravity loading, the spherical shape is recovered; 2) since any feed under the lens will be limited by the supporting post for the lens to a minimum angle of $\theta/2$ from zenith, this part of the sky cannot be viewed, but this is only a small percentage, υ, of the total sky given by (with θ in radians)

$$\upsilon \approx 12.5 \times \theta^2 \approx 50 \times (d/D)^2\,;\ \% \qquad \text{(B4)}$$

* This calculation is due to Paul Thompson, ATNF vacation student

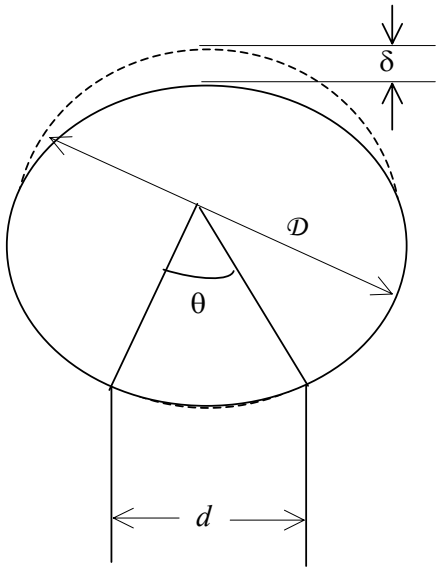

Figure B10: Spherical deflection due to gravity

B3.3.6 MANUFACTURING AND INSTALLATION COSTS

The total quantity of material required for the SKA lenses is directly proportional to the lens diameter. Figure B11 shows the obvious square-law relation between the element diameter and the number of elements, *n*, required.

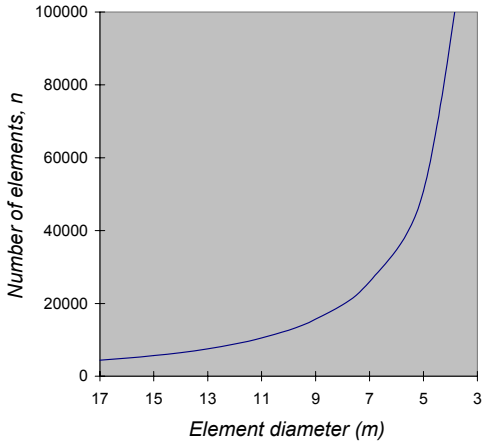

Figure 11: Number of SKA elements v. element diameter

For our maximum value for the diameter of 10 m (which, as discussed above, is limited by the loss through the lens) we need almost 13, 000 elements increasing to nearly 80,000 elements for a 4m diameter lens. Aside from the rapid increase in the number of elements, the lens cannot be much smaller than this if it is to operate down to 0.3 GHz effectively. Therefore, for our purposes here, we consider lens diameters in the range 4-10m only. Within this range the number of elements remains large and given this quantity, it would be advantageous to spend a reasonably large sum of money in tooling-up to construct the lenses. Since the process in making a lens is not especially sophisticated as it basically requires foaming into a mould, we estimate a figure of around US$30M or less should suffice to design a largely automatic and portable process to manufacture the lenses. For simplicity and in view of having no additional information we assume this estimate is independent of lens diameter.

A peculiar advantage of the Luneburg lens solution is that, with a little thought, it can involve a minimal amount of earth works with subsequently significant cost savings especially having in mind the likelihood of the antennas being located in remote sites. As the lenses are static they need only be supported sufficiently high above the ground to allow for feed movement. A possible low-cost scheme is outlined in Fig. B12 where a number of key parameters has been identified.

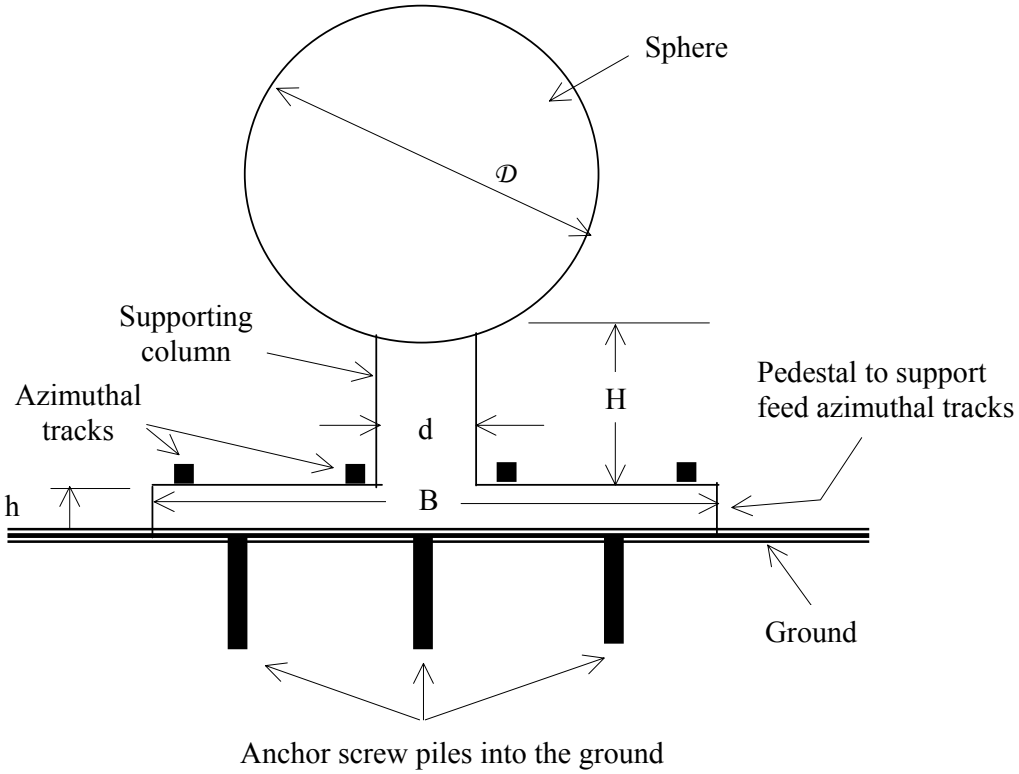

Figure B12: Schematic sketch of the lens installation on the ground

The concept behind the construction illustrated schematically in Fig. B12 is to minimise cost, especially with regard to materials, machinery and the amount of earth works required. The whole structure is based around polystyrene foam. This material, given its cheapness, insulation properties, longevity and its ease of moulding into any shape desired, is used extensively in the packaging and building industries. For the SKA application we envisage portable automated tooling assemblies to fabricate everything *in situ*. We have already mentioned such tooling to construct the lens. To this we add a separate and far less accurate or elaborate tooling set-up to mould the supporting column and pedestal assembly as shown in Fig. B12. The column supports the lens and the pedestal provides a flat surface on which to mount the feed azimuthal tracks. The pedestal would not be completely filled-in but, to reduce the amount of material required, have a number of spokes as shown in Fig. B13.

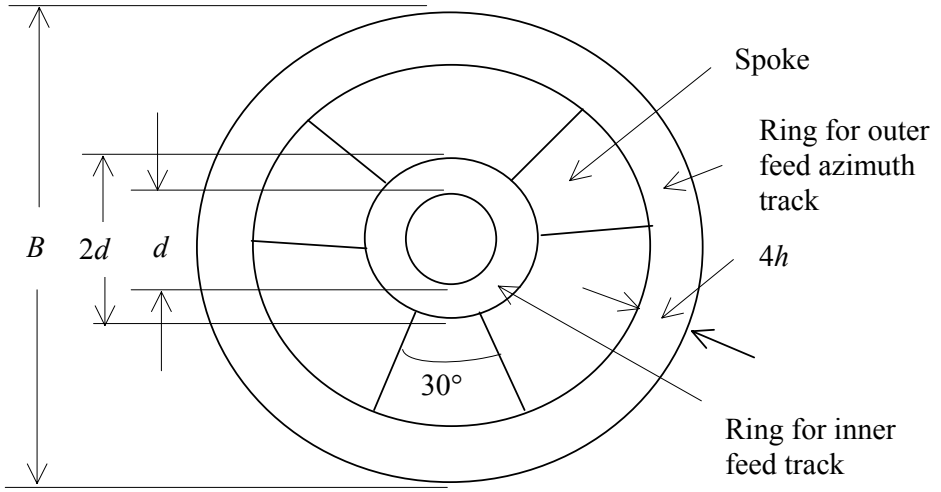

Figure B13: Details of the support base for the lens

By fabricating *in situ*, we need only take to the site the pre-foamed stage polystyrene resin granules and the rutile powder for mixing into the moulding process to form the variable dielectric lens thus minimising substantially transportation costs. The only earth works required are the rough clearance (as necessary) of the ground area within the circle of diameter B and the drilling of location holes for the screw piles that hold the structure to the ground (Fig. B12)[#].

Of the various parameters in Figs. B12 and B13, the column diameter d needs to be large enough to support the lens. Calculations show that a value for $d \approx D/4$ provides sufficient support and, from equation (B4), blocks-out a small percentage of the sky around zenith of just over 3%. The base diameter B needs to be large enough to support the feed outer azimuthal track. This is a function of the focal length f and the radial feed movement required. From our feed design given later we have $B \approx 2f + 3$ metres. The height of the pedestal h needs only be sufficiently large to smooth out the small-scale ground variations and should be proportional to B. To this end we set h/f to be ~ 0.05. The height H needs to be large enough to allow for the feed movement and for our feed design we have $H \approx f - D/2 + 1.5$ metres. We calculate the total amount of foam required as a function of both f/D and lens diameter and add the amount of rutile we need as deduced from the 10m-diameter lens example in Fig. B9.

The cost of foam and rutile materials, together with fixed set-up costs such as tooling, equipment and labour, will dominate the cost of building the structure shown in Figs B12 and B13. The lowest cost we are likely to achieve is US$1k/tonne for the foam and $US1.5k/tonne for the rutile.[#] These are unlikely to change greatly over the next

[#] The plausibility of the structural scheme presented here has been verified by building and structural experts within CSIRO Building, Construction and Engineering. Many more detailed calculations, such as those relating to estimation of material creep, insulation of the lens by an outer later of foam, the establishment of daily and annual dimensional variations that can be tolerated etc.are of course required.

[#] I am indebted for these costings to Richard Donelson (CMST) and Mike O'Shea (CMS) of Clayton, Victoria.

decade unless there is a substantial increase in petroleum prices, in which case this would affect the cost of the foam.

Other cost components include the feed azimuth and altitude tracks, and to finish the structure, a thin layer of a tough coating material (such as a gel coat) to protect the foam from birds and vermin. It will also provide further protection to UV radiation and the ingress of water, although foam is inherently highly impervious to both of these effects. The remaining cost is that of the support arm fitted to the azimuthal tracks to drive the feed in elevation plus the cost of the feed and LNA. Again, given the quantity of track, elevation arms and feeds, it will be essential to allow for the development of automatic tooling.

The cost estimates (rounded to the nearest US$m) for the antenna components are itemised in Table B2. What is immediately striking about these figures is the domination of the material costs. This is shown in both the f/D and D dependency on cost. For smaller lenses where the number of elements increases substantially, this domination still applies. Note that we have re-compiled an original version of Table B2 with new performance assumptions for uncooled systems; these assumptions are the same ones used in Section 15 and Appendix D.

While our first estimates are for component costs alone, more extensive studies are needed to determine fabrication and installation costs. A rough first estimate might allow US$30m to cover the cost of machinery and tooling costs to manufacture the antennas on-site. To this we must add the labour and accommodation costs. Assuming each person costs US$100k per year and that we need around 100 persons over four years to construct the SKA antennas, the labour component adds another US$40m to the cost.

TABLE B2

Estimated costs in US$m for the construction of the antenna component of the SKA

		f/D					
D	**Item**	**0.5**	**0.6**	**0.7**	**0.8**	**0.9**	**1**
4m	**Lenses in Array**	**151,059**	**150,603**	**150,285**	**150,051**	**149,871**	**149,730**
	Foam	110	114	118	124	130	137
	Rutile (1.5%)	213	173	145	124	108	96
	Azimuth tracks	21	23	25	27	29	31
	Coating	23	23	23	23	23	23
	Feed arm	344	343	342	342	341	341
	Feed & LNA	104	104	104	103	103	103
	Total	815	779	756	742	734	730
5m	**Lenses in Array**	**99,221**	**98,852**	**98,595**	**98,406**	**98,261**	**98,147**
	Foam	139	144	149	156	163	172
	Rutile (1.5%)	274	222	185	159	139	123
	Azimuth tracks	16	18	19	21	22	24
	Coating	23	23	23	23	23	23
	Feed arm	226	225	224	224	224	223
	Feed & LNA	68	68	68	68	68	68
	Total	747	699	670	651	639	633
8m	**Lenses in Array**	**41,801**	**41,563**	**41,398**	**41,276**	**41,183**	**41,110**
	Foam	236	243	251	261	273	287
	Rutile (1.5%)	472	381	319	273	238	211
	Azimuth tracks	10	11	12	13	14	15
	Coating	25	25	25	25	25	25
	Feed arm	95	95	94	94	94	94
	Feed & LNA	29	29	29	28	28	28
	Total	867	783	729	694	672	659
10m	**Lenses in Array**	**28,085**	**27,891**	**27,756**	**27,657**	**27,581**	**27,521**
	Foam	307	316	326	339	354	371
	Rutile (1.5%)	620	500	417	357	311	276
	Azimuth tracks	8	9	10	10	11	12
	Coating	26	26	26	26	26	26
	Feed arm	64	63	63	63	63	63
	Feed & LNA	19	19	19	19	19	19
	Total	1,045	934	862	815	784	767

B3.3.7 A PREFERRED DESIGN

B3.3.7.1 Choice of f/D

From the above information, we can begin to arrive at a suitable design for the Luneburg lens SKA antenna element. The choice of parameters for the lens is very simple; a value for f/D and for D is the only requirement. In terms of feed illumination angle, maximum permittivity, blockage issues, loss, cost and weight, it is obvious that an $f/D \geq 0.7$ is highly desirable. However, the larger the f/D the further (for a given D) the lens needs to be supported from the ground and the larger the feed antenna required with smaller maximum feed angle, θ_{max} (Fig.B1). Choosing an f/D in the range 0.7-0.8 seems a good choice given these conflicting requirements. The maximum permittivity in the centre of the lens is only 1.5 to 1.6 and with $\theta_{max} \sim 42^o$ (Fig. B3), we now show that this is an excellent fit to an available wide-band feed.

B3.3.7.2 Feed Design

To a first approximation, if we set the half power beamwidth (HPBW) equal to θ_{max}, the feed radiation pattern level at θ_{max} will be in the vicinity of 12-15 dB below the on-axis value and this gives close to optimum η/T performance. Given the two engineering drivers of low cost and wide bandwidth, frequency independent antennas [B19] are an ideal place to start for the feed design where we required HPBW ~ 42º. Since the lens has a focal surface, it would appropriate if the phase centre of the feed remained on this surface across the 0.3 – 5 GHz bandwidth. A possibility is the flat spiral antenna [B19] but, aside from its broad beamwidth, it has a bi-directional radiation pattern that is unsuitable for the application here. If placed over a ground plane to suppress the back radiation the performance is relatively poor with quite a restricted bandwidth. Another possibility is a broadside periodic design [B20]. This antenna type has received little attention to date but for our application is unsuitable as it is difficult to see how it could be designed for dual polarisation. Log-periodic antennas are well studied [B21] but difficult to achieve the required HPBW of ~ 42º with pattern symmetry. Some more recent designs have investigated the Vivaldi fin-line [B22], [B23] but, while these may be useful in dense, active, arrays (and possibly as a cluster feed for a lens), they offer little promise as isolated elements; they tend to be very large for a given HPBW and require special treatment, such as the use of absorbers, to achieve a reasonable radiation pattern.

From a survey of possible suitable feed designs, we favour the zigzag antenna described in [B19], [B24] and shown in Fig. B14(a). This antenna is pyramidal in shape with the same zigzag configuration on all four sides. It provides dual linear polarisation, is very simple in construction, compact in size for its beamwidth and essentially self-scaling in frequency with a HPBW which is highly symmetrical, particularly as the HPBW becomes narrower. Our requirement of ~ 42º HPBW is ideally suited to this design.[*] The only disadvantage, which applies to all end-fire antenna types, is that since the phase centre moves along the antenna with frequency, we will need radial movement of the feed to retain optimum performance.

[*] It is interesting to note that this particular zigzag design appears to be the basis of the feed for the Allen Telescope [6].

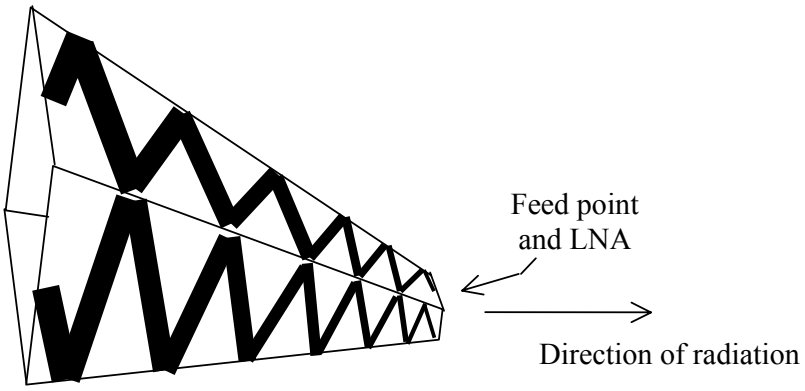

Figure B14(a) Dual polarisation frequency independent zigzag antenna

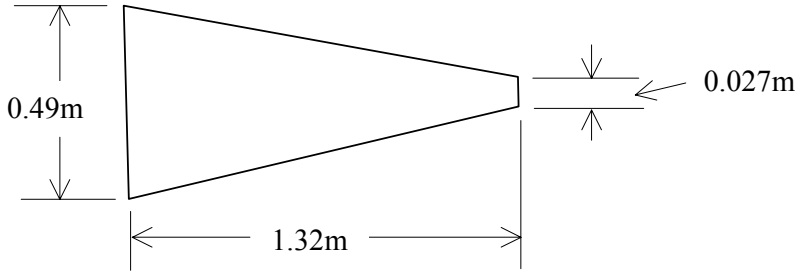

Figure B14(b) Outline dimensions for a 0.3 – 5 GHz feed

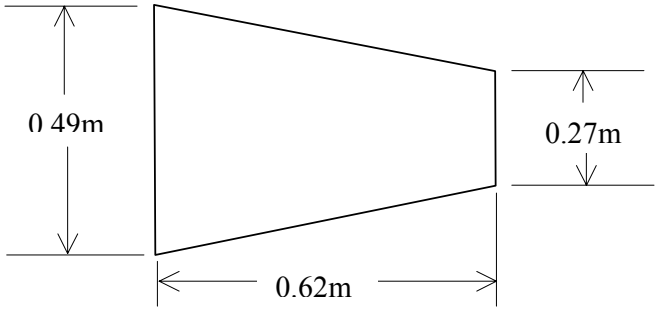

Figure B14(c): Outline dimensions for a 0.3 – 0.5 GHz feed

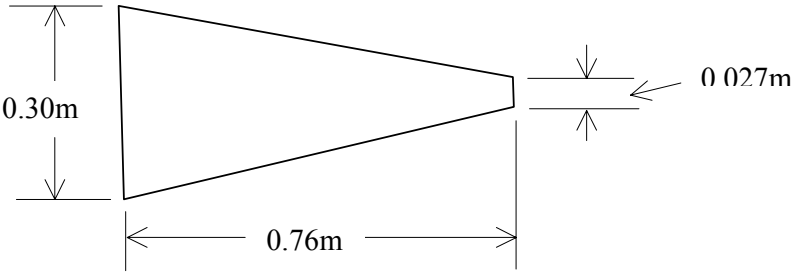

Figure B14(d): Outline dimensions for a 0.5 – 5 GHz feed

From the design information in [B19], we have designed an antenna with an HPBW ~ 42º with as short a length as possible. Alternative designs are shown in Fig. B14. Note that the length of the feed is 1.32m to cover the entire 0.3 – 5 GHz band. If we reduce the lower limit to 0.5 GHz the feed length reduces considerably to 0.76m. Given the rapidly increasing feed dimensions with frequency, there may be a case to cover the 0.3 – 0.5 GHz band with a separate feed of length 0.62m as shown in Fig. B14. This latter feed could be in a fixed position with little loss in gain at the band extremities. Another advantage of splitting the band in this way is to limit the amount of radial feed movement required. In our calculations and costing above, we allowed 1.5 m for the feed travel but this can be almost halved by using a separate lower band feed.

Given the basic simple structure of the zigzag antenna, it is conceivable that it can be made, together will a low-cost uncooled LNA, very cheaply and a figure of US$100 would seem to be a conservative estimate. This figure has been included in Table B2.

While we have concentrated on the zigzag feed, other antenna types may be appropriate in the future as time and money allow. For example, a multi-beam phased array feed based around the THEA feed design [B25] would be an alternate means of providing multiple beams within the FOV. However, it will be difficult to surpass the zigzag antenna's economic advantage. At frequencies below 300 MHz, however, the zigzag design may be too bulky and simple dipole feeds (Section 7-4) are a more likely option.

B3.3.7.3 Choice of lens diameter

As mentioned earlier, the Luneburg lens solution to the SKA antenna element will involve small diameter lenses probably no larger than 7m in diameter with a lower limit of 4m set by the need to operate down to 0.3 GHz. Figure B15 shows an outline of a possible Luneburg lens configuration where two feeds cover the 0.3 – 5 GHz bandwidth as discussed earlier. As mentioned earlier, we have performed an accurate finite-element analysis on the structural deformation of the lens under gravity for a 5m and 7m diameter lens and the results are given in Appendix C.

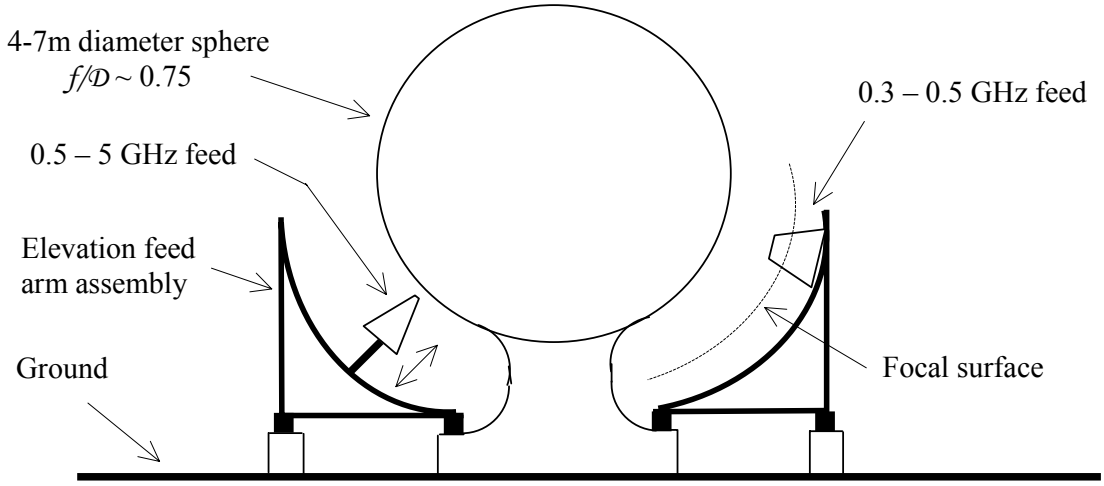

Figure B15: Outline of a preferred option

ACKNOWLEDGMENTS

The author is indebted to a number of people in preparing this appendix: to Drs W. Brouw, J.D. Bunton, R.N. Norris and P. Hall on astronomy and general SKA matters; to Drs B. MacA. Thomas, J.S. Kot and A.J. Parfitt on antenna related issues; to R.G. Gough on receiver issues; to Dr P Paevere, S Burn, M Syme, P. Thompson, B.F. Parsons and B. Wilcockson on structural and mechanical issues; and to Dr R. Donelson and M. O'Shea on materials for artificial dielectrics.

REFERENCES

[B1] A.R. Taylor and R. Braun (Eds), "Science with the Square Kilometer Array", University of Calgary, March 1999. [Available at: http://www.ras.ucalgary.ca/SKA/science/science.html]

[B2] G.A. Hampson, R.De Wild and A.B. Smolders, " Efficient Multi-Beaming for the Next Generation of Radio Telescopes", *Perspectives on Radio Astronomy: Technologies for Large Antenna Arrays* (ASTRON), edited by A.B. Smolders and M.P. van Haarlem, pp265-276.

[B3] G.L. James, A.J. Parfitt, J.S. Kot and P. Hall, "A Case for the Luneburg Lens as the Antenna Element for the Square Kilometre Array Telescope", The Radio Science Bulletin, June 2000, pp32-37.

[B4] G.L. James and A.J. Parfitt, "A Proposal for the 1kT Antenna", *URSI General Assembly*, Toronto, Canada, August 13-21, 1999, p549.

[B5] J. D. Bunton, Cylindrical Reflector SKA, SKA concept to be submitted, June 2002.

[B6] P. Dewdney, "The Large Adaptive Reflector for the SKA", *The URSI Large Telescope Working Group Meeting and 1kT International Technical Workshop*, Sydney, Australia, 15-18 December, 1997, Section C2.

[B7] J.W. Dreher, "The One Hectare Telescope (1HT) project", *Perspectives on Radio Astronomy: Technologies for Large Antenna Arrays* (ASTRON), edited by A.B. Smolders and M.P. van Haarlem, pp33-36.

[B8] B. Peng *et al*., "The Technical Scheme for FAST", *ibid.,* pp43-48.

[B9] J.D. Bregman, "Design Concepts for a Sky Noise Limited Low Frequency Array", *Perspectives on Radio Astronomy: Technologies for Large Antenna Arrays* (ASTRON), edited by A.B. Smolders and M.P. van Haarlem, pp23-32.

[B10] C. Jackson, "SKA Science: A Parameter Space Analysis", http://www.mso.anu.edu.au/~cjackson/downloads/

[B11] C.J. Lonsdale, "Frequency-Dependent Tradeoffs in Array Configurations", SKA Meeting, UC Berkeley, July 2001.

[B12] G. Niu et al., "Noise Modeling and SiGe Profile Design Tradeoffs for RF Applications', *IEEE Trans Electronic Devices*, Vol. 47, November 2000, pp2037-2044.

[B13] R.D. Ekers, Discussion paper on the SKA specifications, SKA Meeting, Bologna, January, 2002.

[B14] C.J. Lonsdale and R.G. Cappallo, "Concepts for a Large-N SKA", *Perspectives on Radio Astronomy: Technologies for Large Antenna Arrays* (ASTRON), edited by A.B. Smolders and M.P. van Haarlem, pp243-250.

[B15] R.K. Luneburg *The Mathematical Theory of Optics*, University of California Press, Berkeley, 1964.

[B16] S. Cornbleet, "A Simple Spherical Lens with External Foci", *The Microwave Journal*, May 1965, pp65-68.

[B17] H. Mosallaei and Y. Rahmat-Samii, "Non-Uniform Luneburg Lens Antennas: A Design Approach based on Genetic Algorithms", *IEEE AP-S*, Orlando, July 1999, pp431-437.

[B18] L. Li, D.B. Hayman, G.C. James and S.J. Barker, "Test Report for Luneburg Lens at Ku-Band", CSIRO Report, TIPP 1412, November, 2001 and "Test Report for Lunburg Lens at S-Band", CSIRO Report TIPP 1429, December 2001.

[B19] P.E. Mayes, *Frequency-Independent Antennas*, Chapter 9 in *Antenna Handbook* (Van Nostrand Reinhold) edited by Y.T. Lo and S.W. Lee, 1993.

[B20] K.K. Mei and D. Johnstone, "A Broadside Log-periodic Antenna", Proc. IEEE, Vol. 54, June 1966, pp889-890.

[B21] C.E. Smith (ed) Log Periodic *Antenna Design Handbook* (Smith Electronics, Inc), 1966.

[B22] A.K.Y. Lai, A.L. Sinopoli and W.D. Burnside, "A Novel Antenna for Ultra-Wide_Band Applications", *IEEE Trans Antennas and Propagation*, Vol. 40, July 1992, pp755-760.

[B23] Li-C.T. Chang and W.D. Burnside, "An Ultrawide-Bandwidth Tapered Resistive TEM Horn Antenna", *ibid*., Vol. 48, December 2000, pp1848-1857.

[B24] P.E. Mayes, "Balanced Backfire Zigzag Antennas", IEEE Int. Convention Record, 1964, pp153-165.

[B25] D.H. Schaubert and T-H Chio, "Wideband Vivaldi Arrays for Large Aperture Antennas", *Perspectives on Radio Astronomy: Technologies for Large Antenna Arrays* (ASTRON), edited by A.B. Smolders and M.P. van Haarlem, pp49-57.

APPENDIX C:

FINITE ELEMENT STATIC STRESS ANALYSIS OF A LUNEBURG LENS

WEI WU
CSIRO TELECOMMUNICATIONS AND INDUSTRIAL PHYSICS
PO BOX 218, LINDFIELD, NSW 2070, AUSTRALIA

With the use of dielectric materials to construct the Luneburg lens, there are questions about the degree of asymmetry suffered by the lens as a consequence of material creep and gravitational forces. Both effects, which stabilize over time, can be calculated accurately and, if necessary, the lens can be manufactured with a pre-distorted shape to counteract these effects if they are severe. We have yet to calculate the effects of creep but we have undertaken an initial study of the effects of gravitational forces on the lens geometry; some sample data are presented in this Appendix.

Our study makes use of accurate finite element stress analysis software where the problem is modelled as shown in Figure C1. The lens is approximated by five 'onion' rings and is supported on a circular column. The material properties and dimensions are noted below in the two examples quoted; one is for a 5 m diameter lens while the other refers to a 7 m diameter lens.

These initial results as presented below indicate that the lens distortion due to gravitational forces is not likely to have a significant adverse impact on the performance up to the maximum expected operating frequency of 5 GHz. However, in order to obtain definitive quantitative data on the lens performance, we intend doing a full electromagnetic analysis on the lens geometry under gravitational stress (the software has already been written). A similar study will be undertaken when we have results of lens distortion due to material creep.

EXAMPLE 1: LENS DIAMETER OF 5 METRES

Dimensions and Material Properties

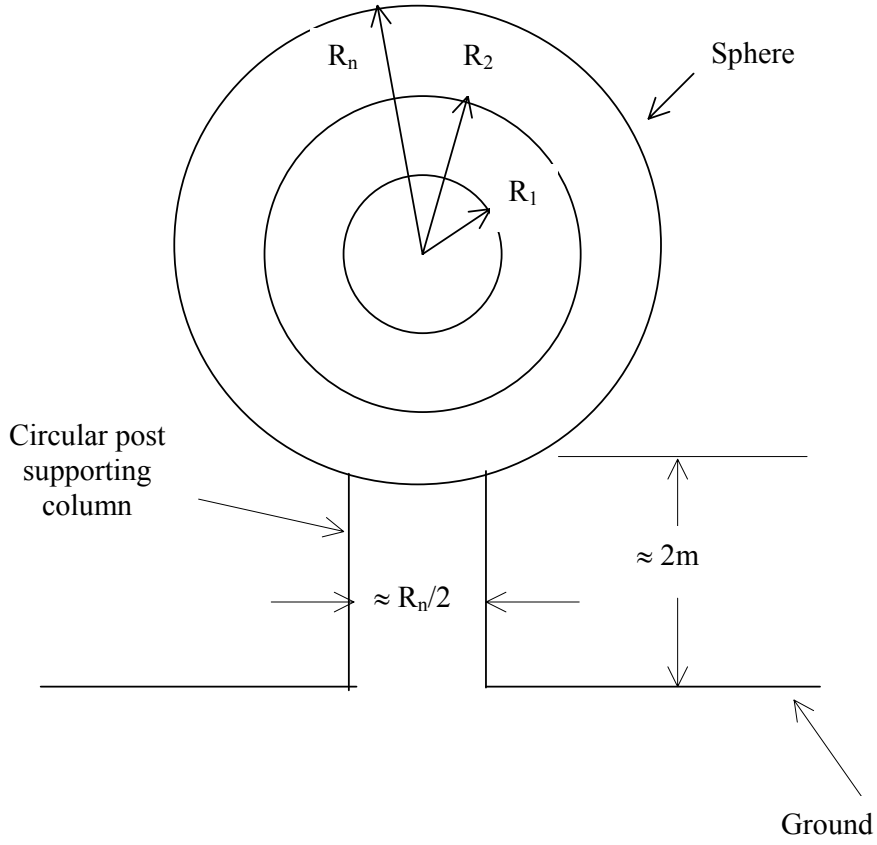

Figure C1

n	R_n	Weight
1	0.5m	71 kg/m^3
2	1.0m	67 kg/m^3
3	1.5m	63 kg/m^3
4	2.0m	50 kg/m^3
5	2.5m	33 kg/m^3

The basic material in the sphere and column is low-density polystyrene foam. where, in this example, we assume a density of 20 kg/m^3 and a Young's modulus, E, of $\sim 1.3 \times 10^6$ Pa. The extra weight in the table is due to the doping of rutile which, given the small quantities of doping, we assume has no affect on the structural properties of the composite material.

Region to be Modelled

Since the sphere and cylindrical support are axisymmetric, only a cross-section area in X-Y plane (see Figure C2) needs to be studied. The centre of the sphere is defined as the centre of the X-Y plane. The gravity force is assumed in Y-direction. Different colours show different densities.

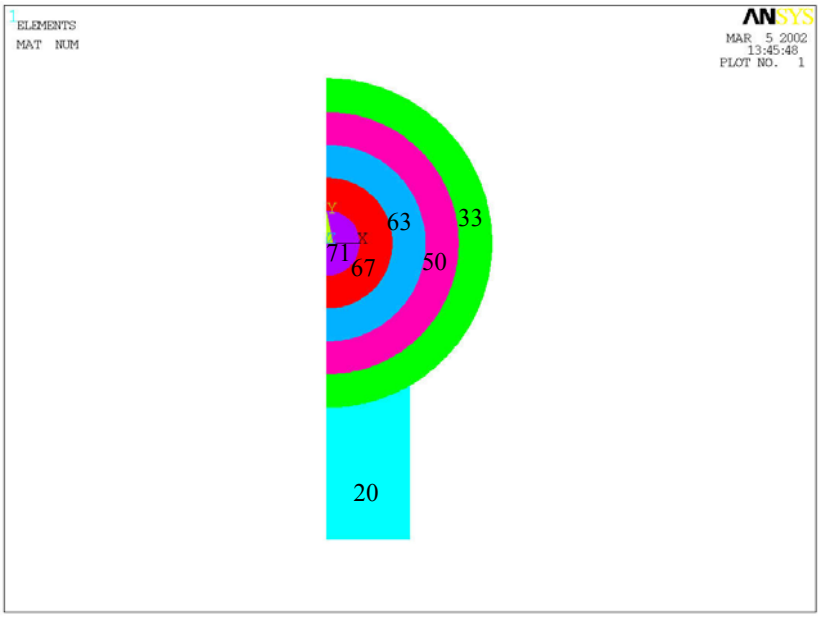

Figure C2: Region to be modelled

3 Results

The contours of displacements in meters under gravity are shown in the Figures below in the alternate order of:

Displacements along X-direction, U_x

Displacements along Y-direction, U_y

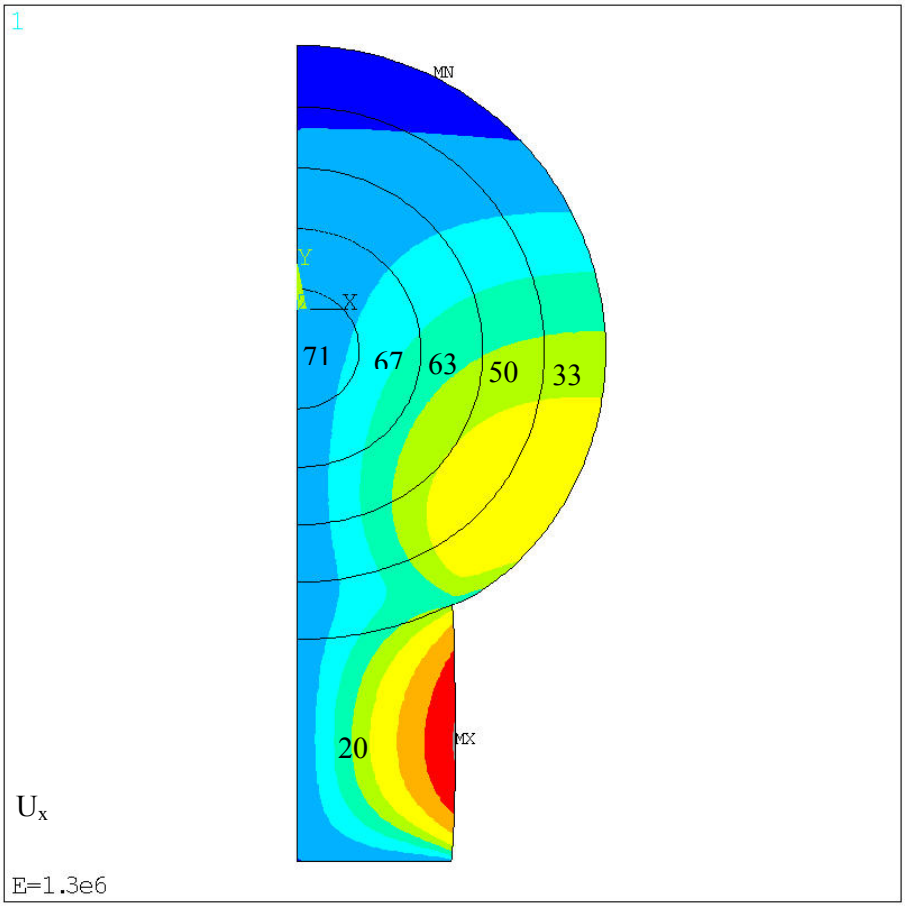
1
MN
71
67
63
50
33
20
MX
Ux
E=1.3e6
ANSYS 5.7
MAR 6 2002
12:04:45
PLOT NO. 1
NODAL SOLUTION
STEP=1
SUB =1
TIME=1
UX (AVG)
RSYS=0
PowerGraphics
EFACET=1
AVRES=Mat
DMX =.016034
SMN =-.897E-04
SMX =.001718
-.897E-04
0
.200E-03
.400E-03
.600E-03
.800E-03
.0011
.0014
.0017

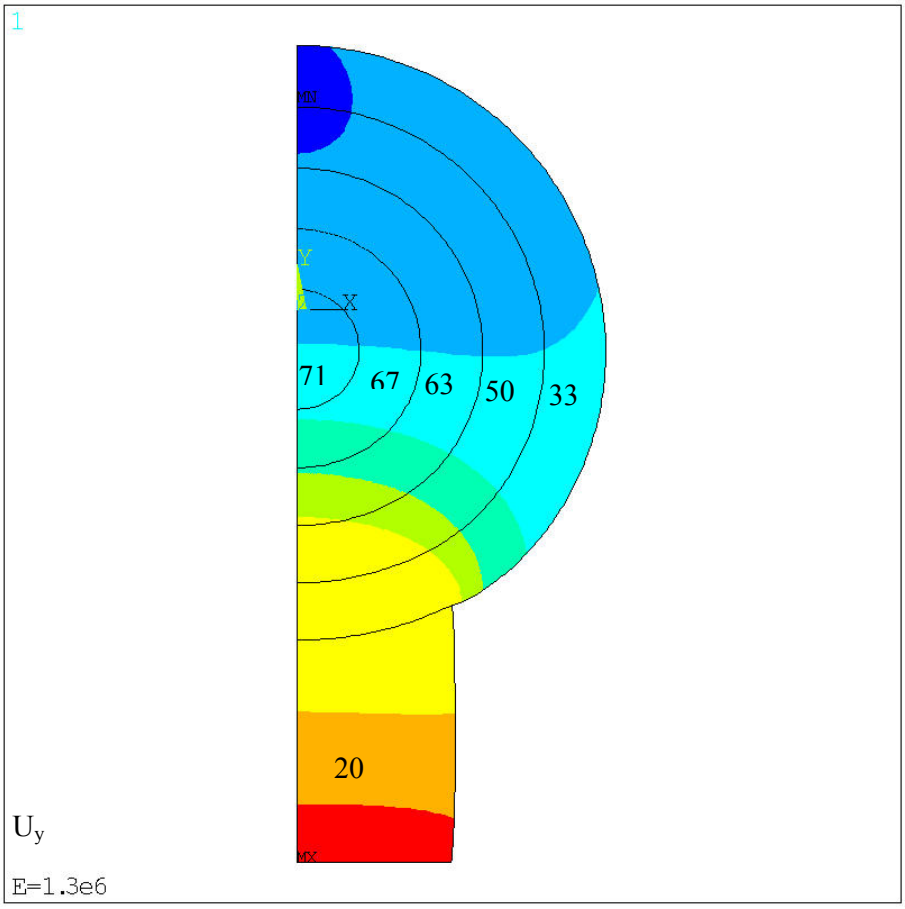
1
MN
71
67
63
50
33
20
MX
Uy
E=1.3e6
ANSYS 5.7
MAR 6 2002
12:19:18
PLOT NO. 1
NODAL SOLUTION
STEP=1
SUB =1
TIME=1
UY (AVG)
RSYS=0
PowerGraphics
EFACET=1
AVRES=Mat
DMX =.016034
SMN =-.016034
-.016034
-.016
-.015
-.014
-.013
-.012
-.006
-.002
.100E-10

EXAMPLE 2: LENS DIAMETER OF 7 METRES

The results following are for a 7 m diameter lens using the same procedures as in the first example.

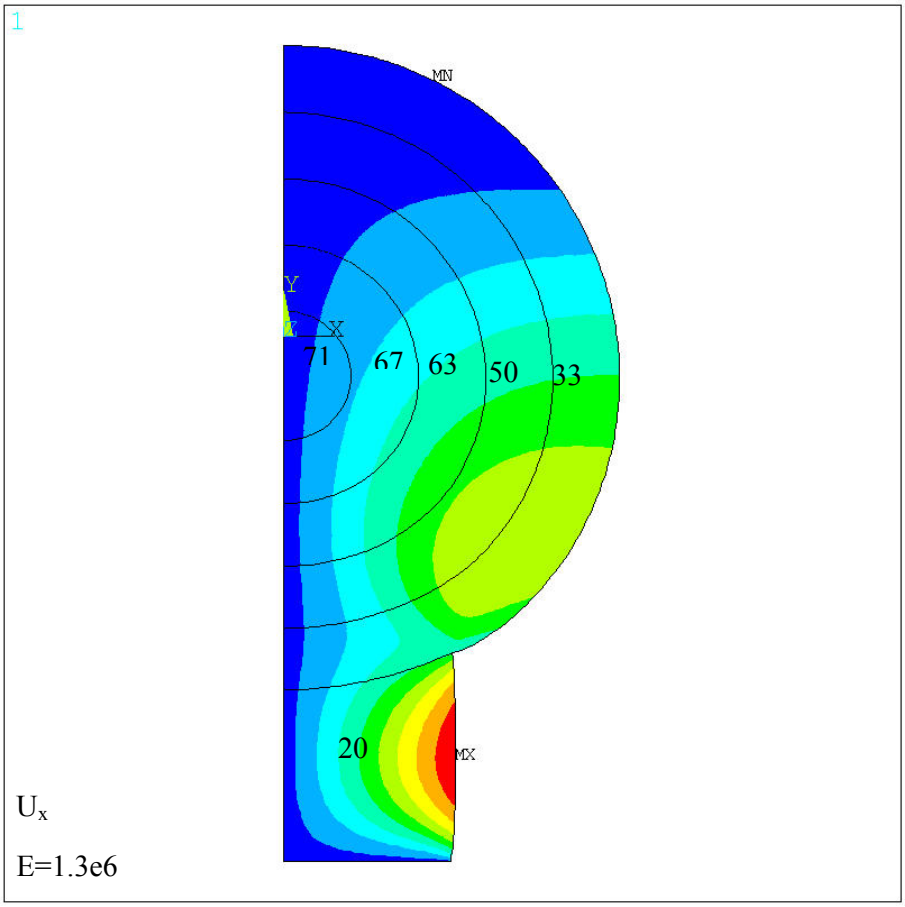

U_x

E=1.3e6

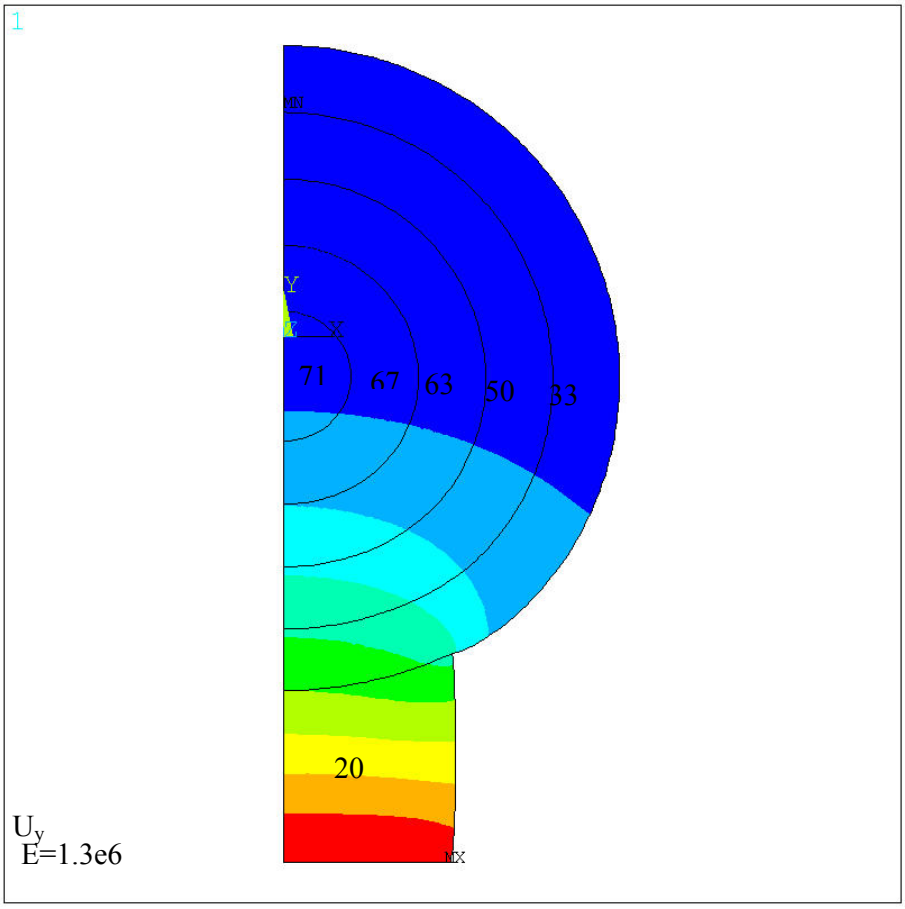

U_y

E=1.3e6

APPENDIX D: COST EQUATION FOR A LUNEBURG LENS SKA

This spreadsheet provides a preliminary cost equation for an SKA built from Luneburg lenses. It was derived at 1.4 GHz and 7 m. The model should scale reasonably for lenses between 5 m and 10 m in diameter. In its current form the model should not be applied to other frequencies. Special care should also be taken for lenses outside of the current suggested diameter range. Finally, parameters in the model scale with the number of widely placeable beams, except for signal transport parameters which are currently fixed for two widely placeable beams.

Colour Code

Bold type	input parameter
Normal type	calculated parameter
Primed'	scaled to 2010 cost
Red	contentious number
Light blue background	parameter label
Light green background	parameter description
Light yellow background	parameter units
Tan backrgound	parameter equation

Send Feedback To

Aaron.Chippendale@csiro.au
Australia Telescope National Facility

SYSTEM

INPUT PERFORMANCE PARAMETERS

Parameter	Description	Default Value	Units
f_0	Frequency of interest	**1.4**	GHz
SFOM	Sensitivity figure of merit	**20,000**	$m^2.K^{-1}$
T_p	Ambient physical temperature	**300**	K
N_p	Number of polarisations per receiver	**2**	none
N_{ccdc}	Number of data channels per core cluster; ea 40 Gb/s or 2 GHz RF capacity	**10**	none
N_{sdc}	Number of data channels per station; ea 40 Gb/s or 2 GHz RF capacity	**10**	none
$D_{station}$	Diameter of station	**250**	m
NS_{tot}	Number of stations in array	**300**	none
S_{kmcore}	Stations x km within core	**20000**	km
NS_{core}	Number of stations in compact core	**147**	none
NS_{spiral}	Number of stations in spiral	**153**	none
$N_{lens/cc}$	Number of lenses in a core cluster	**10**	none
$N_{LBFEEDS}$	Number of LF (eg 0.3-1.5GHz) feeds. One feed has two polarization channels	**1**	none

$N_{HBFEEDS}$	Number of HF (eg 1.4-5GHz) feeds. One feed has two polarization channels	**1**	none
v_L	Sampling rate for low freq feed	**5**	Gs/s
v_H	Sampling rate for high freq feed	**10**	Gs/s

CALCULATED PERFORMANCE PARAMETERS

Parameter	Description	Formula	Evaluation	Units
NB_w	Number of widely placeable beams	$(N_{LBFEEDS} + N_{HBFEEDS})$	2	none
$v_{data/station}$	RF bandwidth of data out of station	N_{sdc} *x 2GHz*	20	GHz
$v_{data/cc}$	RF bandwidth of data out of core cluster	N_{ccdc} *x 2GHz*	20	GHz

FEED ARM

INPUT COST PARAMETERS

Parameter	Description	Default Value	Units
$c_{armsteel}$	Cost of fabricated steel per arm for a 5 m diameter lens	**450**	USD
$c_{azmotor}$	Cost of azimuth motor	**200**	USD
$c_{altmotor}$	Cost of altitude motor	**100**	USD
c_{encode}	Cost of encoders and limit switches	**250**	USD
$c_{miscarm}$	Miscellaneous cost for a single feed arm	**100**	USD

CALCULATED COST PARAMETERS

Parameter	Description	Formula	Evaluation	Units
$C_{armsteel}$	Cost of fabricated steel per arm for a lens of diameter D	$c_{armsteel}\,(D/5)^2$	882	USD
c_{arm}	Cost of a single feed arm	$C_{armsteel} + 2c_{azmotor} + c_{altmotor} + c_{encode} + c_{miscarm}$	1732	USD

LUNEBURG LENS

INPUT PERFORMANCE PARAMETERS

Parameter	Description	Default Value	Units
η_a	Aperture efficiency	**65.0%**	none
α	Percentage rutile inclusions in foam, by volume, required to achieve an artificial ε_r of 2	**1.50%**	none
ρ_{foam}	Density of foam	**20**	$kg.m^{-3}$
ρ_{rutile}	Density of rutile	**4250**	$kg.m^{-3}$
D	Lens diameter	**7**	m
f/D	Focal ratio	**0.7**	none
δ	Loss tangent of foam	**0.0001**	

INPUT COST PARAMETERS

Parameter	Description	Default Value	Units
c_{foam}	Cost of foam	**1**	USD.kg^{-1}
c_{rutile}	Cost of rutile	**1.5**	USD.kg^{-1}
c_{track}	Cost of azimuth track	**5**	USD.m^{-1}
c_{coat}	Cost of protective coating	**3**	USD.m^{-2}

CALCULATED PERFORMANCE PARAMETERS

Parameter	Description	Formula	Evaluation	Units
$\sqrt{\bar{\varepsilon}_r}$	Root mean permittivity of lens	$e^{\frac{0.088}{f/D}}$	1.13	USD.kg^{-1}
dB(L_{lens})	Dielectric lens loss	$100 \times \delta . D . f \sqrt{\bar{\varepsilon}_r}$	0.111	dB
L_{lens}	Dielectric lens loss	dB -> ratio	1.03	none
T_{lens}	Equivalent noise temperature of lossy lens	$(L_{lens}-1)T_P$	7.78	K
η_r	Radiative efficiency of lens	L_{lens}^{-1}	97.5%	none
AL_g	Geometric collecting area of single lens	$\pi D^2/4$	38.5	m^2
AL_e	Effective collecting area of single lens	$\eta_a \eta_r AL_g$	24.4	m^2
S_{lens}	Surface area of lens sphere	πD^2	154	m^2

f	Focal length	$D \times f/D$	4.90	m
VL_{sphere}	Total volume of single lens (sphere only)	$\pi D^3/6$	180	m^3
τ	Volume of rutile (percentage of single lens volume)	$0.2\alpha(f/D)^{-1.14}$	0.451%	none
ML_{sphere}	Mass of a single lens sphere	$VL_{sphere}((1-\tau)\rho_{foam} + \tau\rho_{rutile})$	7,014	kg
B_3	Intermediate calculation for foam volume	$2f+3$	12.8	m
VL_{foam}	Total volume of foam in sphere, column and inner base	$\frac{D^3}{2}\left[0.95 + 0.2\frac{f}{D} + \frac{0.15}{D}\right] + 0.0025 f\left[(6.4f + 4B_3)B_3 + D^2\right]$	204	m^3
ML_{foam}	Mass of foam in sphere, column and inner base	$\rho_{foam}\, VL_{foam}$	4083	kg
VL_{rutile}	Volume of rutile in sphere	$\tau\, VL_{sphere}/100$	0.809	m^3
ML_{rutile}	Mass of rutile in sphere	$\rho_{rutile}\, VL_{rutile}$	3439	kg
ML_{tot}	Total mass of lens including sphere, column and inner base	$ML_{foam} + ML_{rutile}$	7522	kg
l_{track}	Length of azimuth track	$\pi(2f + 3 + D/2)$	51.2	m

CALCULATED COST PARAMETERS

Parameter	Cost Parameters	Formula	Evaluation	Units
C_{foam}	Total cost of foam for one Lens element	$c_{foam}ML_{foam}$	4,083	USD
C_{rutile}	Cost of rutile	$c_{rutile}ML_{rutile}$	5,158	USD
C_{track}	Cost of azimuth track	$c_{track}l_{track}$	256	USD
C_{coat}	Cost of protective coating	$c_{coat}S_{lens}$	462	USD
C_{arm}	Cost of feed arms for a single lens	$c_{arm}NB_{w}$	3464	USD
C_{lens}	Cost of single lens element	$C_{foam} + C_{rutile} + C_{track} + C_{coat} + C_{arm}$	13,423	USD
C_{area}	Cost of effective collecting area	C_{lens}/AL_{e}	551	$USD.m^{-2}$
$C_{area(lossless)}$	Cost of effective lossless collecting area	$C_{area}T_{lens}$	4,280	$USD.m^{-2}$

FRONT END

INPUT PERFORMANCE PARAMETERS

Parameter	Description	Default Value	Units
T_{lna}	Equivalent noise temperature of first LNA stage	**25**	K
χ	Proportion of receivers requiring rework	**5%**	none
β	Relative noise contribution of receiver after first LNA stage	**10%**	none

INPUT COST PARAMETERS

Parameter	Description	Default Value	Units
C_{MMIC}	Cost of MMIC for a single polarization LNA	**40**	USD
$C_{off\text{-}chip}$	Cost of off-chip components for a single polarization LNA	**20**	USD
C_{asm}	Cost of assembling a single polarization LNA	**20**	USD
C_{test}	Cost of testing a single polarization LNA	**20**	USD
C_{feed}	Cost of a zig-zag feed (including baluns)	**100**	USD

C_{cool}	Cost of cooling	**0**	USD

CALCULATED PERFORMANCE PARAMETERS

Parameter	Description	Equation	Evaluation	Units
T_{RX}	Receiver noise temperature	$T_{lna}(\beta + 1)$	27.5	K

CALCULATED COST PARAMETERS

Parameter	Description	Equation	Evaluation	Units
C_{RX}	Cost of dual polarisation LNA	$N_p(1 + \chi)(C_{MMIC} + C_{off\text{-}chip} + C_{asm} + C_{test})$	210	USD
C_{FE}	Cost of dual polarisation front end	$C_{RX} + C_{feed} + C_{cool}$	310	USD

NOISE PARAMETERS

INPUT PERFORMANCE PARAMETERS

Parameter	Description	Default Value	Units
T_{cmb}	Brightness temperature of cosmic microwave background radiation	**2.73**	K
T_{gxy400}	Brightness temperature of galactic foreground at 400 MHz (upper limit for off plane directions - about 70% of the sky)	**30**	K
n	Average logarithmic slope of galactic brightness temperature (3.6 degrees off the plane)	**-2.91**	
$dB(L_{feed})$	Feed loss at 1.4 GHz	**0.1**	dB
T_{atm}	Brightness temperature of atmosphere at 1.4 GHz (zenith at sea level, 20% humidity, 1013 hPa)	**4.41**	K
γ	Spillover response	**8%**	none
T_{cal}	Noise contribution of calibration signal	**2**	K

CALCULATED PERFORMANCE PARAMETERS

Parameter	Description	Equation	Evaluation	Units
T_0	Zero frequency intercept of galactic brightness temperature model	$T_{gxy400}/0.4^n$	2.09	K
T_{gxy}	Brightness temperature of galactic foreground at frequency f_0	$T_0 f_0^{\ n}$	0.783	K
T_{spill}	Spillover noise contribution (half on sky, half on ground)	$\gamma(T_{cmb} + T_{gxy} + T_{atm} + T_p)/2$	12.3	K
L_{feed}	Feed loss ratio	dB -> ratio	1.02	none
T_{feed}	Equivalent noise temperature of the feed loss at frequency f_0	$(L_{feed} - 1)T_P\sqrt{\frac{f_0}{1.4}}$	6.99	K
T_{sky}	Brightness temperature of sky background	$T_{cmb} + T_{gxy} + T_{atm}$	7.92	K
T_{sys}	System temperature	$T_{sky} + T_{lens} + L_{lens}(T_{feed} + T_{spill}) + L_{lens}L_{feed}T_{RX}$	64.4	K

SHORT-HAUL SIGNAL TRANSPORT

INPUT COST PARAMETERS

Parameter	Description	Default Value	Units
$c_{VCSEL10}$	Cost of VCSEL 8λ E-band array. This is highly integrated package with 0.25 μm CMOS driver and includes Array Waveguide WDM . Directly Modulated.	**400**	USD
$c_{PINRx10}$	Cost of PIN photodiode 8λ E-band band array. This is highly integrated package with limiting amps and includes Array Waveguide WDM .	**150**	USD
$c_{2\lambda MUX}$	Additional 2 λ MUX for distribution of 10G sysclk and 1Mb/s control/monitor data. 10G O/E Rx.	**200**	USD

CALCLATED COST PARAMETERS

Parameter	Description	Equation	Evaluation	Unist
C_{opt10}	Cost of photonics for 10G link. Excludes fiber, connectors.	$(C_{VCESL10} + C_{PINRx10})$	550	USD
$c_{shphotonics}$	Cost of 2 dual polarization photonics. Two channels @2.4G and two @10G. Also includes datacomms	$NB_wN_pC_{opt10} + C_{2\lambda MUX}$	2,400	USD

LONG-HAUL SIGNAL TRANSPORT

INPUT PERFORMANCE PARAMETERS

Parameter	Cost Parameters	Default Value	Units
N_{EDFA}	Total Number of optical amplifiers. Nominal quantity given spiral dimensions.All seven arms accounted.	**175**	none
$N_{Repeaters}$	Number of O/E-E/O regenerators based on 14500 km of long haul lines, repeater every 80 km per fiber strand used.	**30**	none
$N_{trunkfiber}$	Number of fibers for longhaul. Nominal (1) but can be increased as beamformer outputs exceed 13 wavelengths	**1**	none

INPUT COST PARAMETERS

Parameter	Cost Parameters	Default Value	Units
$C_{lasermod}$	Cost of a laser and external modulator and drive electronics	**3000**	USD
C_{optrx}	Cost of PIN or APD photodiode and limiting amp CDR ccts	**1000**	USD
C_{mux}	Cost optical add /drop WDM channel	**100**	USD
$C_{Gclk\&hub}$	Costs non-FO associated with 10Gclk and datacomms 1Gb/s hub	**1000**	USD
C_{EDFA}	Cost of EDFA and DCM. This is a bidirectional arrangement, needs two circulators and two WDM add/drop	**10000**	USD

CALCULATED PERFORMANCE PARAMETERS

Parameter	Description	Equation	Evaluation	Unist
$N_{trunkfiber}$	Every 78 λ requires a separate fiber for long-haul.	ceiling$(N_{sdc}/10\ ,1)$	1	none
B_{LHdata}	Aggregate data rate to Central Site from long-haul stations	$NS_{spiral}N_{sdc}$ x 40Gb/s	61,200	Gb/s

CALCULATED COST PARAMETERS

Parameter	Description	Equation	Evaluation	Unist
$C_{singlerepeater}$	Average cost of a single repeater based on average number of wavelengths . 78 wavelengths/2 x 6 stations on spiral	$78/2 \times (C_{lasermod} + C_{optrx} + 2C_{mux})$	163,800	USD
$C_{totalrepeaters}$	Total cost of trunk repeaters for 7 spirals.	$N_{trunkfiber} N_{repeaters} C_{singlerepeater}$	4,914,000	USD
$C_{trunkEDFA}$	Cost of optical amplifier stations >200 km from center	$N_{trunkfiber} N_{EDFA} C_{EDFA}$	1,750,000	USD
$C_{30\text{-}200EDFA}$	Cost of optical amplifier stations for intermediate range (30<d<200 km) from center. Seven spirals each with 6 beamformed stations, each on a separate fiber.	$6 \times 7 \times C_{EDFA}$	420,000	USD
$C_{totalEDFA}$	Total cost of optical amplifiers.	$C_{30\text{-}200EDFA} + C_{trunkEDFA}$	2,170,000	USD
$C_{spiralRx}$	Cost of 40Gb/s Optical Rx's for 7 spiral arms. Considers nominal (13) beamformers per spiral arm. (6) are full DWDM on a single fiber. (7) will use individual fibers	$7 \times NS_{spiral}/7 \times (N_{sdc} C_{optrx} + C_{Gclk\&hub} + (N_{sdc}+3) C_{mux})$	1,881,900	USD

OPTICAL FIBER

INPUT PERFORMANCE PARAMETERS

Parameter	Description	Default Value	Units
$D_{avestation}$	Average connection length in station R = 125 m	**0.125**	km
$D_{ave2.5}$	Average connection length in r < 2.5	**2.5**	km
k	Trunk infrastructure dark fiber free access coefficient. For k% = 0, no access. For k%= 100, free access to adequate existing cabling on trunk routes from telcos.	**30%**	none
L_{acc30}	Accumulated station x spiral length for 2.5< r <30 200 km x 7 spirals = 1400 km	**0**	km
L_{12core}	Length of 12 core trunk route fiber. Use optimum figure ~ 14700 km outside 30 km radius	**16100**	km

INPUT COST PARAMETERS

Parameter	Description	Default Value	Units
$C_{trench/km}$	Cost of trenching 1 km of cable	**10000**	USD
C_{fiber6}	Cable cost $/km 6 core	**2000**	USD
$C_{fiber12}$	Cable cost $/km 12 core	**2600**	USD
$C_{fiber36}$	Cable cost $/km 36 core	**6000**	USD
$C_{fiber144}$	Cable cost $/km 144 core	**15800**	USD

CALCULATED PERFORMANCE PARAMETERS

Parameter	Description	Equation	Evaluation	Unist
$N_{stnstrands}$	Number of fiber strands at the station J-Box.	$2(N_{LBfeeds} + N_{HBfeeds})N_{lens/station}$	704	none
$N_{cable144}$	Number of parallel 144core cables per station required to get to central site (where beamforming is not used)	Ceiling(($N_{stnstrands}$/144) , 1)	5	none
$L_{144core}$	Length of 144 core cable required	$N_{cable144}(NS_{core}D_{ave2.5} + L_{acc30})$	1,838	km
L_{6core}	Length of 6 core intra-station cable required to connect station antennas to the station J-Box	$NS_{tot}N_{lens/station}D_{avestation}$	6,600	km

CALCULATED COST PARAMETERS

Parameter	Description	Equation	Evaluation	Unist
$C_{144core}$	Cost of 144 core cable	$L_{144core}C_{fiber144}$	29,032,500	USD
C_{12core}	Total cost of 12 core fiber cable	$L_{12core}C_{fiber12}$	41,860,000	USD
C_{6core}	Total cost of 6 core fiber cable	$L_{6core}C_{fiber6}$	13,200,570	USD
$C_{fibertotal}$	Total cost of fiberoptic cable	$C_{6core} + C_{12core} + C_{144core}$	84,093,070	USD
$C_{trenching}$	Cost of trenching trunk (multiplied by existing fiber infrastructure factor) and cost of trenching spiral arms r < 30 km	$(L_{accc30} + L_{12core}(1\text{-}k))C_{trench/km}$	112,700,000	USD

DIGITAL SIGNAL PROCESSING

INPUT PERFORMANCE PARAMETERS

Parameter	Cost Parameters	Default Value	Units
v_{cor}	Correlated bandwidth (full Stokes)	**3**	GHz
n_{ce}	Correlated entities (inputs)	**2500**	none

INPUT COST PARAMETERS

Parameter	Cost Parameters	Default Value	Units
c_{cor}	Correlator cost per GHz of dual polarization bandwidth per baseline in 2002 dollars	**174**	USD
MF_{cor}	Moore factor for correlators	**32**	none
c_{bf}	Cost of beamforming (in 2002 dollars) per polarization lens GHz	**120**	USD
MF_{bf}	Moore factor for beam formers	**32**	none
c_{scor}	Cost of station correlators per baseline (1 pol, 32 + 8 (for RFI) 0.61 MHz channels)	**3.12**	USD
c_{scomp}	Cost of station computer	**4000**	USD
MF_{scor}	Moore factor for station correlators	**32**	none

c_{bbrx}	Cost of baseband receiver without LNA or ADC	**250**	USD
c_{adc10}	Cost of 8b 10Gs/s ADC today	**4000**	USD
$c_{frame/mux10}$	Cost of framing and muxing 10 Gs/s signals	**3200**	USD
$c_{deframe/mux10}$	Cost of deframing, demuxing and delaying 10 Gs/s signals	**3200**	USD
$c_{filterbank10}$	Cost of 8k channel zoomable filterbank for 10 Gs/s signals	**9400**	USD
MF_{adc}	Moore factor for ADCs	**4**	none
$MF_{antelec}$	Moore factor for antenna electronics	**32**	none

CALCULATED PERFORMANCE PARAMETERS

Parameter	Description	Equation	Evaluation	Unist
n_{cb}	Correlated baselines	$n_{ce}(n_{ce}-1)/2$	3,123,750	none
$n_{bfinner}$	Number of beamformers in the inner array	$NS_{core}N_{lens/station}/n_{lens/cc}$	2,587	none
n_{sb}	Number of station baselines	$N_{lens/station}(N_{lens/station}-1)/2$	15,401	none

CALCULATED COST PARAMETERS

Parameter	Description	Equation	Evaluation	Units
C_{cor}	Correlator cost today (X only)	$v_{cor} n_{cb} c_{cor}$	1,630,597,500	USD
C_{cor}'	Correlator cost in 2010	C_{cor}/MF_{cor}	50,956,172	USD
$C_{bfinner}$	Cost of central array beamforming in 2002	$v_{cor} N_{lens/station} c_{bf} NS_{core} N_p$	18,628,644	USD
$C_{bfinner}'$	Cost of central array beamforming in 2010	$C_{bfinner}/MF_{bf}$	582,145	USD
$C_{bfspiral}$	Cost of station beamforming in 2002	$v_{cor} N_{lens/station} c_{bf} NS_{spiral} N_p$	19,388,997	USD
$C_{bfspiral}'$	Cost of station beamforming in 2010	$C_{bfspiral}/MF_{bf}$	605,906	USD
C_{scor}	Cost of station correlators in 2002 (1 pol, 32 + 8 (for RFI) 0.61 MHz channels)	$NS_{tot}(n_{sb} c_{scor} + c_{scomp})$	15,615,648	USD
C_{scor}'	Cost of station correlators in 2010 (1 pol, 32 + 8 (for RFI) 0.61 MHz channels)	C_{scor}/MF_{scor}	487,989	USD
C_{adc10}'	Cost of 8b 10 Gs/s ADC in 2010	c_{adc}/MF_{adc}	1,000	USD
$C_{adc/v}'$	Cost of 8b ADC per Gs/s	$C_{adc10}'/(10\ \text{Gs/s})$	100	USD
$C_{antelec10}$	Cost of 10 Gs/s electronics per polarisation	$c_{bbrx10} + c_{frame/mux10} + c_{deframe/dmux10} + c_{filterbank10}$	16,050	USD
$C_{antelec10}'$	Cost of 10 Gs/s per polarisation in 2010	$(C_{antelec} - c_{bbrx10})/MF_{antelec} + c_{bbrx10}$	744	USD
$C_{antelec/v}'$	Cost of antenna electronics per Gs/s in 2010	$C_{antelec10}'/(10\ \text{Gs/s})$	74	USD
C_{antdsp}'	Cost of DSP per antenna (including baseband rx, frame/deframe, mux/demux, filterbank)	$N_p(NH_{BFEEDS} v_H + N_{LBFEEDS} v_L)(C_{antelec/v}' + C_{adc/v}')$	5,231	USD

SKA

CALCULATED PERFORMANCE PARAMETERS

Parameter	Description	Equation	Evaluation	Units
A_e	Required effective collecting area for 1.4 GHz spec	$T_{sys}SFOM$	1,287,476	m^2
N_{lens}	Number of lens elements required	A_e / AL_e	52,802	none
$N_{lens/station}$	Number of lens elements at each station	N_{lens} / NS_{tot}	176	none

CALCULATED COST PARAMETERS

Parameter	Description	Equation	Evaluation	Units
ΣC_{lens}	Cost of lens elements for the entire array	$N_{lens}\ C_{lens}$	708,763,923	USD
ΣC_{FE}	Cost of feeds and LNAs for the entire array	$NB_w N_{lens} C_{FE}$	32,737,413	USD
$\Sigma C_{antdsp}'$	Cost of DSP per antenna (including baseband rx, frame/deframe, mux/demux, filterbank)	$N_{lens} C_{antdsp}'$	276,221,919	USD
$C_{shphotonics}$	Cost of all short-haul photonics. Evaluation excludes fiber cable costs.	$N_{lens} c_{shphotonics}$	126,725,468	USD
$C_{longhaul}$	Total long-haul photonics cost outside (2.5 km) core radius from center. Evaluation excludes fiber costs.	$C_{spiralRx} + C_{totalEDFA} + C_{totalrepeaters}$	8,965,900	USD
$C_{fibertotal}$	Total cost of fiber optic cable	$C_{6core} + C_{12core} + C_{144core}$	84,093,070	USD
$C_{trenching}$	Cost of trenching	$C_{trenching}$	112,700,000	USD
$C_{bfinner}'$	Cost of central array beamforming	$C_{bfinner}'$	582,145	USD
$C_{bfspiral}'$	Cost of station beamforming	$C_{bfspiral}'$	605,906	USD
C_{scor}'	Cost of station correlators	C_{scor}/MF_{scor}	487,989	USD
C_{cor}'	Cost of central correlator	C_{cor}'	50,956,172	USD
C_{SKA}	Cost of the SKA	$\Sigma C_{lens} + \Sigma C_{FE} + \Sigma C_{antdsp}' + C_{shphotonics} + C_{longhaul} + C_{fibertotal} + C_{trenching} + C_{bfinner}' + C_{bfspiral}' + C_{scor}' + C_{cor}'$	1,402,839,904	USD

APPENDIX E: LENS BEAM PATTERNS

Fig. E1 shows computed beam patterns for a 7 m diameter Luneburg lens at 0.1 and 1.4 GHz. For modelling purposes, the lens was divided into ten dielectric shells. Dipole feeds were used at both frequencies. Gain values are relative only.

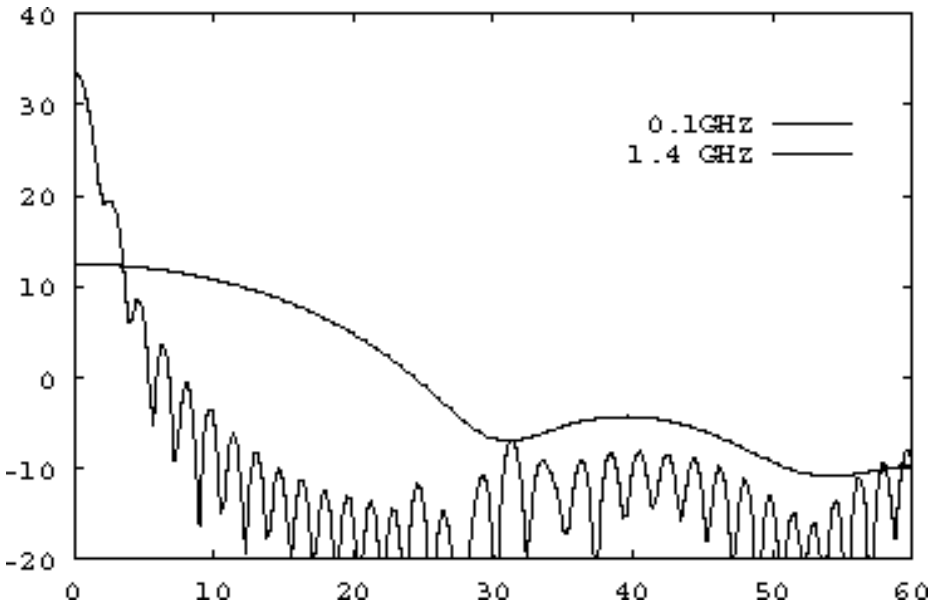

Fig. E1. Luneburg lens beam patterns at 0.1 and 1.4 GHz, assuming simple dipole feeds. The beam cuts are in the 45° plane. Gain values are relative only.

APPENDIX F: DESIGN COMPLIANCE MATRIX

In compiling this summary, we acknowledge the format introduced by the US SKA Consortium in their "Large N – Small D" concept description.

Table F1. Luneburg Lens SKA Compliance Matrix

Parameter	Design Goal	Falls Short	Meets	Exceeds
A_{eff}/T_{sys} 0.1 GHz 0.3 GHz 1.4 GHz 5.0 GHz	 **7.3×10^3 m^2K^{-1}** **2.0×10^4 m^2K^{-1}** **2.0×10^4 m^2K^{-1}** **2.0×10^4 m^2K^{-1}**	 7.0×10^2 m^2K^{-1} 6.0×10^3 m^2K^{-1} 1.3×10^4 m^2K^{-1}	 2.0×10^4 m^2K^{-1}	
Total frequency range	**0.2 - 20 GHz**	0.2 - 5 GHz		
Imaging field-of-view (800 MHz BW) 1.4 GHz (full array) 1.4 GHz (central array)	**1 deg^2**	 0.03 deg^2 0.14 deg^2	Can meet by increasing data link and signal processing capacity (Section G4)	
Number of instantaneous pencil beams (within a feed FOV and assuming correlator-limited BW) 3 GHz BW 800 MHz BW 30 MHz BW	**100**	 1 3	Can meet by adding more feeds and/or beamformers (Sections G3, G4) 100	
Max. primary beam sep. Low frequency High frequency	 **100 deg** **1 deg**			 > 120 deg > 120 deg
Number of spatial pixels	**10^8**		~ 10^8	
Angular resolution 1.4 GHz	 **0.1 arcsec**			 0.018 arcsec
Surface brightness sensitivity at 1.4 GHz (8 hrs integration, 800 MHz BW) 0.1 arcsec (300 km array) 13 arcsec (central array)	 **1 K**			 0.7 K 0.3 mK
Instantaneous bandwidth	**0.5 +f/5 GHz**			Up to 3 GHz correlator BW for f < 5 GHz
Number of spectral channels	**10 000**	8 192		
Number of simultaneous frequency bands	**2**			Flexible within data transport limits (Section 9.4)
Clean beam dynamic range	**10^6**	?	?	?
Polarization purity	**-40 dB**		Expect to meet (optics is unblocked and simple).	
Cost	**$US 1 billion**	$US 1.4 billion		

APPENDIX G: DESIGN EXTENSIONS AND UPDATES

G1 Introduction

We consider briefly three areas in which the performance of the proposed Luneburg lens array can be made to approach more closely the SKA design goals (Appendix A). These areas are the operating frequency range, the number of widely separated beams (or feeds), and the imaging field-of-view. These initial updates are for guidance only and it is certain that more detailed design work will yield better architecture and cost estimates.

G2 Frequency Extension

Modelling of the performance of the 7 m Luneburg lens shows that it is still an effective concentrator at 10 GHz (Fig. G1). Note that with a suitable LNA, the sensitivity approaches 1 x 10^4 m^2K^{-1}, or half the SKA design goal. Mechanical specifications for the antenna (Table 7-1) are adequate to allow effective pointing at the higher frequency. While there may be some capacity for operation at even higher frequencies, the granularity of the inclusions in the artificial dielectric becomes a factor at short wavelengths. We believe therefore that a particular manufacturing process would need detailed assessment for its potential above 10 GHz.

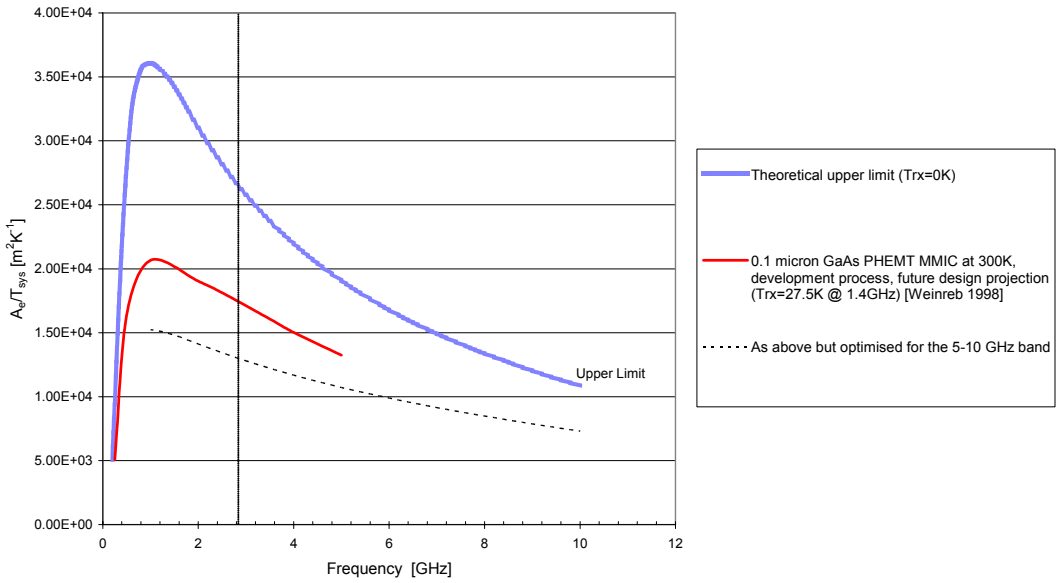

Fig. G1. Performance of Luneburg lens SKA extended to 10 GHz, assuming the 5-10 GHz range is covered by an optimized, uncooled, LNA and associated broadband feed.

It is unlikely that the baseband receiver architecture shown in Fig. 9-2 could be implemented directly at 10 GHz for an SKA operational by 2015. Instead, highly-integrated receivers, perhaps similar to emerging commercial radio-on-chip (RoC) devices, might be used as low-cost front-ends to feed the digital filterbanks. These packages, with on-board quantizers supporting >1 GHz instantaneous bandwidth,

would integrate well with the proposed array and antenna signal distribution topology. In view of the potential of the RoC technology, we propose a more detailed study in the coming year.

G3 Additional Feeds

While Section 15.2 canvasses a few options for adding feeds based on incremental numbers of moveable feed arms, more than one feed can of course be added to existing feed arms, giving much greater array utility in science areas such as surveys and SETI. With full-bandwidth (5 GHz) RF capacity, this saves about $US140 million of the ~$US300 million increment implied as the cost per additional feed in Table 15-1.

An interesting possibility is to assess the potential of RoC technology (having smaller instantaneous bandwidths) in conjunction with a larger number of feeds (~10) to exploit the proposed signal transmission infrastructure in a different way. The challenge is really to use two Luneburg lens attributes – wideband optical beamforming and multiple feed capability – in a scientifically optimum way. In parallel with the RoC assessment, we plan to look more closely at the scientific merits of approaches which maximize the number of beams.

G4 Increased Field-of-View

We have looked at two options to increase the imaging FOV of the Luneburg lens SKA. In the original concept description it was assumed that beamforming in the central array (diameter < 4 km) was at the level needed to give the equivalent of 300 stations in the whole SKA. We now consider two extensions, the first of which increases the beamforming and correlation capacity to give the central array an imaging FOV of 1 deg^2. The second increases the data transport capacity beyond the central array by an order of magnitude, giving a corresponding increase in the FOV across the entire array.

The proposed correlator has 2500 inputs and, with ~25 000 antennas in the central array, 10 lenses need to be combined in a beamformed sub-array if the correlator is devoted wholly to the central array and one feed per antenna. The sub-array beamwidth is ~0.246° with a beam area of ~0.047 deg^2 . The originally-proposed correlator has a 3 GHz full-Stokes bandwidth and, for 800 MHz observing bandwidth (appropriate for 1.4 GHz observing), about 3 "cluster" beams can be processed simultaneously, giving the reference design (Table 15-1) an imaging FOV of 0.14 deg^2. To obtain a 1 deg^2 coverage from the central array requires 7.1 times more processing power; we estimate that this can be provided at an additional cost of $US315 million, with all but $US4 million being accounted for by an expanded correlator. For reference purposes, we note that this cost might drop by a factor of five if one uses four-bit processing rather than the eight-bit scheme we proposed.

Considering now the wider array, the FOV of the reference array we have discussed is limited by both the data transport links and the correlator. For the station data channel capacity summarized in Table 9-1, 12 dual-polarization beams can be processed for an 800 MHz bandwidth, giving a FOV of ~0.03 deg^2. By doubling the capacity of the data links and station beamforming, at an estimated cost of $US 10 million, the correlator and link capacities are better matched, and the FOV increased to 0.06 deg^2.

While a full 1 deg^2 FOV for the entire array would be expensive and unnecessary, it is possible to buy an order-of-magnitude increase over the reference array (that is, a FOV of 0.3 deg^2) by spending an additional $US 300 million. This cost is split between correlator, data links and beamformers, with these components being estimated at $US 214 million, $US 80 million and $US 6 million, respectively. (Again, the correlator component could be reduced by a factor of five for four-bit processing).

Finally, we note that if both the central and wider array upgrades were made simultaneously, the cost would be about $US 400 million, or $US 150 million if the four-bit processing option is adopted.

APPENDIX H: DOCUMENT HISTORY

Table H1. Record of Amendments

Date	Revision	Comments
15 June 2002	a	Original release
	b, c	Typographical corrections
15 July 2002	d	Appendix F, G added. Document history added. Typographical corrections.